SELECTIVE ETHYLENE PRODUCTION FROM ETHANE DEHYDROGENATION OVER GALLIUM CATALYSTS; THE ROLE OF STRUCTURE CONFINEMENT AND SURFACE SILANOL GROUPS OF SUPPORTS

KITTIPONG PRAKOBTHAM

A THESIS SUBMITTED IN PARTIAL FULFILMENT OF THE REQUIREMENT FOR THE DEGREE OF MASTER OF SCIENCE IN PETROCHEMICALS AND HYDROCARBONS CHEMISTRY

DEPARTMENT OF CHEMISTRY FACULTY OF SCIENCE

KING MONGKUT'S INSTITUTE OF TECHNOLOGY LADKRABANG

2019

KMITL-2019-SC-M-015-069

Thesis Title	Selective ethylene production from ethane dehydrogenation over gallium catalysts: the role of structure confinement and surface silanol groups of supports
Student Name	Kittipong Prakobtham
Student ID	59605026
Degree	Master of Science (Petrochemicals and hydrocarbon chemistry)
Department	Chemistry
Year	2019
Thesis Advisor	Dr. Kittisak Choojun
Thesis Co-advisor	Prof. Dr. Tawan Sooknoi

Abstract

The effect of silanol and confinement of supports used in gallium catalysts with MFI structure including, HZSM-5 (Si/Al ratio 28, 40, 250, and 500), Ga-Silicalite (OH, (OH(550)), and F), and SiO_2 (devisil) was evaluated for the ethane dehydrogenation. For HZSM-5, 2%.Ga-HZSM-5 (28) and 2%.Ga-HZSM-5 (40) show the activity higher than others due to the synergistic of gallium in exchangeable site and Brønsted acid site resulting in the BTX as a side product. Furthermore, the severe deactivation is observed. While, the absent of Brønsted acid site in 2%.Ga-HZSM-5 (250) and 2%.Ga-HZSM-5 (500) provides high ethylene selectivity (99%) and stability that is derived from the gallium extra-framework species. When gallium loading is increased from 2%, 3% to 4% in HZSM-5 (500), the conversion is also enhanced signifying the higher amount of extra-framework Ga species. *In situ* XANES, EXAFS, and H_2-TPR suggest that these extra-framework Ga species could be dimeric Ga oxide $[Ga_2O_2]^{2+}$. Moreover, the reduction of $[Ga_2O_2]^{2+}$ forming $[HGaOH]^{+}$ species which are in virtual equilibrium and the later one functions as hydrogenolysis. With the different supports, the activity of gallium catalysts is in the order of 3%.Ga-Silicalite (OH) > 3%.Ga-Silicalite (OH(550)) ~ 3%.Ga-HZSM-5 (500) > 3%.Ga-SiO_2 (Davisil) > 3%.Ga-Silicalite (F). This is the result of

the number of surface silanol and the confinement of supports plays significant role for gallium dispersion. In addition, this combination affects the Ga stability as observed in *in situ* XANES reduction at 900 °C.

Keywords: Ethane dehydrogenation, extra-framework Ga, surface silanol and structure confinement

Acknowledgement

The author desires to appreciatively thank my advisor, Dr. Kittisak Choojun, and my co-advisor, Prof. Dr. Tawan Sooknoi, for suggestions, inspiration, carefulness, reassurance, experimental instrument, and knowledge in catalysis throughout this research

I would like to gratefully acknowledge chairperson and committee, Dr. Amnat Permsubscul, and Assoc. Prof. Dr. Siriporn Jongpatiwut for judgment and valuable comments.

Moreover, I would like to acknowledge the financial support from the Faculty of Science, King Mongkut's Institute of Technology Ladkrabang for the equipment, chemicals, and facilities.

Sincerely thanks to Suranaree University of Technology, Scientific and Technological Research Equipment Centre, Department of Chemistry, Chulalongkorn University for the characterization of catalyst in this research.

Unforgettable, I would like to grateful to my friends in Catalytic Chemistry Research Unit (CCR group) for their help, advice, support, and encouragement.

Finally, I deeply appreciate and thank our parents and family for their love and support.

Mr. Kittipong Prakobtham

TABLE OF CONTENTS

TABLE OF CONTENTS (Continued)

TABLE OF CONTENTS (Continued)

LIST OF TABLES

LIST OF FIGURES

LIST OF FIGURES (Continued)

LIST OF FIGURES (Continued)

LIST OF SCHEMES

CHAPTER 1
INTRODUCTION

1.1 Motivation

Ethylene is used extensively as a building block for a wide array of products including, plastics, rubbers, fuel blending agents, and chemical intermediates [1-3]. The production of ethylene is mainly via steam cracking, catalytic cracking, and ethane dehydrogenation [4]. However, the crude oil and natural gas, primary sources to produce ethylene, is nonrenewable and the concern of its depletion is raising. While, the production of light alkanes, especially ethane, is nowadays increased from shale gas extraction process [5]. As a result, the cost of these light alkanes has decreased substantially, leading to an opportunity to use ethane as a feedstock for ethylene production.

Currently, many researchers have paid attention on catalytic ethane dehydrogenation (EDH) at relatively lower temperature (550-650 °C) [6-9]. The first class of catalysts is the nobel metal over various supports, for example, palladium on silica. Palladium [10] and platinum-based catalysts [11] typically provide high conversion. However, deactivation is usually observed due to the metal sintering. Moreover, the nobel metals favored hydrogenolysis leading to high methane selectivity and they are relatively expensive. The second class is the metal oxides, including, chromium oxide, vanadium oxide, and gallium oxide. Nakagawa *et al*., [12] showed that the catalytic activity is in the order of β-Ga_2O_3 (19.6%) > Cr_2O_3 (12.1%) > V_2O_5 (9.8%), where the selectivity to ethylene is 95.0%, 93.8%, and 97.1%, respectively. This trend is also seen in propane dehydrogenation indicating that gallium oxide is capable to activate C-H bond in light alkane. In 2017, Chun-Tao Shao *et al.,* [13] shows that gallium oxide on HZSM-5 has a higher initial activity as compared to SiO_2, SBA-15, and Al_2O_3. However, the gallium oxide on HZSM-5 catalyst gives a higher deactivation rate due to coke formation. Ausavasukhi *et al*., [9] reported that the reduction of gallium oxide over HZSM-5 resulted in gallium hydride complex (GaH_2^+) species and deactivation can be suppressed over the reduced catalyst. Nevertheless, the exact nature of the gallium active sites is still under debate, particularly for the catalysts with

different Si/Al ratio. This is because the incorporated gallium in HZSM-5 with different acidity could be either located at the exchangeable site or exist as the gallium extra-framework.

In this research, it is challenging to understand relation between the nature of gallium species in HZSM-5 with various acidity, and their activity. Furthermore, the stability of Ga species is also evaluated using the different supports; Silicaite (OH), Silicalite (OH(550)), Silicalite (F), and SiO_2 (Davisil) that possess surface silanol and/or structure confinement. Therefore, we thus reason to study the activity, selectivity, and stability of Ga supported catalysts towards ethane dehydrogenation. The Ga species on the supports can be regulated by its acidity. X-ray spectroscopy will be used to elucidate the oxidation state and coordination of the Ga incorporated. The crystallinity, acidity, and reducibility of the Ga supported catalysts will also be characterized. The ethane dehydrogenation performance will be investigated for the effect of Ga loading, contact time, and acidity of catalyst.

1.2 Objectives

1.2.1 To selectively produce ethylene via direct dehydrogenation of ethane over Ga catalysts

1.2.2 To understand the nature of gallium species in Ga-HZSM-5 with various acidity.

1.2.3 To understand the effect of acidity of catalysts, the nature of gallium species, Ga loading and contact time on the ethane conversion, and supports.

1.3 Scopes of the study

The scopes of this thesis are as follow:

1.3.1 Preparation of gallium loaded MFI including, HZSM-5 with different Si/Al ratio (28, 40, 250, and 500), Silicalite (OH), Silicalite (OH(550)), and Silicalite (F) and SiO_2 (Davisil) catalysts by wet-impregnation method.

1.3.2 Characterization of catalysts by temperature-programmed reduction (TPR), NH_3-temperature-programmed desorption (NH_3-TPD), X-ray powder

diffraction (XRD), gas adsorption analysis (BET), X-ray fluorescence (XRF), Temperature programmed reduction (TPR), X-ray adsorption (XAS).

1.3.3 Testing on catalytic activity in a fixed-bed continuous flow reactor.

1.3.4 Study on the effect acidity of support HZSM-5 (x), (where x is Si/Al ratio = 28, 40, 250, and 500), Silicalite (OH), Silicalite (OH(550)), Silicalite (F), and SiO_2 (Davisil), nature of active Ga species in HZSM-5 (500), and stability of Ga with different supports

1.3.5 Products are analyzed and identified by online gas chromatography with flame ionization detector (GC-FID).

1.4 Expected Results

The appropriate condition for high ethane conversion and ethylene selectivity without severe deactivation can be obtained. Together with an understanding on the nature of gallium species, the knowledge could be applied to design catalyst for industrial application.

CHAPTER 2
THEORY

2.1 Ethane

2.1.1 General information [14]

Ethane is a C_2 hydrocarbon with the molecular formula C_2H_6. It is a colorless and odorless substance with an extremely flammable properties at standard temperature and pressure. The density of ethane is 0.5446 g/cm^3. The boiling point and melting point of ethane is −88.5 °C (−127.3 °F) and −182.8 °C (−297.0 °F), respectively. Ethane is only sparingly soluble in water. It is a precursor for ethylene, chemical intermediates for polymers, drugs, etc.

2.1.2 Sources and productions [14]

Ethane is one of the main components in natural gasses. Moreover, it is largely obtained as a byproduct from petroleum refining. Though, this raises the concern of the depletion of petroleum supply. Recently, the Shale-gas technology provides the large alternative source of natural gasses in which ethane is one of the key components. Ethane is most efficiently separated from methane by liquefying it at cryogenic temperatures. Even though, there are various strategies to extract ethane, the most economical process presently in wide use employs a turboexpander. In this process, chilled gas is expanded through a turbine, reducing the temperature to about −100 °C (−148 °F). This process can recover ethane more than 90% from natural gasses.

2.1.3 Applications [14, 15]

The industrial importance of ethane is based upon the ease of a transformation to ethylene (C_2H_4) and hydrogen by a pyrolysis or cracking once it passes through a hot tube at a temperature above 1,000 °C. Like propane and to a lesser extent butane, ethane is a major raw material for the huge ethylene petrochemical industry, which produces such important products as polyethylene plastic, ethylene glycol, and ethyl alcohol. Unlike propane liquid, ethane is not in common use as an industrial or

domestic fuel. Experimentally, ethane is under investigation as a feedstock for other commodity chemicals. Oxidative chlorination of ethane has long appeared to be a potentially more economical route to vinyl chloride than ethane chlorination. Many processes for producing this reaction have been patented, but poor selectivity for vinyl chloride and corrosive reaction conditions (specifically, a reaction mixture containing hydrochloric acid at temperatures greater than 500 °C) have discouraged the commercialization of most of them. Ethane can be used as a refrigerant in cryogenic refrigeration systems. On a much smaller scale, in scientific research, liquid ethane is used to vitrify water-rich samples for electron microscopy (cryo-electron microscopy). A thin film of water, quickly immersed in liquid ethane at −150 °C or colder, freezes too quickly for water to crystallize. With slower freezing methods, ice crystals can disrupt soft structures, damaging the samples.

2.2 Ethylene

2.2.1 General information [4]

Ethylene or Ethene is an unsaturated C_2 hydrocarbon with the molecular formula $C_{2s}H_4$. It is a flammable gas at room temperature and atmospheric pressure. The density of ethylene is 1.178 kg/m^3 in the gas phase. Ethylene has a boiling point of −103.7 °C (−154.7 °F) and melting point of −169.2 °C (−272.6 °F). It is a colorless flammable gas with a faint "sweet and musky" odor when it is pure.

2.2.2 Sources and productions [4]

Ethylene is produced in the petrochemical industry by steam cracking and catalytic reaction. In the first process, gaseous or light liquid hydrocarbons are heated to 750–950 °C, inducing numerous free radical reactions followed by an immediate quench to stop these chain reactions. This cracking process converts large hydrocarbons into both smaller saturated and unsaturated molecules. . Ethylene is separated from the resulting mixture by repeated compression and distillation. In a related process used in oil refineries, high molecular weight hydrocarbons are cracked over zeolite catalysts. Heavier feedstocks, such as, naphtha and gas oils require at least two "quench towers" downstream of the cracking furnaces to recirculate pyrolysis-

derived gasoline and process water. When cracking a mixture of ethane and propane, only one water quench tower is required.

2.2.3 Applications [16]

Ethylene is the raw material used in the manufacture of polymers such as polyethylene (PE), (PET), (PVC) and polystyrene (PS) as showed in **Figure 2.1**.

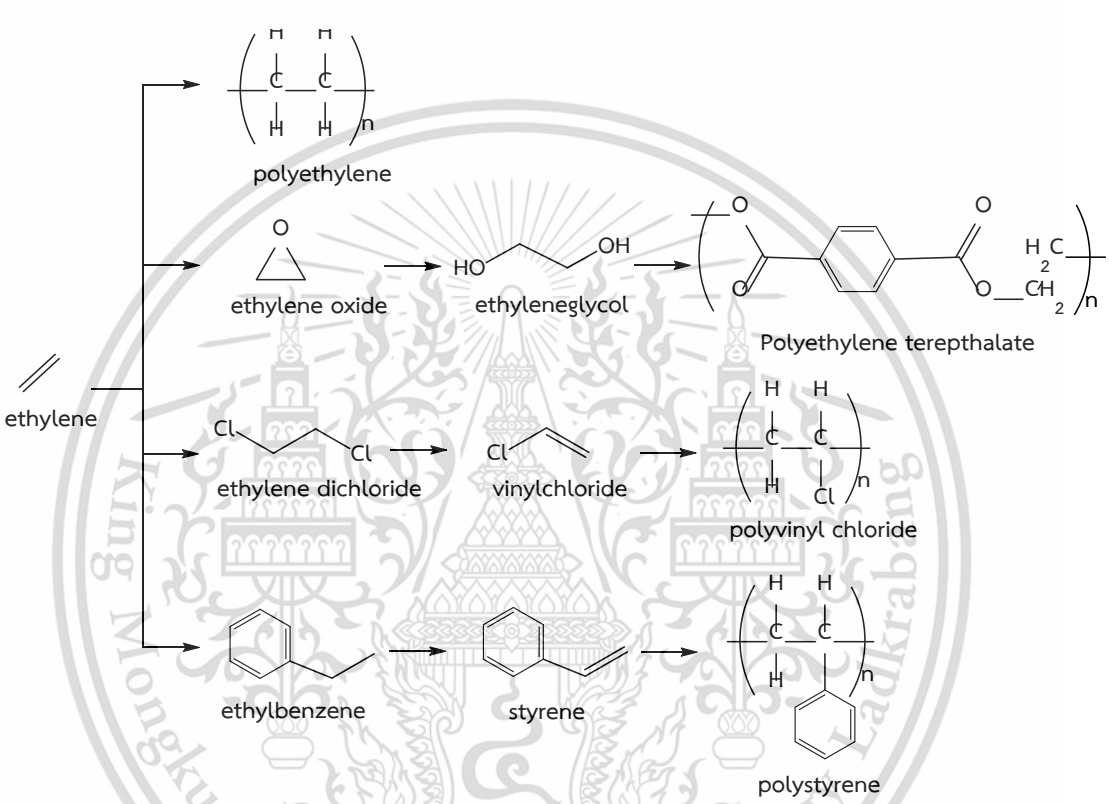

Figure 2.1 Derivatives of ethylene. [17]

These products are used in a wide variety of industrial and consumer markets, such as, the packaging, transportation, electrical, electronic, textile and construction industries as well as consumer chemicals, coatings and adhesives. The largest outlet, accounting for 60% of ethylene demand globally, is polyethylene. Low density polyethylene (LDPE) and linear low density polyethylene (LLDPE) mainly go into film applications, such as, food and non-food packaging, shrink and stretch film. High density polyethylene (HDPE) is used primarily in blow molding and injection molding applications, such as, containers, drums, household goods, caps and pallets. HDPE can

also be extruded into pipes for water, gas and irrigation, and film for refuse sacks, carrier bags and industrial lining.

Another use of ethylene to convert is ethylene oxide (EO) which is a primarily precursor for ethylene glycol. Most monoethylene glycol (MEG) is used to make polyester fibersfor textile applications, PET resins for bottles, and polyester film. MEG is also used in antifreeze applications. Other EO derivatives include ethyoxylates (use in shampoo, kitchen cleaners, etc), glycol ethers (use as solvents, fuels, etc) and ethanolamines (surfactants, personal care products, etc).

Ethylene dichloride (EDC), another product deriving from the chlorination of ethylene. It can then be cracked to make vinyl chloride monomer (VCM). Nearly all VCM is used to make polyvinyl chloride which has its main applications in the construction industry.

Ethylene can react with benzene to make ethylbenzene which is further processed into styrene. The main outlets for styrene are polymers and synthetic rubbers, such as, polystyrene, acrylonitrile-butadiene-styrene (ABS) and styrene butadiene rubber (SBR). Other ethylene derivatives include alpha olefins which are used in LLDPE production, detergent alcohols and plasticizer alcohols; vinyl acetate monomer (VAM) which is used in adhesives, paints, paper coatings and barrier resins; and industrial ethanol which is used as a solvent or in the manufacture of chemical intermediates for ethyl acetate and ethyl acrylate. Ethylene is one of the largest-volume petrochemicals. The consumption of derivative ethylene is 2015-16 show in **Figure 2.2**.

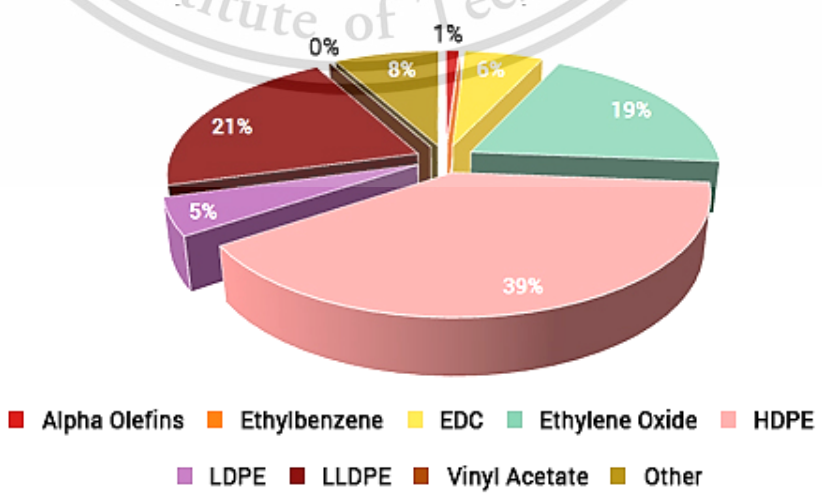

Figure 2.2 Consumption of derivative ethylene in 2015-16. [18]

2.3 Dehydrogenation reaction [19, 20]

Dehydrogenation is a chemical reaction that involves the removal of hydrogen from an organic molecule. The reaction is reversible. This reaction is of importance in industry to convert the low-value alkanes to more valuable olefins. In general, the dehydrogenation reaction can be classifiedinto two strategies that are the direct dehydrogenation and oxidative dehydrogenation. The oxidative dehydrogenation is an exothermic reaction that requires lower reaction temperature than that of the direct dehydrogenation which is an endothermic reaction. However, the oxidative dehydrogenation requires an oxidant, such as, oxygen and halogen. Due to the oxidant use, it may cause the over oxidation reaction forming an unpleasant byproduct, such as, carbon dioxide and halogenated organic molecule.

Considering the direct ethane dehydrogenation (EDH), ethylene and hydrogen would be the product from this reaction. This reaction is normally catalyzed by several types of catalysts. Ausavasukhi *et al.,* supported on zeolite [9], Wu *et al.,* supported on silica [10], and Fu *et al.,* supported on alumina [21] can successfully facilitate the dehydrogenation of ethane. The reaction mechanism involves in this reaction is list as the following and shown in **Figure 2.3**. In the first step, ethane must adsorb and follow by C-H cleavage on the catalyst surface to form ethylidene intermediate on the metal surface and leave H atom as metal-hydride on the support. After that, the intermediate will rearrange to form another hydride on the metal surface and ethylene in which it will leave the catalyst's surface Finally, hydrideon the support and catalyst surface will couple to form H_2 as a by-product as shown in **Figure 2.3**.

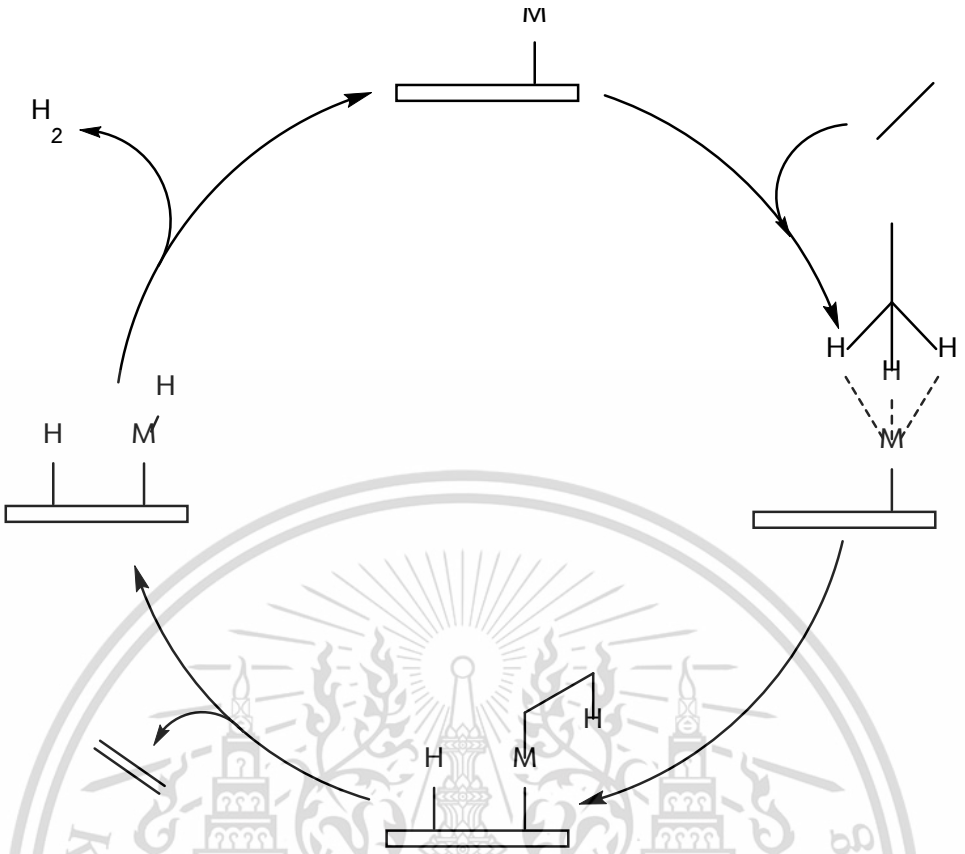

Figure 2.3 Mechanism of dehydrogenation of ethane. [19]

2.4 Catalyst

2.4.1 Metal supported zeolite

2.4.1.1 Zeolite [22, 23]

Zeolites are hydrated aluminosilicate minerals made from interlinked tetrahedra of alumina (AlO_4) and silica (SiO_4). In simpler words, they are solids with a relatively open three-dimensional crystal structure built from the elements aluminum, oxygen, and silicon, with alkali or alkaline-earth metals, such as, sodium, potassium, and magnesium, plus water molecules trapped in the gaps between them. Zeolites can be formed in different crystalline structures, which have large open pores (sometimes referred as cavities) in a very regular arrangement and roughly the same size as small molecules.

There are about 40 naturally occurring zeolites forming in both volcanic and sedimentary rocks. According to the US Geological Survey, the most commonly mined structures including, chabazite, clinoptilolite, and mordenite. Dozens more artificial, synthetic zeolites (around 150) have been designed for specific purposes, the best known of which are zeolite A (commonly used as a laundry detergent), zeolites X and Y (two different types of faujasites, used for catalytic cracking), and the petroleum catalyst ZSM-5 (a branded name for pentasil-zeolite).

Zeolites are very stable solids resisting the kinds of environmental conditions that challenge many other materials. High temperatures don't bother them because they have relatively high melting points (over 1000 °C), and they don't burn. They also resist high pressures, don't dissolve in water or other inorganic solvents, and don't oxidize in the air. They are not believed to cause health problems through, for example, skin contact or inhalation, though in fibrous form, they may have carcinogenic (cancer-causing) effects. Since they are unreactive and are based on naturally occurring minerals, they are not believed to have any harmful environmental impacts. Although zeolites might sound incredibly boring, their stable and unreactive nature is not what makes them useful.

The most interesting thing about zeolites is their open "framework" structure, cage-like, in which it can trap other molecules inside. This is how water molecules and alkali or alkaline-earth metal ions (positively charged atoms with too few electrons, sometimes called cations) become a part of zeolite crystals.Though they do not necessarily remain there permanently. Zeolites can exchange other positively charged ions for the metal ions originally trapped inside them (technically this is known as cation exchange) and, as Cronstedt found over 250 years ago, they can gain or lose their water molecules very easily too. This process is called reversible dehydration. Zeolites have regular openings in term of fixed size, which let small molecules pass straight through but trap larger ones; that is why they are sometimes referred to as molecular sieves. Unlike natural zeolites, which occur in random forms and mixed sizes, synthetic zeolites are manufactured in very precise and uniform sizes (typically from about 1 μm to 1 mm) to suit a particular application; in other words, they are made a certain size to trap molecules of a certain (smaller) size inside them.

Although, all zeolites are aluminosilicate, the amount of alumina and silica may be varied. Some contain more alumina, while others contain more silica. Alumina-rich zeolites are attracted to polar molecules, such as, water; while, silica-rich zeolites work better with nonpolar molecules.

The cage-like structure of zeolites makes them useful in all sorts of ways. One of the biggest everyday uses for zeolites is in water softeners and water filters. In ion-exchange water softeners, for example, hard water (rich in calcium and magnesium ions) is piped through a column filled with sodium-containing zeolites. The zeolites trap the calcium and magnesium ions and release sodium ions in their place, so the water becomes softer but richer in sodium. Many everyday laundry and dishwasher detergents contain zeolites to remove calcium and magnesium and soften water so they work more effectively.

Two other very common everyday uses of zeolites are in odor control and pet litter; in both, the porous crystalline structure of the zeolites helps by trapping unwanted liquids and odor molecules. This simple idea, so effective in our homes, has much more important uses outside them: zeolites have proved extremely effective at removing radioactive particles from nuclear waste and cleaning up soils contaminated with toxic heavy metals. (Following the Fukushima nuclear disaster in Japan in 2011, rice farmers spread zeolites on their fields in an attempt to trap any lingering radioactive contaminants). The many other uses of zeolites include concrete production, soil-conditioners, and animal food [22].

Another important use of zeolites is as catalysts in drug (pharmaceutical) production and in the petrochemical industry, where they are used in catalytic crackers to break large hydrocarbon molecules into gasoline, diesel, kerosene, waxes, and all kinds of other byproducts from petroleum. Again, it is the porous structure of zeolites that proves important. The many pores in a zeolite's open structure are like millions of tiny test tubes where atoms and molecules become trapped and chemical reactions readily take place. Since the pores in a particular zeolite are of a fixed size and shape, zeolite catalysts can work selectively on certain molecules, which is why they are sometimes referred as shape-selective catalysts (they can select the molecules they work on in other ways beside shape and size). Like all catalysts, zeolites are reusable over and over again.

In industrial applications, the most important zeolites are LTA, FAU, MFI, and MOR. The dimensions of the zeolite pores allow for the separation of molecules on the basis of their sizes, so-called molecular sieving effect. In catalysis, this property is often referred to shape selectivity. An example is the cracking of alkanes in acid MFI-type zeolites. Here the zeolite pores allow only the linear molecules to enter the pores containing the acid sites that regulate the cracking. Branched molecules are excluded from the pores and hence do not react [23].

2.4.1.2 ZSM-5 zeolite [24]

Zeolite ZSM-5, Zeolite Socony Mobil-5, is one type of family zeolite. It has shape selective property with unique channel structures. The secondary building unit of frameworks of ZSM-5 include mor 8T, case 12T, mel 14T, and mfi 14T as shown in **Figure 2.4**. These secondary building units can be connected to form sheet and the linking of the sheet lead to a three dimensional framework structure by the chains extend along the z-axis. The sheets parallel to [010] and [100] are shown in **Figure 2.5** and **Figure 2.6**.

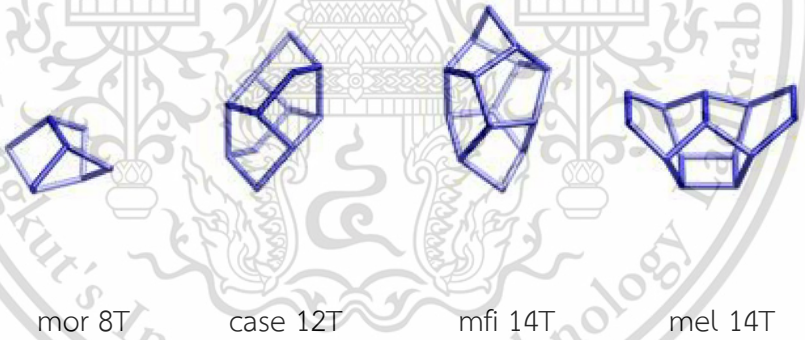

Figure 2.4 The secondary building unit of framework of ZSM-5. [24]

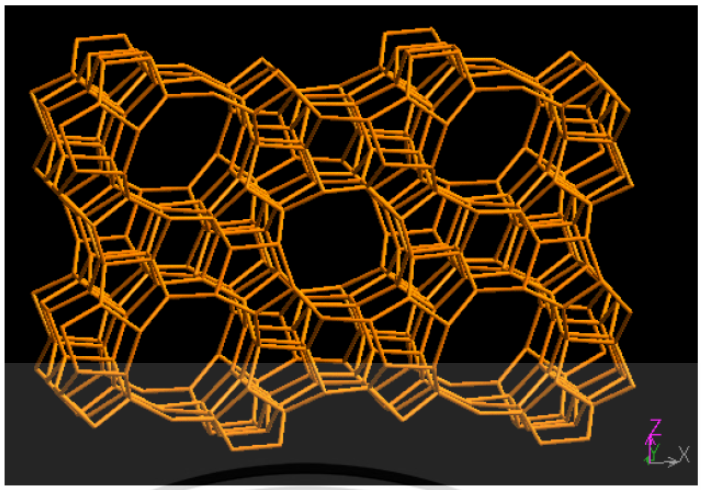

Figure 2.5 Skeletal diagram of the [010]-plane of the ZSM-5 unit cell. [24]

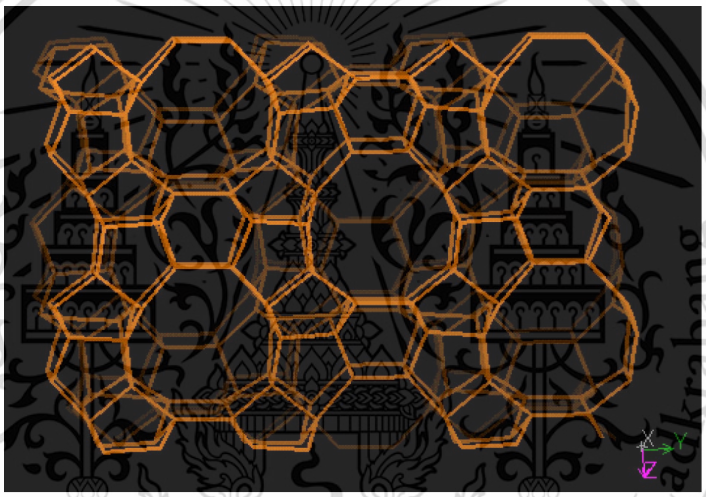

Figure 2.6 Skeletal diagram of the [100]-plane of the ZSM-5 unit cell. [24]

Figure 2.5 shows that the x-axis is horizontal and the z-axis vertical and the 10-membered ring apertures shown are the entrances to the straight channels which run parallel to [010] plane. While, **Figure 2.6** shows that the y-axis is horizontal and the z-axis vertical and the circular 10-membered ring apertures shown are the entrances to channels which run parallel to [100] plane.

ZSM-5 chemical formula is $Na^{+}_{n}(H_2O)_{16}|$ $[Al_nSi_{96-n}O_{192}]$-MFI, n < 27. It is widely used in many catalytic reactions of industrial interest, such as, xylene isomerization, benzene ethylation, and ethanol, methanol-to-gasoline conversion. Their individual catalytic properties are mainly due to their regular framework with a pore size, which is in between the large pore size zeolites (for instance, zeolites X and

Y) and the small pore size zeolite (for instance the A zeolite). The shape selectivity of the pentasil zeolite is catalytically expressed by many featuresas listed the following;

1. The sieving effect, i.e., the capability of zeolite to admit into its pores or to reject reactive molecules having a critical diameter falling within a well-defined range.
2. The (reverse) sieving effect, i.e., the capability of the zeolite to allow product molecules having a certain critical diameter to diffuse out of its pores. Thus, in the case of a product molecule having a diameter exceeding to the pore size of the zeolite, this molecule will have to undergo cracking or rearrangement into a smaller molecule before diffusing out of the zeolite.
3. The effect on the reaction intermediates, i.e., the capability of certain active site to determine the length and structure of reaction intermediate species. ZSM-5 zeolite has pore system, which is believed to be significant for their low coke formation. While most industrial applications of zeolite catalyst make use of these in acid form. Zeolite is also excellent support for metal species. Zeolite supported metal species called a bi-functional catalyst is an acid zeolite on which a metal species phase is deposited. The function of the metal is to catalyze dehydrogenation and hydrogenation reaction; while, H-ZSM-5 possesses excellent dehydration and oligomerization properties which bi-functional catalyst can further undergo a variety of metal species and acidity reactions to form desirable product.

2.4.1.3 Metal supported zeolite [25-28]

Metal supported zeolite is a bi-functional catalyst that each component has the capability of catalyzing a different reaction and compromising each other for the overall reaction. This type of catalyst is widely used in petroleum refining, especially in hydrocracking and hydroisomerization. Because transition states of catalytic mechanism occur both on metal and acid sites, the activity and selectivity of bi-functional catalysts can be determined by the characteristics of the metal sites and

the zeolitic acid sites. In the other words, zeolite support enhances the catalytic activity and selectivity using the acids sites and the microporous properties [25].

The transition metal cations (TMC) that compensate the negative charge of the zeolite skeleton determine substantially the physical, chemical, and catalytic properties of the zeolite. While, non-transition metal cations affect the zeolite properties through their electrostatic field or through their ability to act as Lewis centers. TMC may also act as redox sites in zeolites. TMC, localized in the cation position of the zeolite (as well as randomly located cations or metal or oxide clusters), can be present in various oxidation states in dependence on the manner of the cation introduction into zeolites and on the further zeolite treatment. The properties of the cations are also affected by the type of cation position as well as the coordination of cations by the skeletal oxygen. Furthermore ligands may be bonded to them (H_2O, OH, O, etc.) [26].

In principle, TMC can substitute Si^{4+} or Al^{3+} in the zeolitic structures during synthesis, resulting in a zeolite lattice containing TMC incorporated in the structure. Parameters to be taken into account are (i) the size and charge of the TMC, (ii) the pH of the synthesis medium, and (iii) the ability of the TMC to adopt tetrahedral coordination with O atoms. In most cases, the amount of TMC incorporated in the lattice by hydrothermal synthesis is very limited. The two most common examples are Ti^{4+} and Fe^{3+}. Ti^{4+} exchanged in silicalite, for instance, is called TS-1 and is found to be an active catalyst in converting benzene with hydrogen peroxide into phenol [27, 28]. The presence of Fe^{3+} in the lattice is often due to the presence of an impurity in the zeolite synthesis, but it can also be added as a reagent into the synthesis mixture. One of the problems with TMC in the lattice is thermal stability. Upon high-temperature treatment, some of the TMC in the structure are extracted and found as so-called extralattice TMC, which can be monomeric or dimeric or appear as oligomers. All of them are possible catalytic sites. Aqueous ion exchange is the most commonly used method for preparing zeolites with TMC located at exchange sites. The resulting material contains aqueous TMC in the pores and cavities of the zeolite. Upon high-temperature treatment, water is removed and the TMC coordinate to the surface oxygen of the exchange sites. These sites had been compiled by Mortier a long time ago. They are crystallographically well-defined in the case of zeolites with low Si/Al

ratios, such as, LTA, FAU, and MOR. This is much less so for zeolites with high Si/Al ratios, such as, MFI. Because aqueous solutions of TMC can be acidic, the exchange reaction can be accompanied by side reactions, for example, the exchange of protons and partial lattice destruction. To avoid these side effects, other exchange techniques have been developed, including solid-state exchange or simple buffering of the aqueous solution.

Metal supported zeolites are widely used for many reactions. Cobalt-exchanged zeolites ZSM-5 are active catalysts for alkane ammoxidation [29] and also active for NO_x reduction by methane in presence of excess O_2 [30]. The selective oxidation of NH_3 to N_2 can be occurred over Pd-ZSM-5 [28]. Moreover, Pd-ZSM-5 is an active catalyst for methane combustion [31]. In addition, cobalt, copper, rhodium, ruthenium, and platinum supported ZSM-5 are active for catalytic decomposition of N_2O to N_2 and O_2 [32].

2.4.2 Gallium supported ZSM-5 [33, 34]

Gallium is an element in group IIIA of the periodic table. It does not occur as a free element in nature but as gallium (III) compounds in trace amount of zinc ores. It is a soft, silvery white metal, and similar to aluminum at standard temperature and pressure, a brittle solid at low temperature, and a liquid at temperature greater than 29.76 °C. The application of gallium that has received the most attention is the production of semiconducting compounds. For many years this technology was dominated by the elemental semiconductors, silicon, and germanium. But in 1952, German workers reported the achievement of semiconduction in compounds between elements in group III and group V. Of these, the most important are the compounds of gallium with antimony, arsenic or phosphorus. Nowadays gallium arsenide (Ga-As) is undoubtedly the most used. This compound is used in the production of several electronic parts, such as, diodes and transistors, made for voltage rectification, signal amplification, etc. Other gallium arsenide applications are the semiconductor "lasing" and microwave generation and also in several sensors to measure temperature, light or magnetic field.

Gallium supported ZSM-5 is one of the most active catalyst for light alkane dehydrogenation and aromatization [6, 7, 9]. Its high alkane dehydrogenation and

aromatization activity is attributed to the presence of bi-functional sites of non-framework gallium oxide species and zeolitic protons, located close to each other in the zeolite channels [35].

2.5 Literature review

The catalytic dehydrogenation of ethane has an important commercial interest for industry. Therefore, this reaction has been studied by a lot of scientists over 50 years. Nowadays, the dehydrogenation of ethane (EDH) is commercially available. Some processes used for this reaction can be quoted, such as, ABB/Catofin, UOP Oleflex, PDH (Linde), Phillips STAR having in feed gas as ethane, hydrogen, and an inert gas [36].

In 1907, Sabatier *et al.,* reported catalytic dehydrogenation processes. They studied various oxides which were able to catalyze this reaction [37]. And finally, in 1940's, Vladimir *et al.,* found a reforming process with platinum as a catalyst to produce a high octane gasoline from naphtha (for Universal Oil Product Company) [38]. Palladium [10] and platinum [11] were particularly studied, because it has a high activity for activating C-H bonds, and a relatively low activity for the cracking of C-C bounds. However, platinum and palladium catalysts need to be improved because they suffer from rapid deactivation, poor selectivity depending on experimental conditions.

The first report about the dehydrogenation of light alkanes using gallium oxide supported on ZSM-5 was founded in 1988. Gnep *et al.,* [39] reported that the gallium species increase the rate of propane conversion and the selectivity for aromatics. As the result, the gallium oxide has been used as dehydrogenation catalyst. In comparison gallium oxide with other metal oxides, Nakagawa *et al*., [12] studied activity of metal oxides on ethane dehydrogenation in the presence of CO_2. The reaction was operated at 650 ^{o}C in fixed-bed continuous flow reactor at atmospheric pressure. The results showed that the catalytic activity is in the order of β-Ga_2O_3 (19.6%) > Cr_2O_3 (12.1%) > V_2O_5 (9.8%), where the selectivity to ethylene is 95.0%, 93.8%, and 97.1%, respectively. This trend is also seen in propane dehydrogenation indicating that gallium oxide is capable to activate C-H bond in light alkane.

Gallium oxide on different supports shows different activity and stability. Xu *et al.,* [40] reported that the gallium oxide on the basic supports, including MgO, and SiO_2 were inactive in propane dehydrogenation. In contrast with basic supports, the gallium oxide on acid supports, including ZrO_2, Al_2O_3, and TiO_2 were obtained activity. These different activity on different supports might due to one of the effect from metal dispersion. Nowak *et al.,* [41] also reported the dispersion of Ga_2O_3 species varied with different supports. However, the effects of supports on the state of gallium species have not been fully understood, especially the causes of these changes. Shao *et al.,* [13] studied on effect of supported on the propane dehydrogenation using gallium oxide-based catalyst. They use 5%wt.Ga_2O_3 supported on X (where x is HZSM-5, Al_2O_3, SBA-15, and SiO_2) as the catalysts. The result showed that the initial activity is in the order of SiO_2< SBA-15 < Al_2O_3 < HZSM-5. However, the rate of catalysts deactivation is SiO_2< SBA-15< Al_2O_3< HZSM-5. This could be contributed to the coke formation resulting from the acidity of the supports.

Since zeolites can be formed in different geometry and components, the types of zeolites supported gallium oxide catalysts also have the effect towards propane dehydrogenation. Ren *et al*., [42] studied on effect of acidity and pore geometry of zeolite on the propane dehydrogenation. They used 5%wt.Ga_2O_3 supported on HZSM-48 (x), (where x is Si/Al ratio, 130, 160, and 220) and HZSM-5 (200) as a catalysts. The result showed that Ga_2O_3/HZSM-48 (130) having higher activity as compared to Ga_2O_3/HZSM-48 (160) and Ga_2O_3/HZSM-48 (220). The increase in Si/Al ratio, decrease in acidity, led to the decrease in propane conversion. Amongst the various zeolites, it was found that Ga_2O_3/HZSM-5 (200) gave higher stability, as compared to Ga_2O_3/HZSM-48 (130) at 50 h on stream. Choudhary *et al.,* [33], studied on the effect of acidity on propane aromatization over Ga/H-ZSM-5 with 0-3%wt. Ga loading and 35-132 Si/Al ratio. The reaction was operated at 550 ^{o}C in fixed-bed continuous flow reactor at atmospheric pressure. The results showed that an increase in Ga loading led to higher propane conversion and aromatics selectivity. However, an increase in Si/Al ratio led to lower propane conversion and aromatics selectivity.

Not only does the acidity of the supports have an effect towards the gallium oxide catalysts but the acidity of the gallium species, in which it can be manipulated

by the reduction, also have an influence. Ausavasukhi *et al.,* [9] studied the ethane dehydrogenation over 3%.Ga-HZSM-5 using pulse reactor. The reaction was operated at 550-750 °C at atmospheric pressure under He and H_2 as carrier gas. The results showed that the ethane conversion was increased with temperature with 100% ethylene selectivity except for the reaction at 700 and 750 °C under H_2 carrier gas that methane was found as a cracking product. It was interestingly that the different carrier gas gave a significant difference in ethane conversion. It was suggested that after calcination, GaO^+ is the active species provided ~25% ethane conversion under He carrier gas. After the reduction, slightly higher activity was obtained (~30% ethane conversion), presumably due to the formation of more active Ga species (Ga^+). Under H_2 carrier gas, the catalyst show higher activity (~55% ethane conversion), presumably due to the formation of GaH_2^+ that is the most active species. However, GaH_2^+ can decompose in the absence of H_2.

From the literature reviews, the exact nature of the gallium active sites is still under debate, particularly for the catalysts on HZSM-5 with different Si/Al ratio. This is because the incorporated gallium in HZSM-5 with different acidity could be either located at the exchangeable site or exist as the gallium extraframework. It is thus challenging to understand relation between the nature of gallium species in HZSM-5 with various acidities, and their activity.

CHAPTER 3

EXPERIMENTAL DETAILS

3.1 Chemicals and substrates

Chemical reagents	Grade of purity	Manufacturers
1. Gallium nitrate hydrate ($Ga(NO_3)_3.xH_2O$)	99.99%	ACROS ORGNICS
2. Ethane gas	99.50%	LINDE
3. NH_4-ZSM-5 (Si/Al = 28)		ZEOLYST INTERNATIONAL
4. NH_4-ZSM-5 (Si/Al = 40)		ZEOLYST INTERNATIONAL
5. NH_4-ZSM-5 (Si/Al = 250)		ZEOLYST INTERNATIONAL
6. NH_4-ZSM-5 (Si/Al = 500)		ZEOLYST INTERNATIONAL
7. Silicalite (OH) commercial grade		COMPANY CONFIDENTIAL INFORMATION
8. Silicalite (F)		COMPANY CONFIDENTIAL INFORMATION
9. Silicon dioxide (Davisil)		SIGMA-ALDRICH
10. Deionized water		
11. Air zero gas	99.99%	UIG
12. Hydrogen gas	99.99%	PRAXAIR
13. Nitrogen gas	99.999%	UIG
14. Helium gas	99.99%	PRAXAIR

3.2 Apparatus and instruments

1. Catalytic activity testing rig
2. Mass flow controller (AALBORG)
3. Tube furnace with a programmable temperature controller (CARBOLITE)
4. Quartz tube (8.0 mm O.D.)
5. Heating tape with a programmable temperature controller
6. Clamp
7. Gas chromatograph (Agilent 6890 Series)

8. Laboratory glassware
9. Laboratory plasticware
10. Trap condenser
11. Sieve (U.S.A standard sieve, AASHO N-92)
12. Gas adsorption analysis (Autosorb-1C, Quantachrome)
13. Temperature programmed reduction (TPR, Model TCD2-NIFED)
14. Temperature programmed desorption (TPD, Model TCD2-NIFED)
15. Inductively couple plasma mass spectrometer (ICP Quadrupole Mass Spectrometer, Thermo Scientific iCAP Qc ICP-MS)
16. Thermogravimetic analyzer (Perkin-Elmer, Scientific Instrument Service Center, KMITL)

3.3 Preparation of catalysts

3.3.1 Preparation HZSM-5 (x), Silicalite (OH(550)), and SiO_2 (Davisil)

A powder of supports was calcined in the tube furnace with programmable temperature controller under 30 mL/min flow of air zero at 550 °C with heating rate of 2 °C/min for 5 hours.

3.3.2 Gallium loaded HZSM-5 (3%.Ga-HZSM-5 (x))

The gallium loaded HZSM-5 catalysts with different Si/Al ratio (28, 40, 250, 500) will be prepared by wet-impregnation method using gallium nitrate ($Ga(NO_3)_3$) precursor. HZSM-5 (28) and Gallium nitrate hydrate precursor will be weighed (9.79 g and 1.18g), respectively then dissolved using 400 drops of concentrate nitric acid and leaved it until fully dissolve. Then, 40 mL of DI water will be used for dilute the dissolved precursor. The precursor solution will be sprayed on the dried ZSM-5 support. After that, the prepared catalyst will be dried in an oven at 80 °C overnight. The dried catalyst will be calcined in a horizontal tube furnace under 30 mL/min flow of air zero at 550 °C with heating rate of 2 °C/min for 5 hours. Gallium supported on HZSM-5 with different Si/Al ratio will be prepared using similar procedure.

3.3.3 Gallium loaded Silicalite (3%.Ga-Silicalite (x)) and SiO_2 (Davisil)

The gallium loaded Silicalite (x) catalysts, where is x (OH, OH(550), and F) and SiO_2 (Davisil) will be prepared by wet-impregnation method using gallium nitrate ($Ga(NO_3)_3$) precursor. Silicalite-1 (OH) and Gallium nitrate hydrate precursor will be weighed (9.79 g and 1.18g), respectively then dissolved using 400 drops of concentrate nitric acid and leaved it until fully dissolve. Then, 40 mL of DI water will be used for dilute the dissolved precursor. The precursor solution will be sprayed on the dried Silicalite-1 support. After that, the prepared catalyst will be dried in an oven at 80 °C overnight. The dried catalyst will be calcined in a horizontal tube furnace under 30 mL/min flow of air zero at 550 °C with heating rate of 2 °C/min for 5 hours. Gallium supported on Silicalite (OH(550)), Silicalite-1 (F), and SiO_2 (Davisil) will be prepared using similar procedure.

3.4 Characterization of catalysts

3.4.1 Surface area analysis (BET)

Surface area of catalysts will be determined using gas adsorption technique. The sample will be weighed (40-50 mg) and loaded into a cleaned and dried sample cell. After that, the sample will be degassed at 350 °C for 24 hours. The sample cell will be then removed from the out-gassing station after filling up with nitrogen and will be attached to the analysis station. The adsorption isotherm will be measured in a pressure range of 0.05-0.30 P/P_0 at -196 °C.

3.4.2 Temperature programmed reduction (TPR)

In order to investigate the reducibility of catalysts, the temperature programmed reduction (H_2-TPR) will be operated using thermal conductivity detector (TCD). A 100 mg of sample will be put into a quartz tube reactor that is located inside a temperature-regulated furnace. Before the H_2-TPR operation, each sample will be activated under a flow of air zero with a flow rate of 30 mL/min at 450 °C with heating rate of 2 °C/min for 1 h and then cooled down to below 100 °C. A heating rate of 10 °C/min and 30 mL/min of 10% H_2 in Ar will be applied for the H_2-TPR analysis. Water produced from the reduction process will be trapped in a U-shape stainless trap at -196 °C (liquid nitrogen) before entering the TCD.

3.4.3 Temperature programmed desorption (TPD)

3.4.3.1 Ammonia temperature programmed desorption (NH_3-TPD)

Acidity of catalysts was investigated by the temperature programmed desorption of ammonia (NH_3) using the TCD. The catalyst was pretreated with similar procedure as that for H_2-TPR except cooling down to room temperature. The NH_3 was adsorbed with a flow rate of 30 mL/min for 1 h using 1% NH_3 in He and continue with flushing of the excess physisorbed NH_3 using He with a flow rate of 30 mL/min for 1 h. The heating rate of 10 ^{o}C/min was applied for the NH_3 desorption procedure under He flow.

3.4.4 X-ray Florescence (XRF)

The conventional technique to check the chemical composition of catalyst is by X-ray fluorescence spectroscopy. This technique can be done according to the following procedure: the catalyst sample was weighed about 0.5 g and boric acid was weighted about 4.5 g, then sample and boric acid were mixed together, and compressed into alumina pan before bring into the XRF sample holder in XRF instrument.

3.4.5 Inductively couple plasma mass spectrometry

In order to identify gallium content (%loading) of the catalysts, the inductively couple plasma mass spectrometry (ICP-MS) was operated using ICP Quadrupole Mass Spectrometer, Thermo Scientific iCAP Qc ICP-MS. The standard gallium solution was prepared with various concentration (0.01-0.1 ppm) using gallium nitrate solution. The sample solution was prepared by digesting the catalyst in the aqua regia solution (3:1 HCl: HNO_3 v/v) and then diluted with DI water. The intensity of the standard gallium solution was plotted as a calibration curve. The intensity of the sample solution was used for calculating the % Ga loading.

3.4.6 X-ray powder diffraction (XRD)

The structure of catalyst was determined by X-ray diffractometer (XRD). The sample was prepared by packing the catalyst into the sample holder. CuKα X-ray beam was used for analysis at 40 kV and 30 mA. The sample was scanned over the angle ranged from 2θ: 5° to 90° with 2 deg./min. and 0.02 2θ/step increments. X-ray diffraction pattern of the sample was compared with the X-ray diffraction pattern of standard catalyst for structure determination.

3.4.7 X-ray Absorption (XAS)

The energy of the X-ray absorption was used to determine the oxidation state of the metal species and coordination environment of the catalyst. X-ray absorption were measured at SLRI (Synchrotron Light Research Institute, Public Organization) using a Ge (220) double crystal monochromator. The storage ring was operated at 1.2 GeV. Data were collected in the transmission mode on self-supporting sample pellet using gas-filled ionization chambers as detectors.

3.5 Catalytic activity testing

Gas phase catalytic dehydrogenation of propane will be investigated using fixed-bed continuous flow reactor made with quartz tube (8.0 mm O.D.) at atmospheric pressure. The schematic diagram of the catalytic testing rig is shown in **Figure 3.1**. The catalyst will be packed in the middle of reactor while top and bottom of the reactor will be filled with quartz wool and quartz beads. The reactor will be installed inside the temperature-controlled furnace. The gas flow rate will be controlled by AALBORG mass flow controller and measured using bubble flow meter. Before testing, the catalyst will be activated under 30 mL/min flow of air zero at 450 °C with a heating rate of 2 °C/min for 1 h. Then, N_2 will be flushed to eliminate the remaining air in the line. After that, the catalyst will be reduced under 50 mL/min flow of H_2 550 °C with a heating rate of 10 °C/min for 3 h. The reaction will be tested at 600-700 °C.

Ethane will be flowed through the catalyst bed with a varies flow rate of (20-150 mL/min) which the low flow rate < 30 mL/min co-feed carrier gas but the high flow rate > 75 mL/min without carrier gas. The catalytic testing will be continued at least 3 h on stream. The products mixture will be flowed out of the reactor and passed

through a gas sampling loop of the GC. In order to prevent products condensation, the line after the reactor will be heated using temperature-controlled heating tape at 165 °C. The summary of the reactor set up and reaction conditions are shown in **Table 3.1**.

3.6 Products analysis

The total products were analyzed using on online-gas chromatograph with flame ionization detector (GC-FID). The heavy product will be collected in gas sampling loop, then injected into the GC column (Equity-1, 30 m length, 0.53 mm internal diameter, 5 μm film thickness). The following temperature program was used for the analysis: holding at 35 °C for 5 min, followed by the ramping to 85 °C at the rate of 15 °C/min. holding for 2 min., then ramping to 220 °C at rate of 10°C/min., before a final holding at that temperature for 3 min. N_2 was used as a carrier gas (40 cm/sec). Each component was separated as passed though the column with an inert carrier N_2 gas and their presence in the effluent were recorded as a chromatogram. The light product will be collected in gas sampling loop, then injected into the GC column (Rt®-Q-BOND capillary column (length, 30 m; internal diameter, 0.53 mm; film thickness, 0.20 μm). The initial column temperature was 30 °C hold for 7 min, often then ramp at 20 °C /min to 85 °C hold for 4 min, then ramp at 20 °C /min to 140 °C hold 3 min, finally then ramp at 15 °C/min to 225 °C and hold at this temperature for 6.83 min. The temperature of the injection port and FID was kept constant at 250 °C during analysis. N_2 gas was used as a carrier gas. Each component was separated as they pass though the column with an inert carrier N_2 gas and their presence in the effluent were recorded as a chromatogram. Each components will be identified by comparing to the standard gas. The area of each components will be measured, and then the propane conversion and products yield will be calculated.

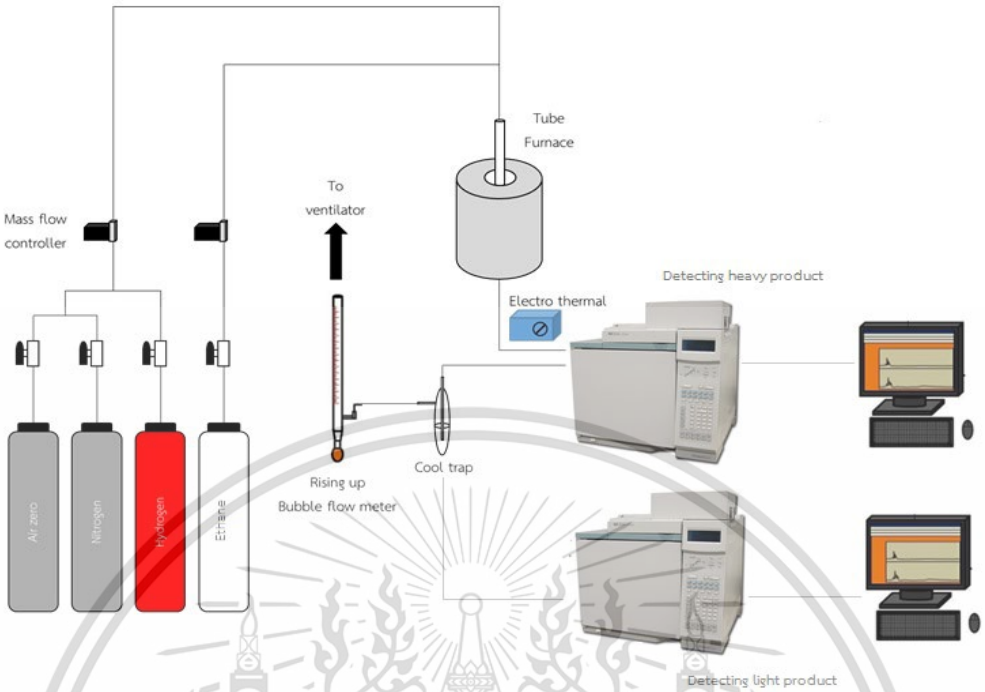

Figure 3.1 Schematic of catalytic testing rig

Table 3.1 Summary of reactor set up and reaction conditions.

Parameters	Value
Reactor outside diameter (mm)	8.0
Bed length (mm)	10-50
Catalyst weight (g)	0.2-0.5
Catalyst pellet size (μm)	600-850
Catalyst activation:	
- Temperature (°C)	450 °C for 1 h
- Heating rate (°C/min)	2
- Gas	Air zero (30 mL/min)
Catalyst reduction:	
- Temperature (°C)	900 °C for 3 h
- Heating rate (°C/min)	10
- Gas	H_2 (50 mL/min)

Table 3.1 Summary of reactor set up and reaction condition (continued).

Parameters	Value
Reaction temperature (°C)	600-700
Reaction pressure (atm)	Atmospheric pressure

CHAPTER 4
RESULTS AND DISCUSSION

4.1 Characterization

4.1.1 Physicochemical properties

Elemental composition, acidity as determined by NH_3-TPD, and specific surface area of Ga supported catalysts are summarized in **Table 4.1.**

Table 4.1 Physical and Chemical properties

Entry	Catalysts	% Metal loading	S_{BET} (m^2/g)	Pore volume (μL/g)	Acidity (mmol/g)
1	HZSM-5 (28)	-	414	210	3.77
2	HZSM-5 (40)	-	420	199	-
3	HZSM-5 (250)	-	397	165	-
4	HZSM-5 (500)	-	402	169	0.41
5	2%.Ga-HZSM-5 (28)	2.30[a]	383	195	4.24
6	2%.Ga-HZSM-5 (40)	2.34[a]	398	185	1.11
7	2%.Ga-HZSM-5 (250)	2.33[a]	359	153	0.38
8	2%.Ga-HZSM-5 (500)	2.46[b]	390	143	0.56
9	3%.Ga-HZSM-5 (500)	3.22[b]	380	145	0.72
10	4%.Ga-HZSM-5 (500)	4.07[b]	374	142	0.81

Table 4.1 Physical and Chemical properties (continued).

Entry	Catalysts	% Metal loading	S_{BET} (m^2/g)	Pore volume (μL/g)	Acidity (mmol/g)
11	SiO_2 (Davisil)	-	330	432	-
12	Silicalite (F)[c]	-	424	481	-
13	Silicalite (OH(550))[d]	-	497	393	-
14	Silicalite (OH)[e]	-	431	356	-
15	3%.Ga-SiO_2 (Davisil)	3.40[b]	309	397	0.06
16	3%.Ga-Silicalite (F)	3.40[b]	382	376	0.03
17	3%.Ga-Silicalite (OH(550))	3.20[b]	433	287	0.52
18	3%wt.Ga-Silicalite (OH)	3.12[b]	416	189	0.75

[a] Determined by ICP-MS [b] Determined by XRF

[c] Silicalite (F) is OH free support.

[d] Silicalite (OH(550)) is support that is calcined 550 ^{O}C.

[e] Silicalite (OH) is support that is not calcined.

From ICP-MS and XRF result, it can be seen that Ga content in all catalysts is similar to the expected value. The 2%.Ga-HZSM-5 (x), where x is Si/Al ratio 28, 40, 250, and 500 (**Table 4.1, entry 5-8**) possesses surface area of 350-400 m^2/g that is slightly lower than the parents support. This is due to pore blocking either inside or outside by the incorporated gallium as observed with the decrease in pore volumes. In a similar manner, 3%.Ga over siliceous supports (SiO_2 (Davisil), Silicalite (F), Silicalite (OH (550)), and Silicalite (OH) shows lower surface area and pore volume as compared to their parents. As the Ga loading is increased from 2% to 4%. the surface area is decreased (**Table 4.1, entry 8-10**) as expected.

The acidity of 2%.Ga-HZSM-5 (28) and 2%.Ga-HZSM-5 (500) (4.24 and 0.56 mmol/g, respectively) (**Table 4.1, entry 5 and 8**) are higher than HZSM-5 (28) and HZSM-5 (500) (3.77 and 0.41 mmol/g, respectively) (**Table 4.1, entry 1 and 4**). Moreover, the total acidity is correlatively enhanced with the Ga loading (**Table 4.1**, **entry 8-10**). This observation could be contributed to the Lewis acidity generated by the incorporated gallium species as reported by A.L Petre [43].

In line with this view, the total acidity of the gallium loaded siliceous supports (**Table 4.1, entry 15-18**) are also enhanced. This emphasizes the presence of Lewis acid from the incorporated gallium oxide. Despite of similar gallium loading, the total acidity of 3%.Ga-Silicalite (F), 3%.Ga-SiO_2 (Davisil), 3%.Ga-Silicalite (OH(550), and 3%.Ga-Silicalite (OH) is varied from 0.03, 0.06, 0.52, and 0.75, respectively. Such difference in acidity is likely to be the result of the gallium dispersion.

4.1.2 Catalyst structures

Crystallinity and local structure of the catalysts before and after gallium loaded are shown in **Figure 4.1.**

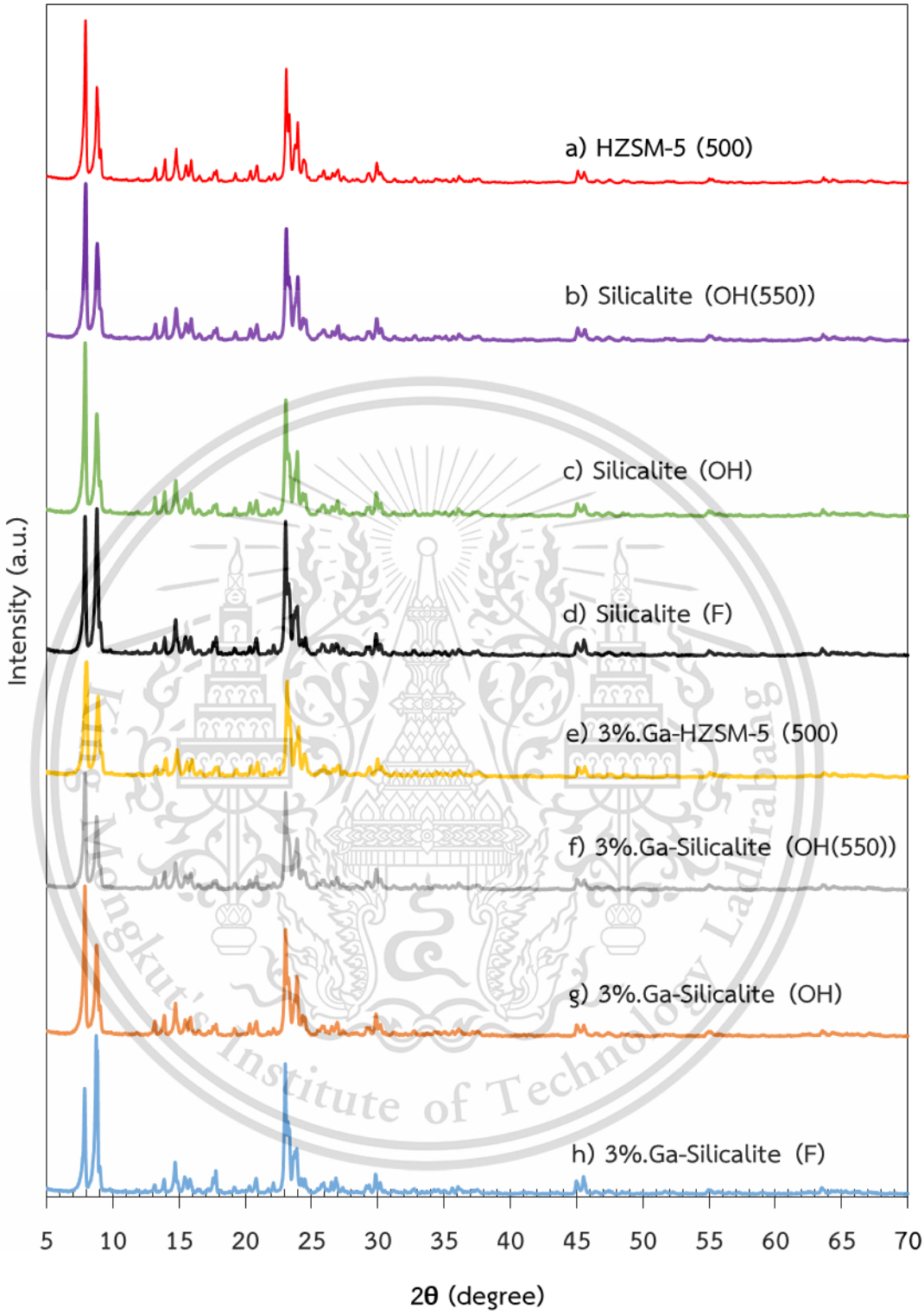

Figure 4.1 XRD pattern of before and after gallium loaded supports a) HZSM-5 (500), b) Silicalite (OH(550)), c) Silicalite (OH), d) Silicalite (F), e) 3%.Ga-HZSM-5 (500), f) 3%.Ga-Silicalite (OH(550)), g) 3%.Ga-Silicalite (OH) and h) 3%.Ga-Silicalite (F)

According to the XRD patterns, the structure of MFI parent supports (HZSM-5, Silicalite (OH(550)), Silicalite (OH), and Silicalite (F) (**Figure 4.1a–d**)) show major peaks at 2θ = 7.92, 8.32, 22.68, 23.13, 23.15 and 24.41 degrees, similar to those reported in literatures [44]. In addition, the higher intensity of Silicalite (F) is due to the preferred orientation at *200* plane since the crystalize size is larger as compared with HZSM-5 (500) as shown by SEM image (**Figure 4.2)**. After loaded gallium (**Figure 4.1e-h**), the crystallinity patterns remain the same without the gallium oxide crystalline phase [45,46]. This indicates that the loaded gallium is well-dispersed over these MFI supports.

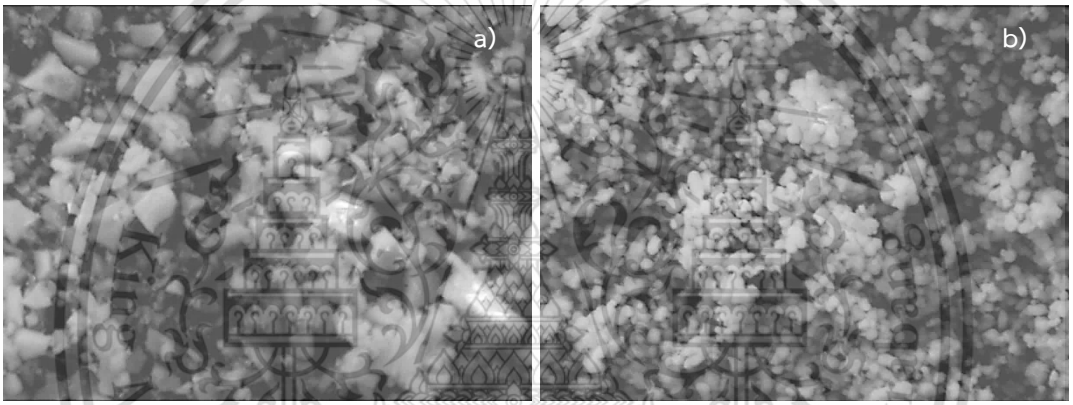

Figure 4.2 SEM images of a) Silicalite (F) and b) HZSM-5 (500)

4.1.3 Catalysts reducibility

The effect of the gallium loading on HZSM5 (500) and the effect of the supports towards the reducibility of gallium were examined by H_2-TPR as shown in **Figure 4.3**. The H_2 consumption, obtained by comparing with H_2 standard pulse, is summarized in **Table 4.2**.

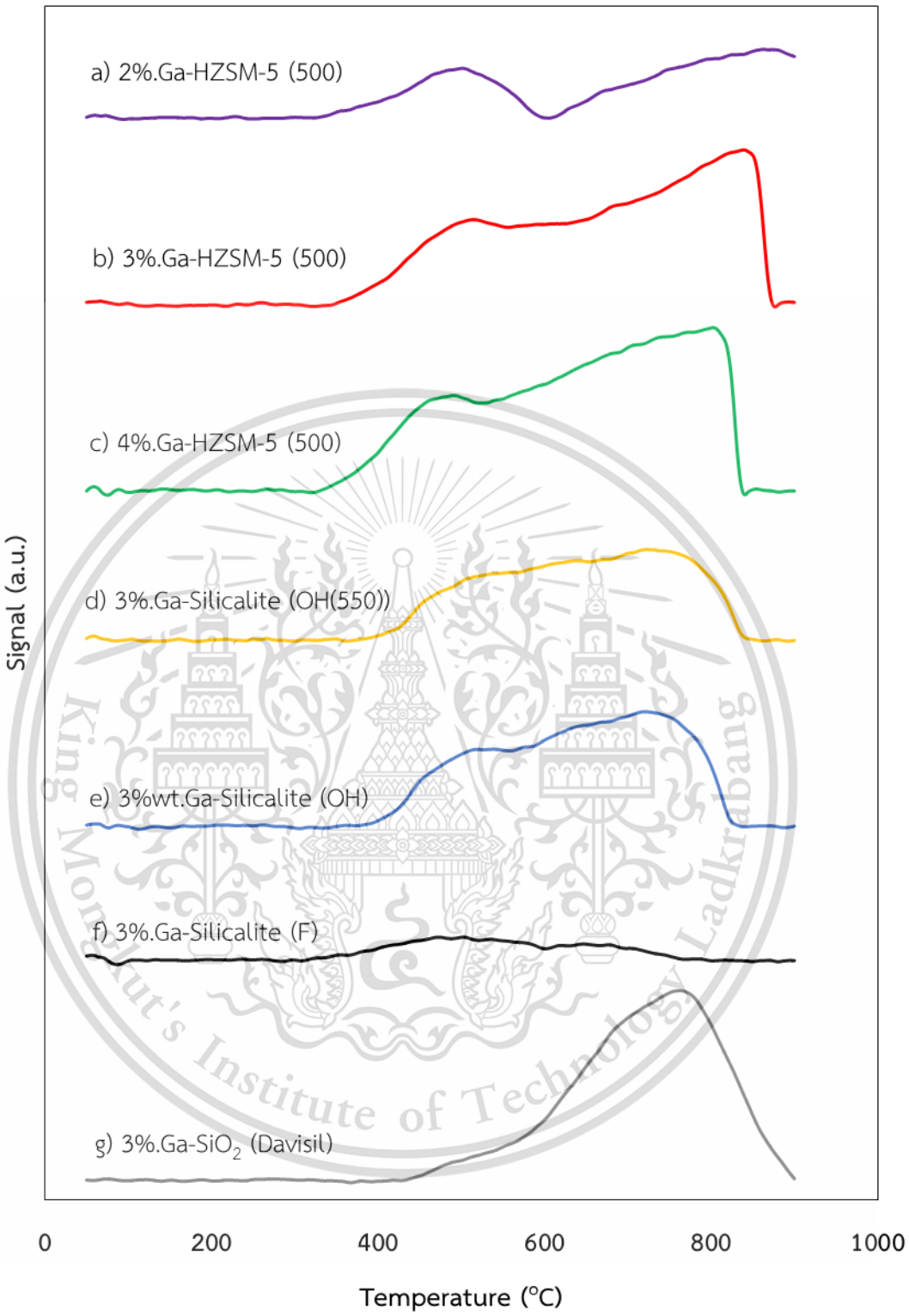

Figure 4.3 H_2-TPR profiles of a) 2%, b) 3%, c) 4% of Ga loading over HZSM-5 (500), d) 3%.Ga-Silicalite (OH(550)), e) 3%.Ga-Silicalite (OH), f) 3%.Ga-Silicalite (F), and g) 3%.Ga-SiO_2 (Davisil) under a flow of 10% H_2/Ar (30 mL/min) at 50-900 °C with a heating rate of 10 °C/min.

Table 4.2 Summarized H_2–consumption of the catalysts

Entry	Catalyst	Ga content (mmol/g)	H_2 consumption (mmol/g)		
			400-600 °C (peak I)	600-900 °C (peak II)	total
1	2.46%.Ga-HZSM-5(500)	0.35	0.08	0.15	0.23
2	3.22%.Ga-HZSM-5(500)	0.46	0.18	0.25	0.43
3	4.07%.Ga-HZSM-5(500)	0.58	0.20	0.35	0.55
4	3.20%.Ga- Silicalite (OH (550))	0.46	0.14	0.23	0.37
5	3.12%.Ga- Silicalite (OH)	0.45	0.13	0.22	0.35
6	3.40%.Ga-SIlicalite (F)	0.49	0.06	0.01	0.07
7	3.40%.Ga-SiO_2 (Davisil)	0.49	0.01	0.42	0.43

According to **Figure 4.3**, all the catalysts show two reduction peaks at 400-600 °C (peak I) and 600-900 °C (peak II) with H_2 consumption (mmol/g), similar to the Ga content. The observed reduction temperature is somewhat higher than the exchangeable Ga species, as reported in literature [47,48]. Moreover, small amount of Ga exchangeable site is presented in HZSM-5 (500) and none of this site is found in Silicalite and SiO_2 (Davisil). Therefore, it could be suggested that the incorporated Ga species exist as highly-dispersed extra-framework Ga.

For 3%.Ga-Silicalite (F) (**Figure 4.3f**), small amount of H_2 consumption can be observed, despite the same Ga loading (**Table 4.2, entry 6**). It is suggested that Ga cannot be easily reduced presumably due to the presence of bulk Ga_2O_3, as reported by M. Saito [49]. This is presumably because the incorporated Ga tends to agglomerate due to the weak interaction with this support. The relatively low energy surface of Silicalite (F) is derived from small amount of surface silanol, as evidenced by *in situ* FTIR (**Figure 4.4**).

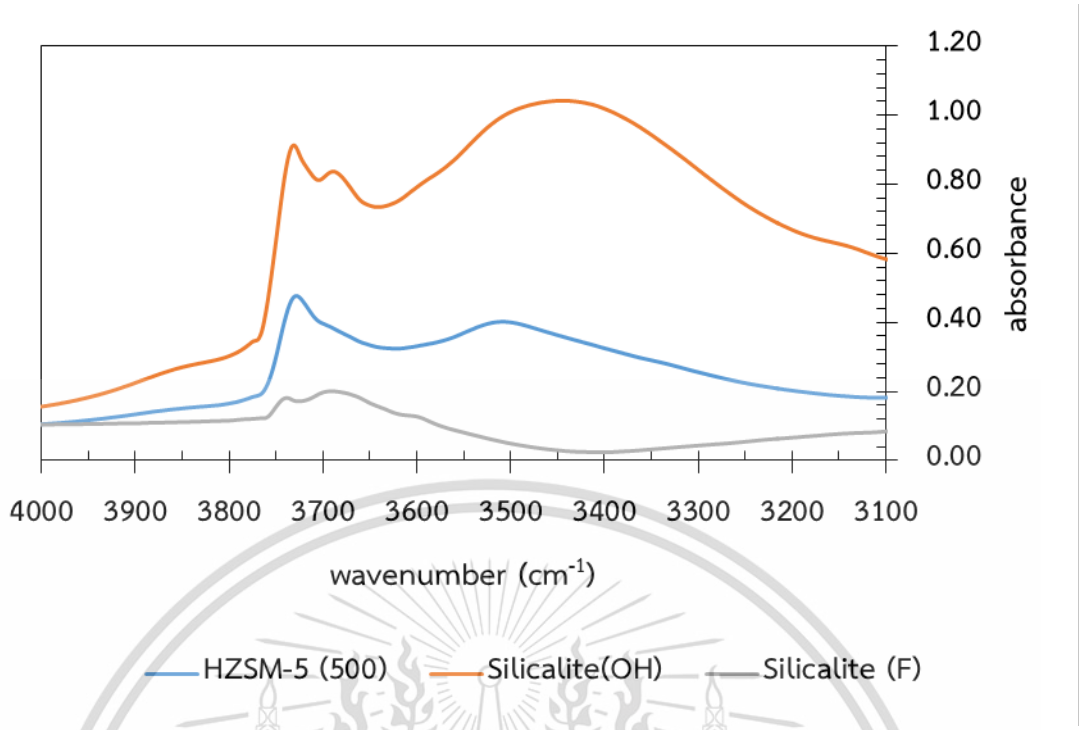

Figure 4.4 *In situ* FTIR spectra of MFI structure under N_2 flow 30 mL/min at 300 °C

As seen from the IR spectra, the relatively less intensity of the bands at 3740 cm^{-1} (isolated external silanol), 3725 cm^{-1} (internal silanol), and 3700-3650 cm^{-1} (internal silanol nests) is observed for Silicalite (F) indicating small amount of silanol. While, these bands are notably pronounced for HZSM-5 (500) and Silicalite (OH). Moreover, the observed peak at 3200-3600 cm^{-1}, which is the vibration of perturbed OH from H_2O, is in the same trend with the amount of silanol. As Silicalite (F) contains relatively less silanol, the incorporated Ga tends to agglomerate providing lower dispersion over Silicalite (F), as compared with HZSM-5 (500). In support with this view, SEM-EDX (**Figure 4.5**) shows the agglomeration and lower dispersion of Ga in Silicalite (F), as compared to HZSM-5 (500).

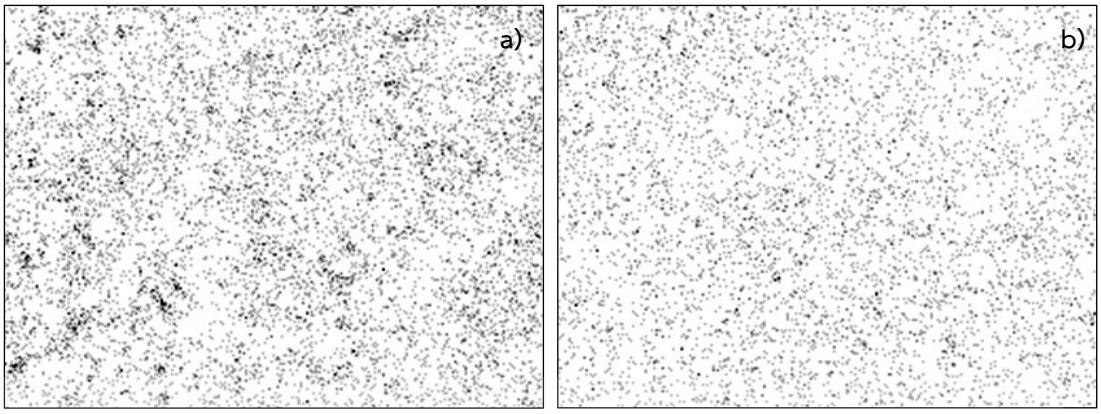

Figure 4.5 SEM-EDX of a) 3%.Ga-Silicalite (F) and b) 3%.Ga-HZSM-5 (500); the dark spots represent an atomic Ga.

Considering for Ga supported SiO_2 (Davisil) (**Figure 4.3g**), a broad H_2-consumption peak at high temperature (0.42 mmol/g) was noticed. This leads to suggestion that the large particle size of Ga_2O_3 is presented in this sample. Despite that SiO_2 (Davisil) possesses exceedingly high surface silanol, the poor Ga dispersion is obtained. Therefore, it seem that both the silanol numbers and the structure confinement are crucial factors for Ga dispersion.

As the %Ga loading is increased from 2%, 3%, 4%.Ga-HZSM5 (500) (**Figure 4.3 a-c**), the H_2 consumption are enhanced (**Table 4.2, entry 1-3**). Interestingly, the reduction temperature peak II is decreased along with increase gallium content (875, 843, and 807 °C, respectively). This could be contributed to the gallium agglomeration of the extra-framework Ga at high Ga loading, as reported by Shao [49].

4.2 Catalytic ethane dehydrogenation

4.2.1 The ability of gallium as an active site

The activity of 2%.Ga-HZSM-5 (28) for ethane dehydrogenation at 650 °C was compared to that of the parent support, as shown in **Figure 4.6**.

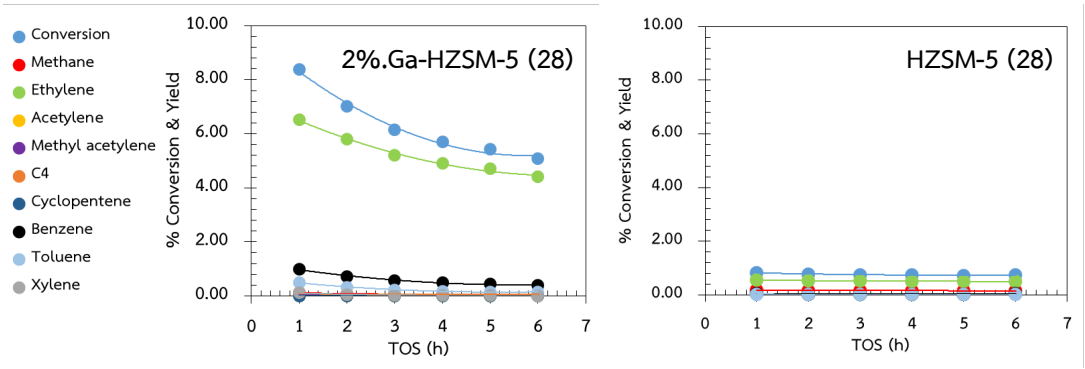

Figure 4.6 Ethane dehydrogenation over a) 2%.Ga-HZSM-5 (28) and b) HZSM-5 (28), (Reaction conditions: temperature = 650 °C, catalyst weight = 0.2 g, W/F = 4 g.h.mol^{-1}, Co-feed (ethane: helium) rate = 1: 2.75 mL/min (total feed = 75 mL/min). Catalyst was activated under a flow of air (30 mL/min) at 450 °C for 1 h with a heating rate of 2 °C/min and reduced under a flow of H_2 (50 mL/min) at 900 °C for 3 h with a heating rate of 10 °C/min.)

It can be seen that when gallium is loaded, the conversion (8.39%) and all products are significantly improved as shown in **Figure 4.6a**, especially for ethylene major product (6.52%). In addition to methane, methyl acetylene, benzene, and toluene other products including acetylene, C4, cyclopentene, and xylene were observed. This clearly indicates that the gallium supported on HZSM-5 (28) can especially facilitate the dehydrogenation (C-H activation) [50]. Although, high selectivity of ethylene was observed, BTX were also produced presumably due to the result of high acidity (4.24 mmol/g) (**Table 4.1, entry 5**) that significantly promoted side reaction, including aromatization, cyclization, and oligomerization [50]. Moreover, the deactivation can be observed. This could be contributed to the coke formation on the catalyst which suppress the feed accessibility to the active site, as seen by the observed decrease in BET and pore volume of the spent catalyst in **Table 4.3**, **entry 2**.

Table 4.3 Textural parameters of fresh and spent 2%.Ga-HZSM-5 (28) catalyst for ethane dehydrogenation.

Entry	Catalyst	S_{BET} (m^2/g)	Micropore volume (μL/g)
1	Fresh of 2%Ga-HZSM-5 (28)	383	195
2	Spent of 2%Ga-HZSM-5 (28)	292	158

In line with this view, TGA of the spent catalyst shows a marked weight loss at (400-600 °C), corresponding to the decomposition of coke deposit [51]. While, the weight loss below 150 °C is represent water desorption and the weight loss at (200–390 °C) indicates desorption of light hydrocarbon as shown in **Figure 4.7**.

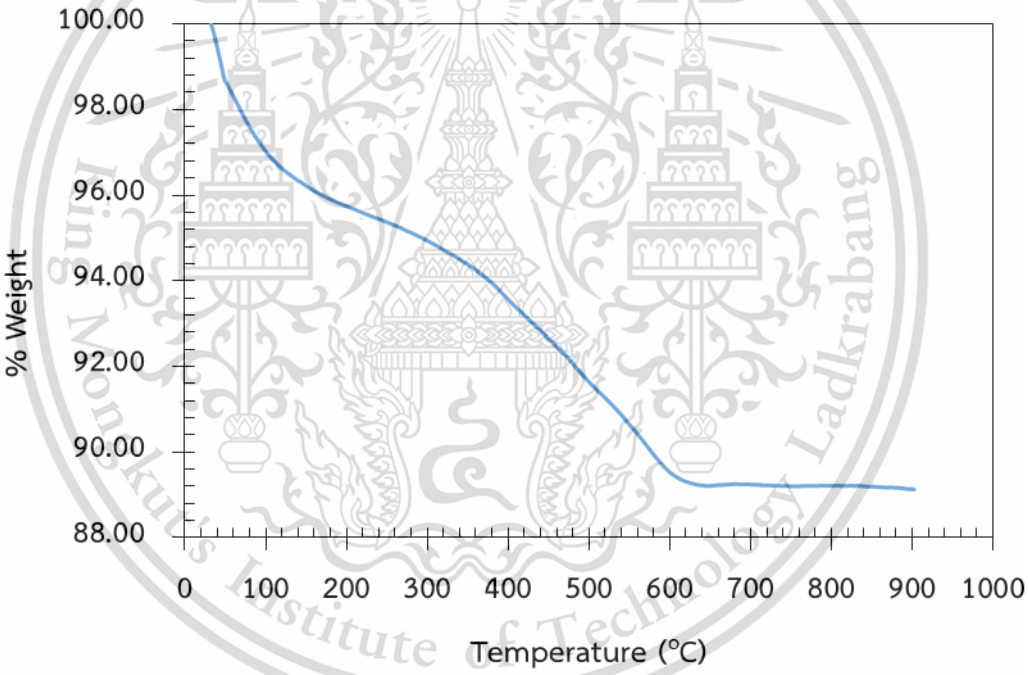

Figure 4.7 TGA profiles of 2%.Ga-HZSM-5 (28) after ethane dehydrogenation reaction. (TGA analysis under Air ZERO)

It can be concluded at this state that the side reaction and severe deactivation are promoted by high acidity of the catalyst. Therefore, the acidity of the catalyst is further investigated to improve the ethylene selectivity and stability.

4.2.2 Effect of Si/Al

The effect of acidity was investigated using catalyst with different Si/Al ratio, but with the same Ga loading. The results are depicted in **Figure 4.8**.

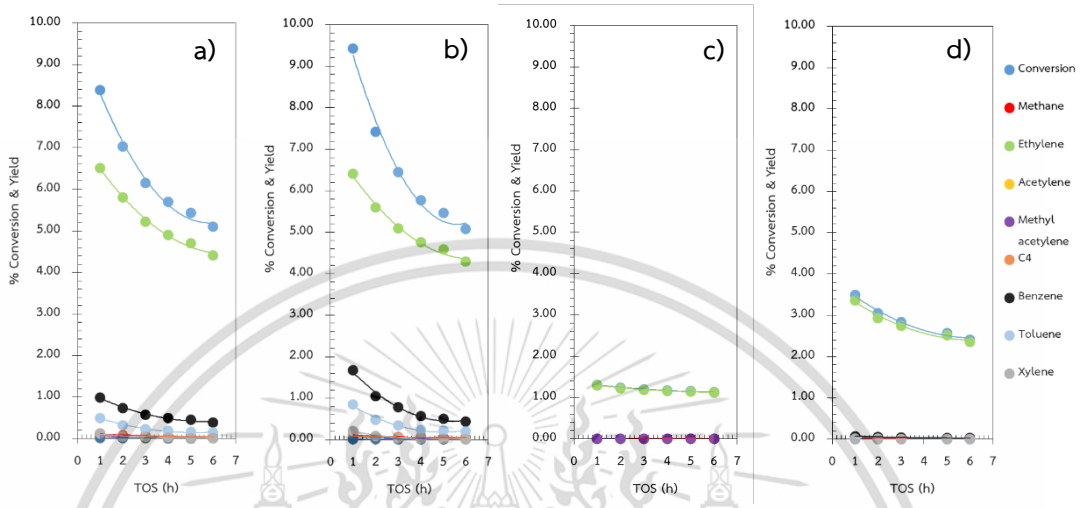

Figure 4.8 Ethane dehydrogenation over a) 2%.Ga-HZSM-5 (28), b) 2%.Ga-HZSM-5 (40), c) 2%.Ga-HZSM-5 (250) and d) 2%.Ga-HZSM-5 (500) (Reaction conditions: temperature = 650 °C, catalyst weight = 0.2 g, W/F = 4 g.h.mol^{-1}, Co-feed (ethane : helium) rate = 1 : 2.75 mL/min (total feed = 75 mL/min). Catalyst was activated under a flow of air (30 mL/min) at 450 °C for 1 h with a heating rate of 2 °C/min and reduced under a flow of H_2 (50 mL/min) at 900 °C for 3 h with a heating rate of 10 °C/min.)

As the acidity is decreased from Si/Al ratio 28 to 40, the similar activity and product distribution are still observed with severe deactivation (**Figure 4.8a and 4.8b**). It is because high number of acid site still remain in 2%.Ga-HZSM-5 (40) (1.11 mmol/g) (**Table 4.1, entry 6**). In order to eliminate of Brønsted acid site, the catalyst with Si/Al ratio 250 and 500 were tested. It can be seen that the conversions over 2%.Ga-HZSM-5 (250) and 2%.Ga-HZSM-5 (500) (1.3% and 3.5%) are significantly dropped, as compared to 2%.Ga-HZSM-5 (40) (9.4%). Nevertheless, these catalysts provide high ethylene selectivity (99%) and stability. It is because these catalysts possess relatively low acidity (0.38 and 0.56 mmol/g) (**Table 4.1, entry 7 and 8**). Therefore, the observed activity in the absence of the Brønsted acid site would be derived from the extra-framework Ga species that especially promoted ethane dehydrogenation. In different

manner, the observed high activity, when acid site is present (2%.Ga-HZSM-5 (28) and 2%.Ga-HZSM-5 (40)), is a result of synergistic effect between the exchangeable Ga species with the Brønsted acid, as reported in literature [48]. Despite high activity, such synergistic activity (Ga/H^+) promoted side reactions that lead to lower stability.

When Si/Al ratio is increased from 250 to 500, the ethane activity is interestingly enhanced from 1.3% to 3.5%. This is presumably due to the increase in the extra-framework Ga. For the similar Ga loaded HZSM-5 with different Si/Al ratio, the incorporated Ga would be primarily interacted with the Brønsted acid site forming the exchangeable Ga species. The excess gallium could interact with internal silanols forming extra-framework Ga species. Therefore, as the Si/Al ratio is increased from 250 to 500, exchangeable site would be decreased, while the extra-framework Ga species would be increased. The selective ethane dehydrogenation is also enhanced.

4.2.3 Effect of extra-framework Ga loading

Upon the increase of gallium loading on HZSM-5 (500) from 2% – 4%, the conversion is increased as shown in **Figure 4.9**.

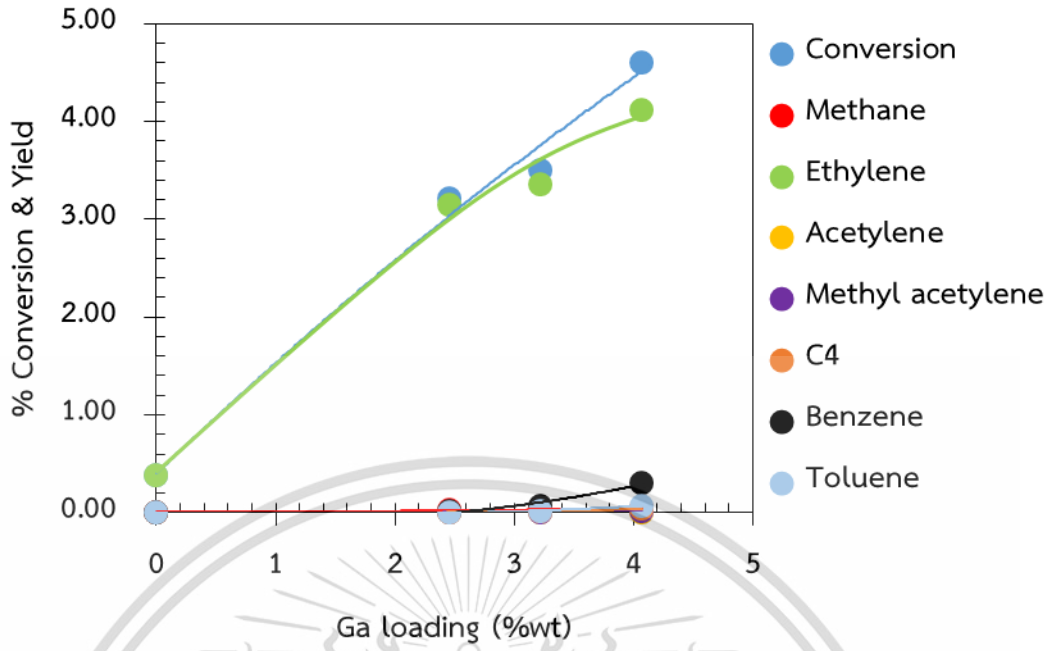

Figure 4.9 Ethane conversion and product yield with different Ga loading (x) over HZSM-5 (500), where x is 2%., 3%., and 4.%. (Reaction conditions: temperature = 650 °C, catalyst weight = 0.2 g, W/F = 4 g.h.mol^{-1}, Co-feed (ethane: helium) rate = 1: 2.75 mL/min (total feed = 75 mL/min). Catalyst was activated under a flow of air (30 mL/min) at 450 °C for 1 h with a heating rate of 2 °C/min and reduced under a flow of H_2 (50 mL/min) at 900 °C for 3 h with a heating rate of 10 °C/min.)

This is because as Ga loading is increased, the extra-framework that is an active site for ethane dehydrogenation is also increased. Accordingly, high selectivity of ethylene are observed for all Ga loading. Small amount of C4, benzene, and toluene are produced at the high Ga loading (4%). This is because the increase in ethylene concentration promoted secondary reactions including, oligomerization and aromatization. In support with this view, a lower ethylene selectivity was observed at high contact time (**Figure 4.10**).

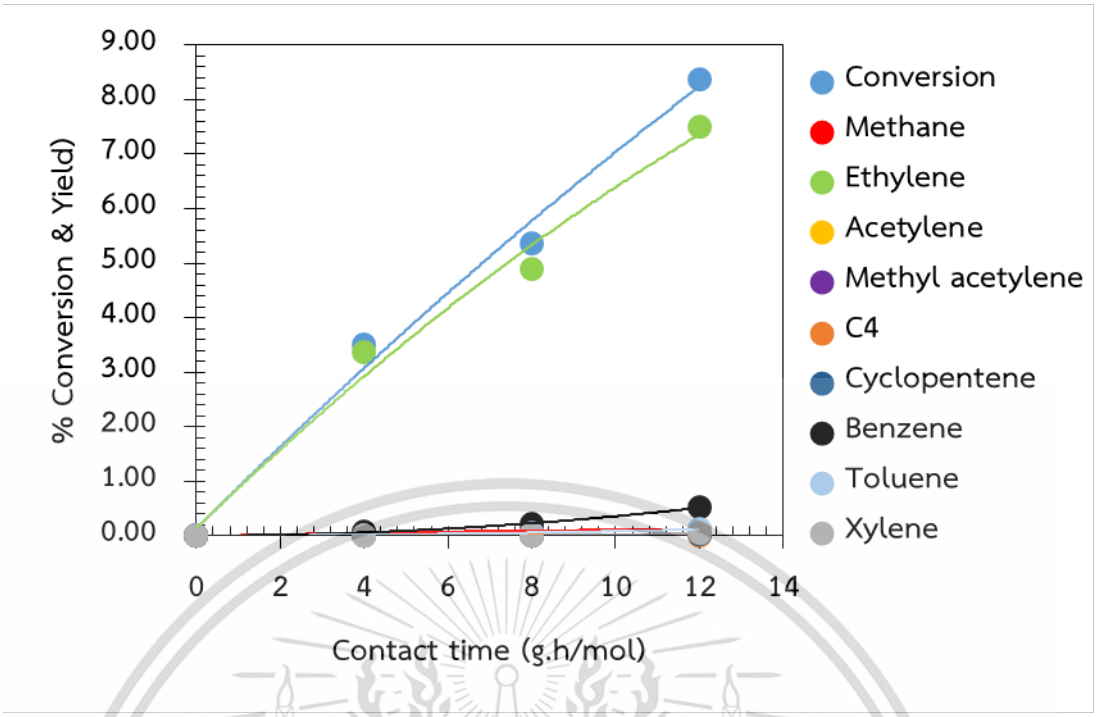

Figure 4.10 Ethane conversion and products yield during different contact times using 3%.Ga-HZSM-5 (500). (Reaction conditions: temperature = 650 °C, Co-feed (ethane: helium) rate = 1: 2.75 mL/min (total feed = 75 mL/min). Catalyst was activated under a flow of air (30 mL/min) at 450 °C for 1 h with a heating rate of 2 °C/min and reduced under a flow of H_2 (50 mL/min) at 900 °C for 3 h with a heating rate of 10 °C/min.)

It can be seen that the C4 and BTX products are produced at higher conversion indicating that the increased conversion, and hence ethylene concentration, promotes the secondary reactions.

4.2.4 The investigation nature of the extra-framework Ga species

To investigate nature of the extra-framework Ga species, the oxidition state of Ga in the 3%Ga-HZSM-5 (500) was primarily determined by *in situ* XANES. The XANES spectrum of 3%.Ga-HZSM-5 (500) is depicted in **Figure 4.11**, as compared with α-Ga_2O_3.

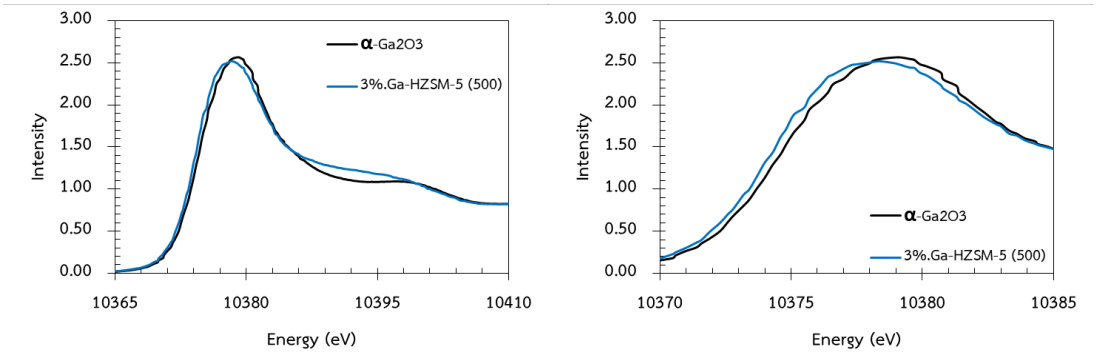

Figure 4.11 *In situ* XANES spectra of α-Ga_2O_3 (black) and 3%.Ga-HZSM-5 (500) (blue), before treatment a) normally range (10365-10410 eV) and b) zoom range (10370-10385 eV)

It can be seen that K-edge energy of 3%.Ga-HZSM-5 (500) (10374.30 eV) is similar to that of the α-Ga_2O_3 (10374.60 eV) suggesting that the extra-framework Ga possesses oxidation state of 3+. The standard α-Ga_2O_3 shows the white line at 10379 eV representing gallium in octahedral environment as reported in literatures [52,53]. In the different manner, gallium (III) species in 3%wt.Ga-HZSM-5 (500) shows the white line at 10378 eV indicating that the gallium is presented in tetrahedral coordination [52,54]. It was suggested that the shift of 1 eV to the lower energies and the spectral shape are consistent with the change of Ga coordination from 6 to 4 [55]. This suggests that the extra-framework gallium species is not formed as bulk α-Ga_2O_3, but could be presented as highly dispersed tetrahedral Ga oxide species.

When the 3%Ga-HZSM-5 (500) was heated under pure O_2 from 50-450 °C, the gallium edge energy and the white line position remain the same, as shown in **Figure 4.12**.

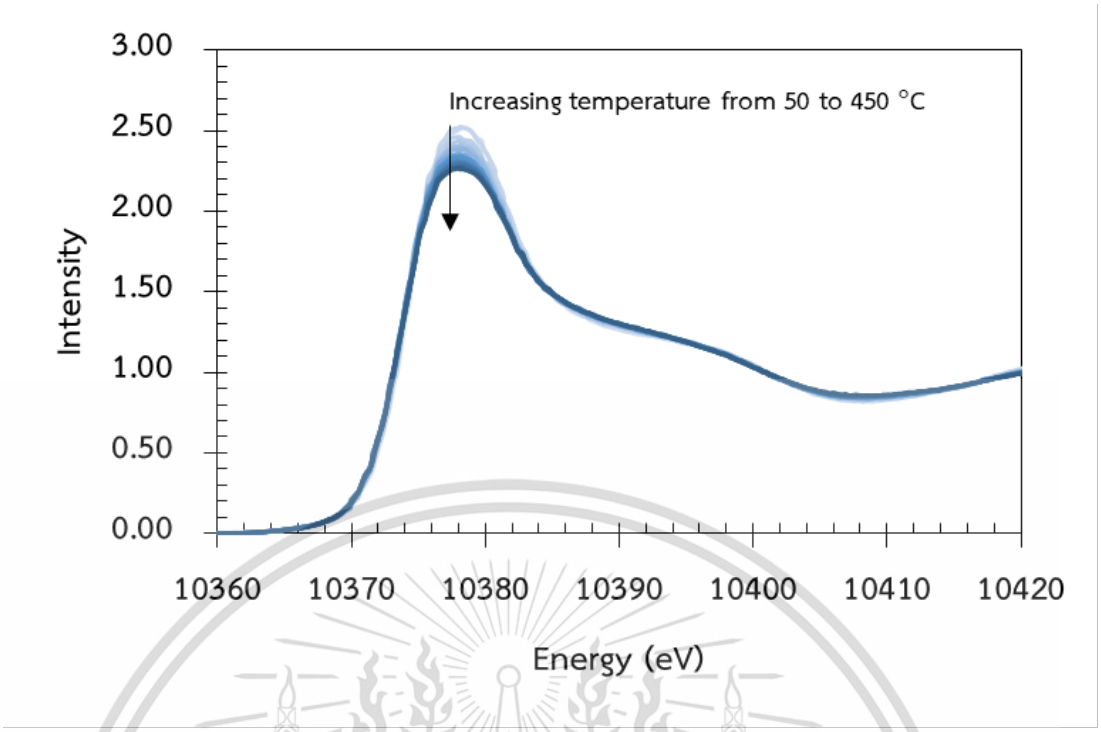

Figure 4.12 *In situ* XANES spectra of 3%.Ga-HZSM-5 (500) under a flow of O_2 (30 mL/min) at 50-450 °C with a heating rate of 2 °C/min.

However, the white line intensity was dropped upon increasing temperature, presumably due to the desorption of coordinated water from the tetrahedral Ga oxide species. This result supports that the extra-framework Ga is highly dispersed.

To validate the coordination of highly-dispersed extra-framework Ga species, the *in situ* EXAFS of 3%.Ga-HZSM-5 (500) is performed and compared with the standard α-Ga_2O_3 oxide. The results are shown in **Figure 4.13**.

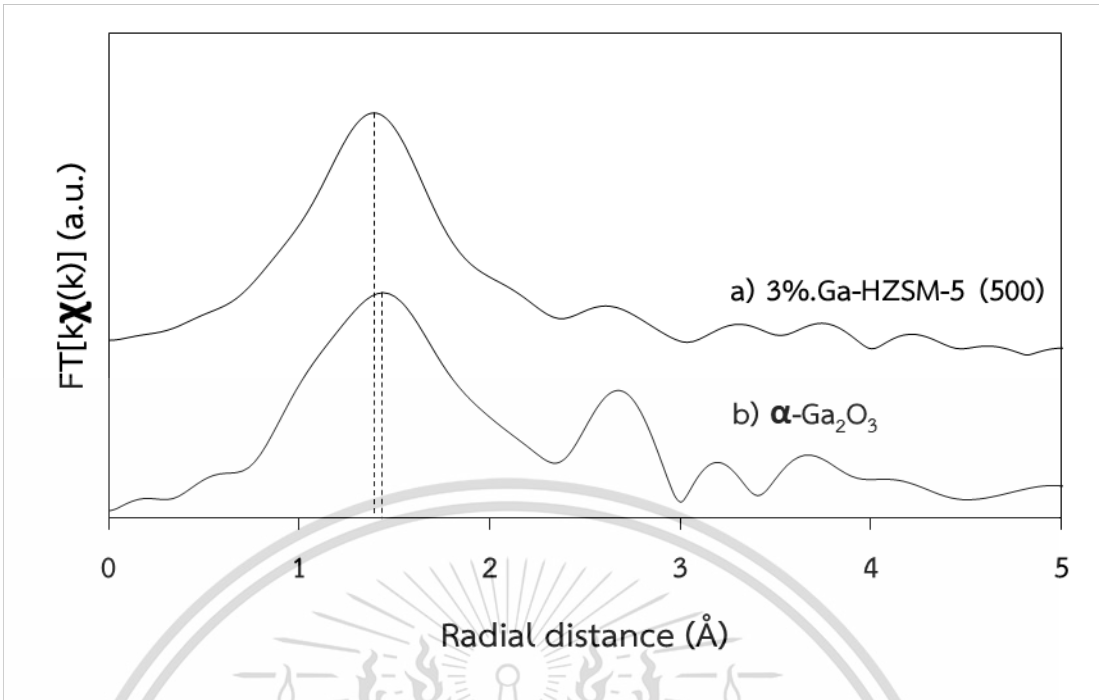

Figure 4.13 Magnitudes of k-weighted Fourier-transformed Ga K-edge in-situ EXAFS spectra of 3%.Ga-HZSM-5 (500) measured at 450 °C under 30 mL/min of O_2 and α-Ga_2O_3 measured at ambient temperature.

As seen from **Figure 4.13**, EXAFS spectra of both 3%.Ga-HZSM-5 (500) and α-Ga_2O_3 show the dominant feature between 1.0-2.0 Å (1^{st} shell) in R-space, corresponding to the backscattering from O atom of Ga-O bond. However, the peak position of 3%.Ga-HZSM-5 (500) shifts to a lower distance, as compared with α-Ga_2O_3, indicating that the coordination number and Ga-O bond length are different. The EXAFS fitting of the first coordination shell was performed using $CaGa_2O_4$ as a model for 3%.Ga-HZSM-5 (500) and standard α-Ga_2O_3 as a model for itself. The result is shown in **Figure 4.14**.

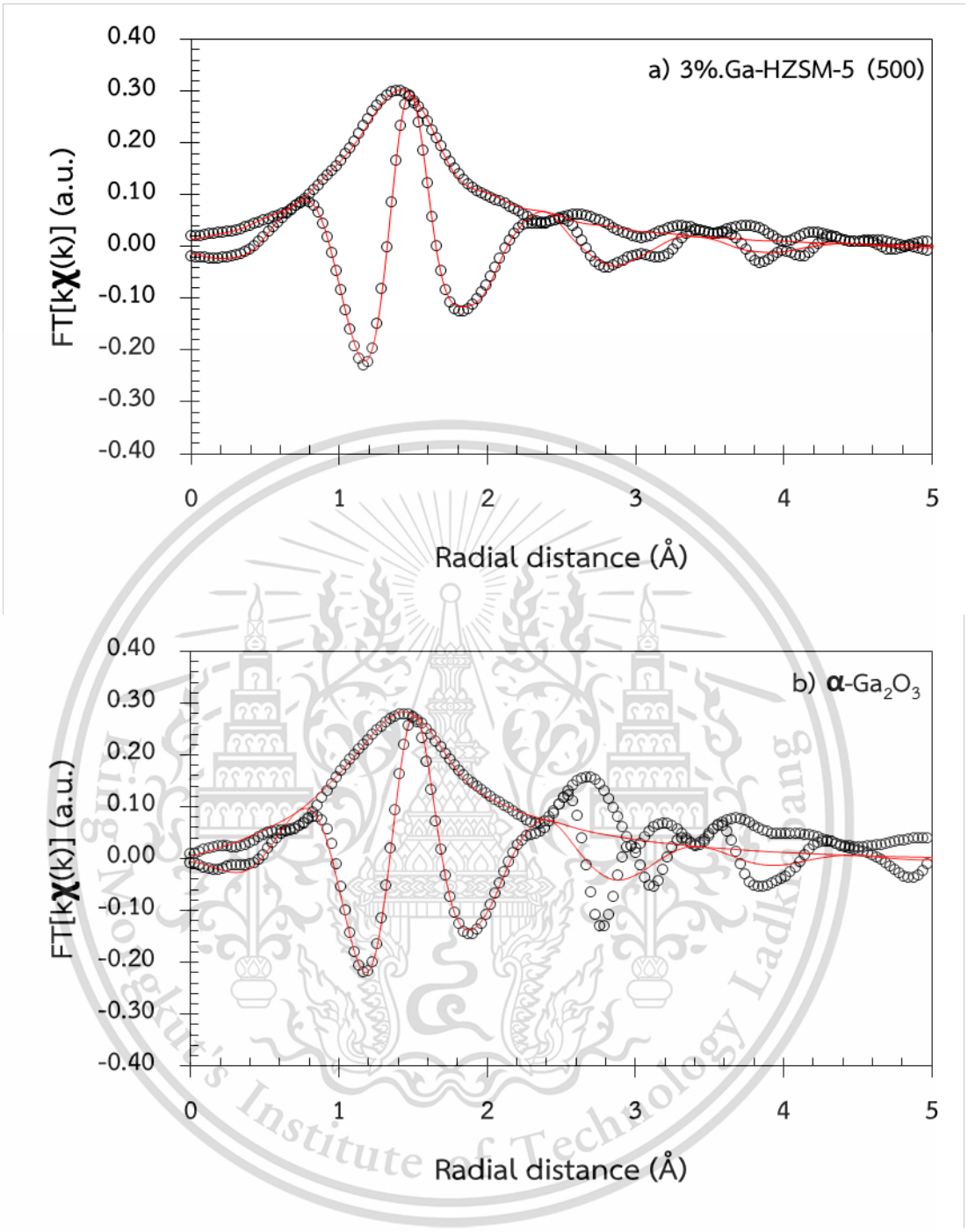

Figure 4.14 Magnitudes and imaginary parts of k-weighted Fourier-transformed fitting Ga K-edge in-situ EXAFS spectra of a) 3%.Ga/HZSM-5 (500) measured at 450 °C under 30 mL/min of O_2 [a] and b) α-Ga_2O_3 [b] measured at ambient temperature. (Noted: dotted line is a raw data and solid line is a fitting) ([a] Fit was performed using $CaGa_2O_4$ as a model structure and [b] it was performed using α-Ga_2O_3 as a model structure)

It can be seen that the satisfactory fits of the spectra was obtained for both samples as evidenced by the close agreement between the solid lines and dotted lines for the first coordination shell. Fitting parameters of 3%.Ga-HZSM-5 (500) and α-Ga_2O_3 are summarized in **Table 4.4**.

Table 4.4 Fitted coordination numbers, interatomic distances, Debye-Waller Factors, energy shift parameters, and R-factor values for fits to Fourier-transformed of 3%.Ga-HZSM-5 (500) samples at 450 °C under flowing pure O_2[a] and α-Ga_2O_3[b] measured at ambient temperature.

Sample	Path	N	S_0^2	σ^2	ΔE_0 (eV)	R (Å)	R-factor
3%.Ga-HZSM-5 (500)	Ga-O	4.000	1.000	0.00752	6.507	1.8662	0.004
α-Ga_2O_3 standard	Ga-O	6.000		0.01409	4.187	1.9166	0.025

[a] Fit was performed using $CaGa_2O_4$ as a model structure and [b] it was performed using α-Ga_2O_3 as a model structure Fit EXAFS spectra, obtained after normalization and background subtraction, were k-weighted; a Hanning window function was applied between k = 3–11 $Å^{-1}$, and fitted coordination were performed from R = 1–2.1 Å.

These results suggest that the extra-framework Ga species in 3%.Ga-HZSM-5 (500) is coordinated to four O-atoms at an interaction distance of 1.87 Å. While, Ga species in α-Ga_2O_3 shows the coordination number of six O-atoms at an interaction distance of 1.92 Å. In support manner, Rodrigues *et al.* [50] reported that the Ga-O bond length of tetrahedral and octahedral site is presented between 1.83-1.86 Å and 1.93-2.07 Å, respectively. This observation confirms that the Ga in 3%.Ga-HZSM-5 (500) is presented in tetrahedral coordination while Ga in α-Ga_2O_3 is presented in octahedral coordination which is corresponding to *in situ* XANES.

Moreover, the 2nd coordination shell (the peak at 2.8 Å corresponded to the backscattering from next-neighboring Ga atoms in the Ga–O–Ga lattice), is absent in 3%.Ga-HZSM-5 (500). While, this peak is clearly pronounced in α-Ga_2O_3**.** To further obtain the more detail for the second coordination shell of extra-framework Ga species

in Ga-HZSM-5 (500), Wavelet transform function of k^2-weighted *in situ* EXAFS was applied using HAMA software. The contour plot presenting the relation between wavenumber space (k-space) and radial space (R-space) are shown in **Figure 4.15**.

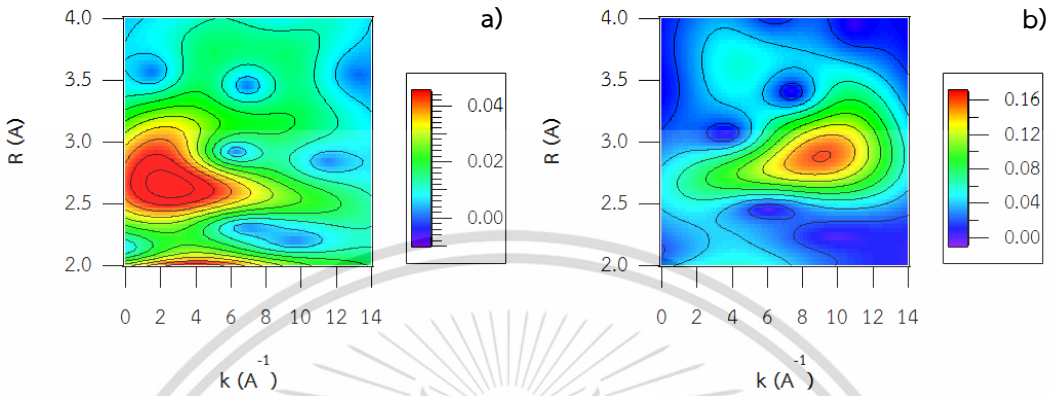

Figure 4.15 Wavelet transforms of the second coordination shell of k^2-weighted Ga K-edge EXAFs spectra measured at 450 °C under 20% O_2 atmosphere: a) 3%.Ga-HZSM-5 (500) and b) α-Ga_2O_3, the data was computed on HAMA software using Morlet function with **κσ** = 15

As seen from **Figure 4.15a**, the 3%.Ga-HZSM-5 (500) shows the feature associated in the second coordination shell with wavelet coordinates (R-space = 2.6-3.0 Å and k-space = 2.0-8.0 $Å^{-1}$). Bell *et al.* [54] reported that the wavelet signal, at 2.5 Å in R-space and 3.0-8.0 $Å^{-1}$ in k-space, is represent backscattering from Ga-O-Al. However, the 3%.Ga-HZSM-5 (500) contain negligible amount of Al (0.29 %). Hence, the observed wavelet signal could be the backscattering from Si in the second coordination shell of Ga, i.e. (Ga-O-Si). In addition, this spectra shows the overlapping feature at R-space = 2.7-3.0 Å and k-space = 7.0-13.0 $Å^{-1}$ that is a result of backscattering from Ga-O-Ga [50].

In contrast, α-Ga_2O_3 (**Figure 4.15b**) shows only wavelet signal at 2.7 Å in R-space and 7.0-13.0 $Å^{-1}$ in k-space that is ascribed to the Ga-O-Ga scattering path. These different in k value for the observed backscattering amplitudes (values of *k*) depends on the atomic number of the atom at the second coordination shell of Ga. In other

words, atom with high atomic numbers give *k*-values higher than that with low atomic numbers [56].

According to XANES and EXAFS data, it is clear that no bulk Ga_2O_3 species is presented in 3%.Ga-HZSM-5 (500). While, the extra-framework Ga species is highly dispersed in tetrahedral environment, presumably with in the silica network, with an oxidation state of 3+. Together with the observed overlapping feature of Ga-O-Ga, it is likely that the dimeric Ga oxide as proposed by Hensen [57] (**Scheme 4.1**) could be the extra-framework Ga species present in 3%.Ga-HZSM-5 (500).

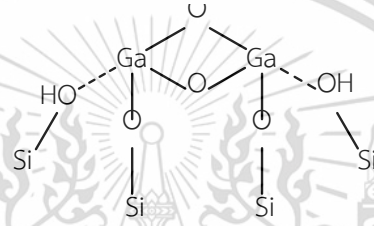

Scheme 4.1 Feature of dimeric extra-framework Ga oxide

The presence of dimeric Ga oxide is also supported by H_2-TPR and *in situ* XANES as shown in **Figure 4.16** and **Figure 4.17**, respectively.

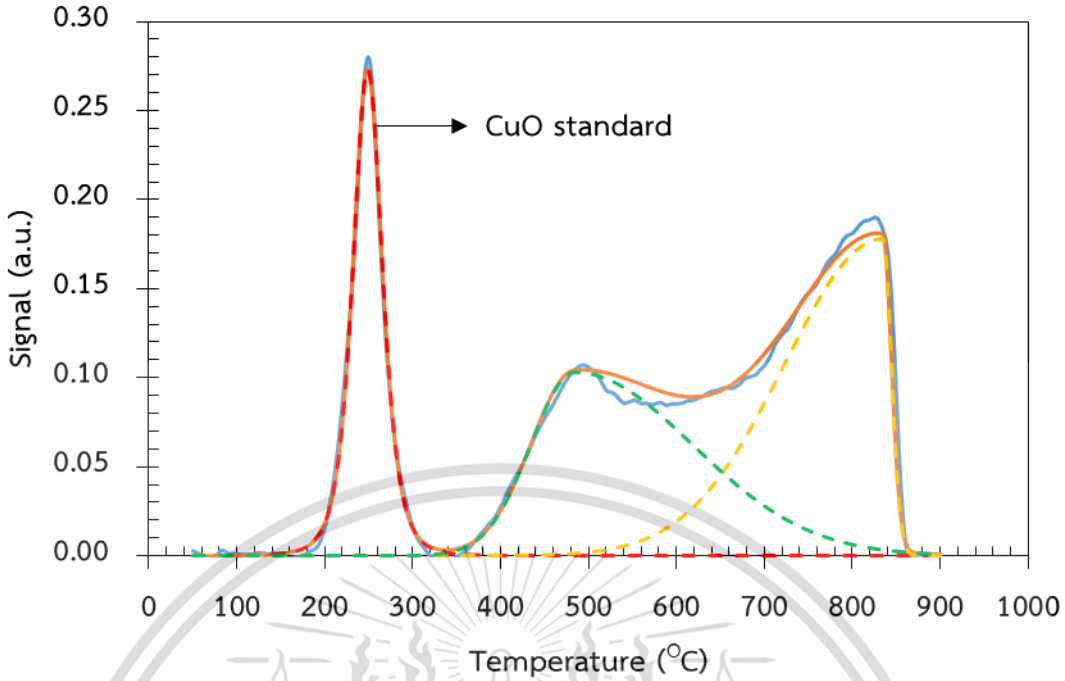

Figure 4.16 H_2-TPR of 3.22%.Ga-HZSM-5 (500) + CuO standard under a flow of 10% H_2/Ar (30 mL/min) at 50-900 °C with a heating rate of 10 °C/min. Noted CuO is internal standard, reduced at 190-300 °C in the perfect symmetry peak as a normal CuO.

It can be seen from **Figure 4.16** that the reduction of the extra-framework Ga oxide species take place at 500 and 832 °C with the hydrogen consumption of 1:1 mol ratio of H_2:Ga (**Table 4.2**). While, the reduction of Ga^{3+} to Ga^{1+} generally involve single step as the formation of Ga^{2+} is not allowed. Therefore, the observed two successive H_2-consumtion could be derived from the consecutive reduction of the dimeric Ga oxide species as proposed in **Scheme 4.2**.

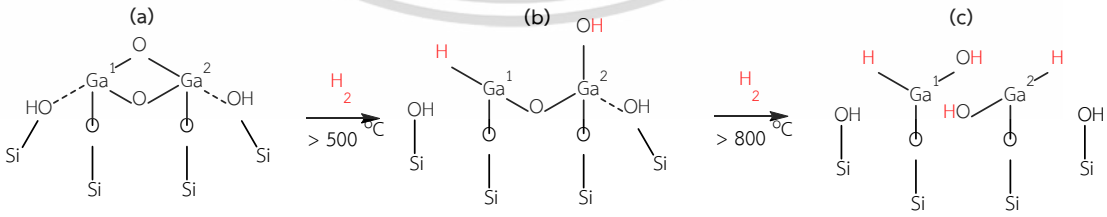

Scheme 4.2 Reduction pattern of dimeric extra-framework gallium oxide

In the support manner, the *in situ* XANES of 3%.Ga-HZSM-5 (500) also shows two steps of edge energy shifts of ~1.5 eV (from 10374.30 to 10372.40 eV) at 750 °C and another ~1.5 eV (from 10372.40 to 10370.6 eV) at 900 °C (**Figure 4.17)**.

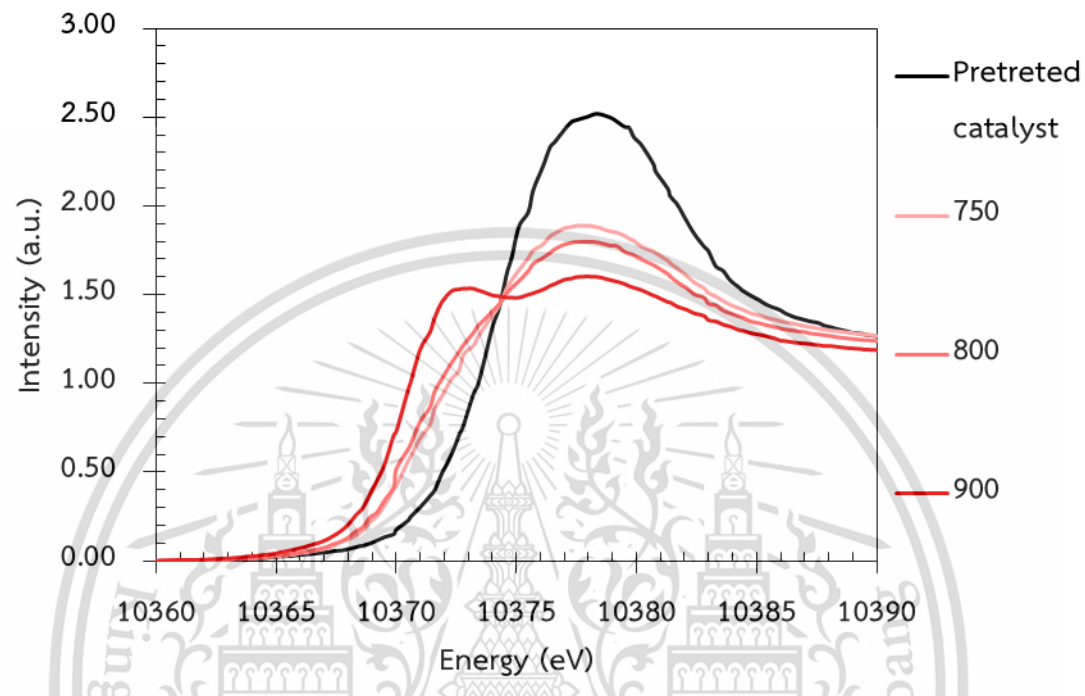

Figure 4.17 Normalized Ga K-edge XANEs for 3%.Ga-HZSM-5 (500), collected at various temperature under mixed N_2 (30 mL/min) + H_2 (15 mL/min).

These shifts indicate the change of Ga coordination, as suggested by Getsoian *et al.* [58] that the edge energy shift of ~1.5 eV is due to the modification of Ga coordination either by (case (i)) replacing O ligand in a 4-coordinate Ga^{3+} with a less electronegative, more strongly **σ**-donating H (hydride) ligand or (case (ii)) a decrease in the coordination number from 4 to 3 around the Ga species. Accordingly, It is suggested that the energy shift at 500-750 °C (~1.5 eV) is a result of the reduction of dimeric Ga oxide species as seen in H_2-TPR. Upon reduction, the surface siloxyl of Ga^1 would be replaced by H (hydride) (case (i)). While, Ga^2-OH species would be formed. Accordingly, the Ga^1 coordination number is decreased from 4 to 3, forming partial reduced Ga species as shown in **Scheme 4.2b** (case (ii)). While, edge energy of the Ga^2 would remain the same. Thus, the average edge energy shift of Ga in dimeric Ga oxide (Ga^1

and Ga^2) for the first reduction (400 °C – 700 °C) is 1.5 eV in total. As the temperature increases to 900 °C, the consecutive reduction take place forming two hydrido hydroxyl Ga species (**Scheme 4.2c**). This results in a decrease coordination number of Ga^2 with hydride as a ligand (case (i) and case (ii)). Hence, another edge shift of 1.5 eV was observed in the *in situ* XANES. However, the reduced form of dimeric Ga species (**Scheme 4.2c**) is somewhat unstable. This is deducted from the observed edge energy shift upon cooled down in N_2 (**Figure 4.18**).

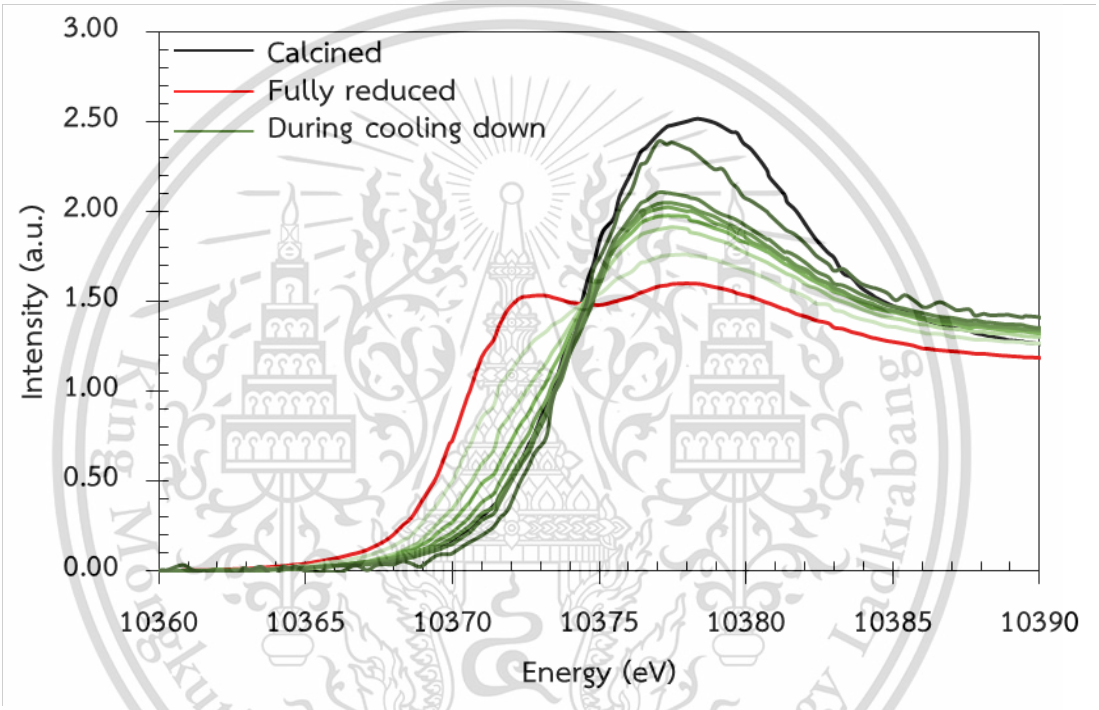

Figure 4.18 Normalized Ga K-edge XANEs for 3%.Ga-HZSM-5 (500), collected at various temperature under switching flows 30 mL/min O_2, mixed 30 mL/min N_2+15 mL/min H_2 and 30 mL/min N_2.

It can be seen that the edge energy after reduced at 900 °C (10370.6 eV) shift back to the original value (10374.3) when H_2 flow is withdrawn. This result suggests that the two hydrido hydroxyl Ga species (**Scheme 4.2c**) decompose to the dimeric Ga species (**Scheme 4.2a**) in the absence of H_2 as shown in **Scheme 4.3**.

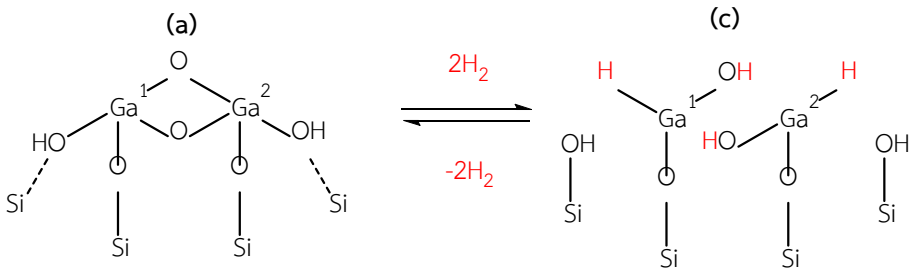

Scheme 4.3 Virtual equilibrium of dimeric extra-framework gallium oxide

In other words, the dimeric Ga oxide (**Scheme 4.2a**) and two hydrido hydroxyl Ga species (**Scheme 4.2c**) are in virtual equilibrium under H_2 partial pressure.

In order to verify the existence of virtual equilibrium between these species, the ethane dehydrogenation reactions under the different H_2 partial pressure, are examined as shown in **Figure 4.19**.

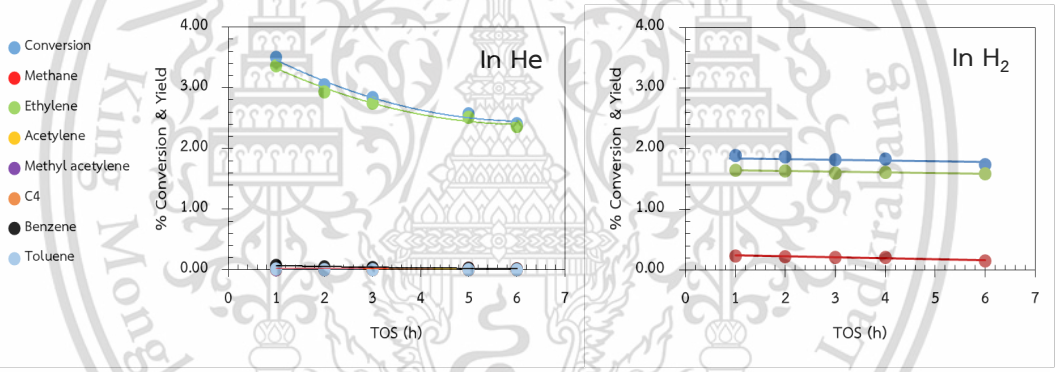

Figure 4.19 Ethane dehydrogenation reaction carry out under a) He and b) H_2 (Reaction conditions: temperature = 650 °C, catalyst weight = 0.2 g, W/F = 4 g.h.mol^{-1}, Co-feed (ethane: carrier gas) rate = 1: 2.75 mL/min (total feed = 75 mL/min). Catalyst was activated under a flow of air (30 mL/min) at 450 °C for 1 h with a heating rate of 2 °C/min and reduced under a flow of H_2 (50 mL/min) at 900 °C for 3 h with a heating rate of 10 °C/min.)

It can be seen that the ethane conversion and ethylene selectivity is decreased in the presence of H_2 gas (**Figure 4.19b**). While, methane is significantly produced (over 10 times) under H_2. This observed decrease in activity suggests that the dimeric Ga oxide (**Scheme 4.2a**), that is an active for ethane dehydrogenation, is reduced to the

two hydrido hydroxyl Ga species (**Scheme 4.2c**) that is not an active for ethane dehydrogenation. This is because the C-H dissociation would not be readily promoted over the reduced Ga species with hydride ligand. In turn, such hydride Ga species would facilitate the hydrogenolysis of ethane. In line with this view, the higher yield of methane was observed in the reaction under H_2 carrier.

According to the observed activity in different H_2 partial pressure, ethane dehydrogenation would be promoted over the dimeric Ga oxide as proposed in **Scheme 4.4**.

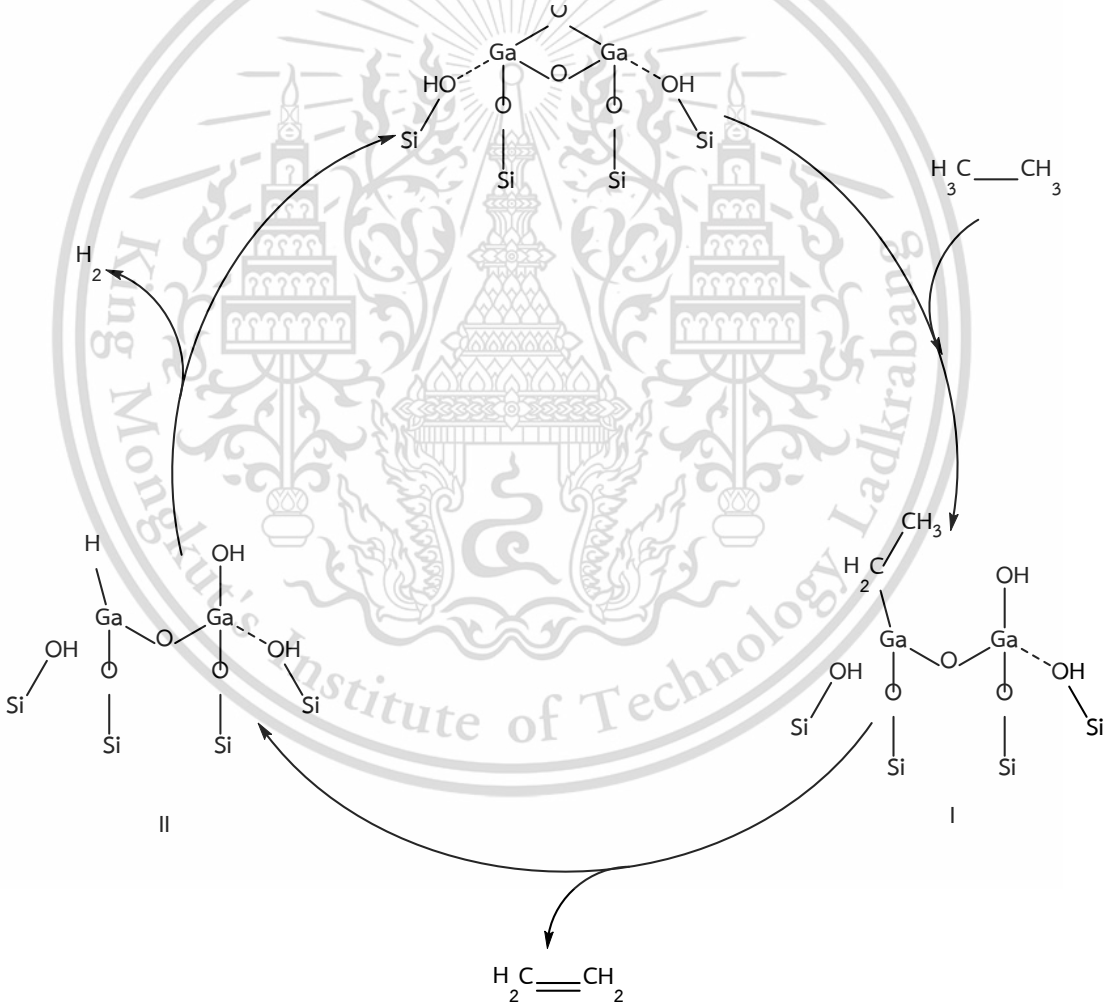

Scheme 4.4 Reaction mechanism of dimeric Ga oxide on ethane dehydrogenation reaction.

It is proposed that the heterolytic C-H cleavage takes place over one of the dimeric Ga oxide species [59], generating gallium hydroxyl ethylidene intermediate (I). The dehydrogenation is suggested to proceed via decomposition of the ethylidene to ethylene, bearing partially reduced dimeric gallium species (II), in a manner similar to that observed by H_2-TPR (**Scheme 4.2b**). Such partially reduced Ga species can be readily decomposed to dimeric Ga oxide via reductive H_2 elimination, as observed by *in situ* XANES (**Figure 4.18**). While, in the presence of H_2, the two hydrido hydroxyl Ga species is formed and would promote only ethane hydrogenolysis, as proposed in **Scheme 4.5**.

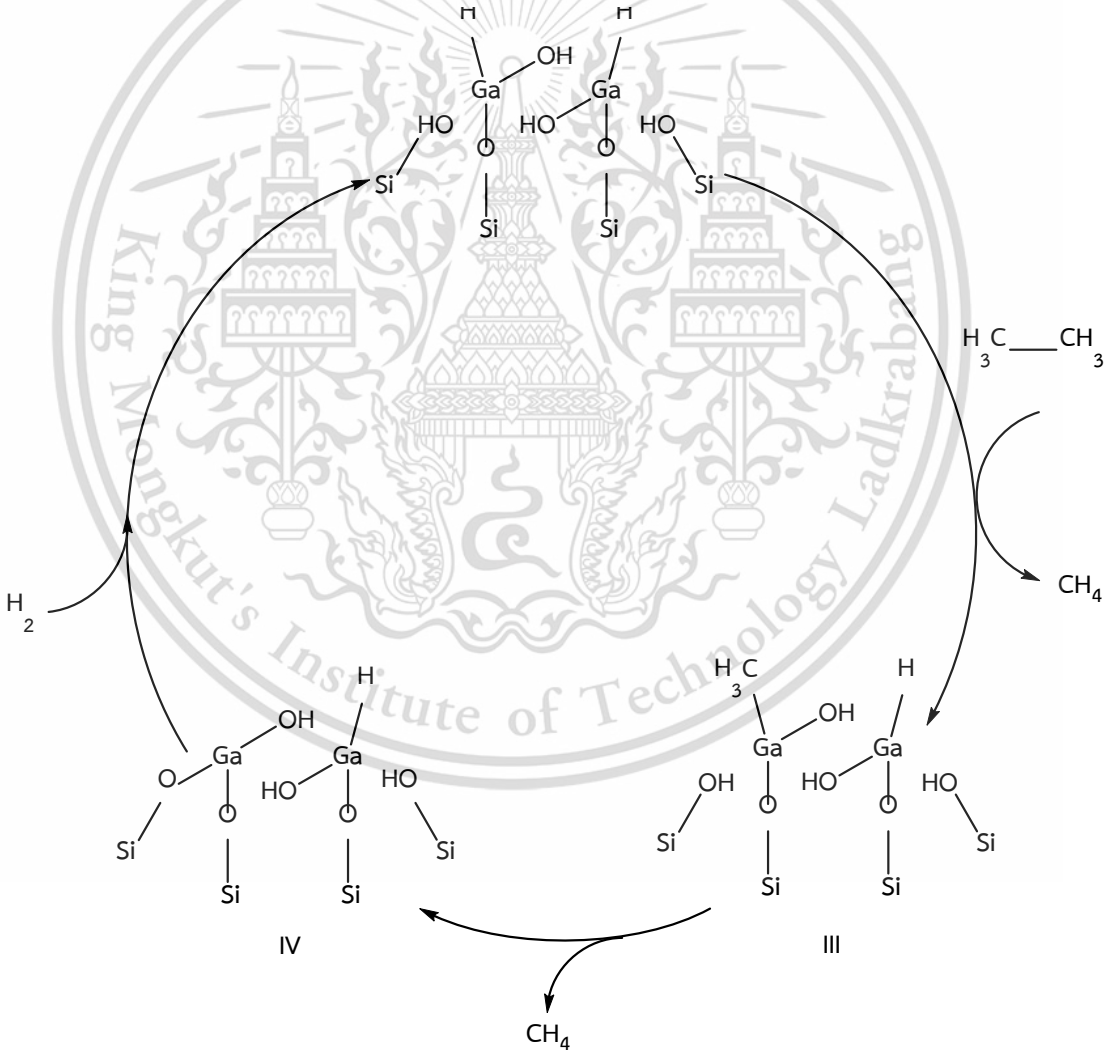

Scheme 4.5 Reaction mechanism of two hydrido hydroxyl Ga species on ethane hydrogenolysis reaction.

It is proposed that the heterolytic C-C cleavage take place over two hydrido hydroxyl Ga species, generating Ga hydroxyl methylidene intermediate (III) and methane. Such methylidene intermediate can be decomposed to another methane and the partially reduced Ga species intermediate (IV) that can be further reduced under H_2 to complete the cycle.

4.2.5 Effect of OH functional surface and Structure confinement

Accordingly to the nature of active species proposed previously (section 4.2.4), concentration and geometrical environment of the surface silanol would play significant role for the dispersion of the extra-framework dimeric Ga species. Therefore, ethane dehydrogenation was studied using Ga incorperated on various supports including, HZSM-5 (500), Silicalite (OH), Silicalite (OH(550)), Silicalite (F), and SiO_2 (Davisil). The result was tabulated in **Table 4.5**.

Table 4.5 OH and confinement factors on the ethane dehydrogenation.

Catalysts	%Conversion	% Yield							% Selectivity of ethylene
		Methane	Ethylene	Acetylene	Methyl acetylene	C4	Benzene	Toluene	
Ga-Silicalite (OH)	5.23	0.04	4.87	0.01	0.01	0.04	0.24	0.02	93.12
Ga-Silicalite (OH (550))	3.37	0.03	3.16	0.01	-	0.01	0.12	0.02	93.77
Ga-HZSM-5(500)	3.50	0.03	3.36	0.01	0.01	0.01	0.07	0.02	96.00
Ga-Silicalite (F)	0.52	0.01	0.51	-	-	-	-	-	98.08
Ga-SiO_2 (Davisil)	0.90	0.01	0.89	-	-	-	-	-	98.89

(Reaction conditions: temperature = 650 °C, catalyst weight = 0.2 g, W/F = 4 g.h.mol^{-1}, Co-feed (ethane: helium) rate = 1: 2.75 mL/min (total feed = 75 mL/min). Catalyst was activated under a flow of air (30 mL/min) at 450 °C for 1 h with a heating rate of 2 °C/min and reduced under a flow of H_2 (50 mL/min) at 650 °C for 3 h with a heating rate of 10 °C/min.)

It can be seen that ethane conversion over Ga supported Silicalite (OH) which possesses high concentration of silanol (as seen by *in situ* FTIR, **Figure 4.4**) gives the relatively high conversion (5.23%). When this support was calcined at 550 °C, the conversion is slightly decreased (3.37%) presumably due to a decrease in silanol groups via the surface dehydroxylation upon the calcination. A similar amount of surface silanol can also be expected for Ga-HZSM-5 (500), as it is calcined at the same temperature. Hence, the conversion of 3%.Ga-HZSM-5 (500) is somewhat similar to 3%.Ga-Silicalite (OH(550)). This is presumably because high Ga dispersion can be obtained from the catalysts with high silanol concentration on the surface as dicussed in previous section (4.1.3) In line with this view, 3%.Ga-Silicalite (F) that possesses small amount of silanol numbers (**Figure 4.4**), and hence low Ga dispersion, give the relatively low conversion (0.52%). The conversion as a function of silanol concentration (intensity of silanol peaks at 3740, 3725, and 3700-3650 cm^{-1}) is shown in **Figure 4.20**.

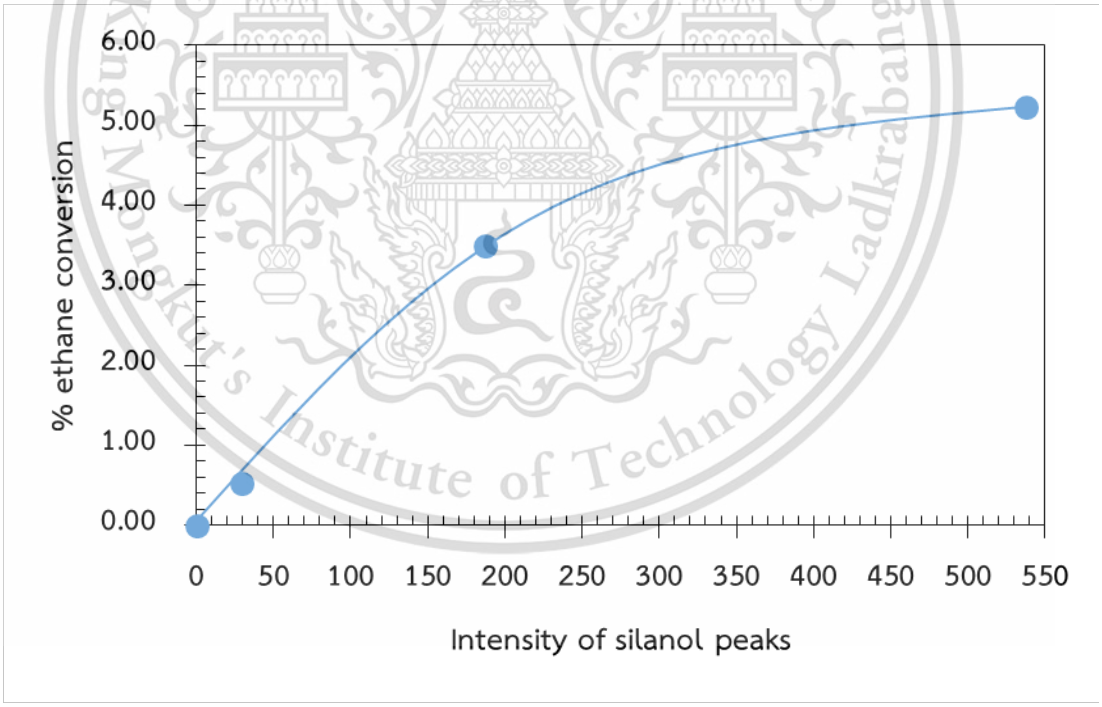

Figure 4.20 Relation between number of silanol vs. ethane conversion (%)

Not only the number of surface silanol, but the structure confinement of the support also affects the Ga dispersion. This is deducted from the observed low activity of Ga-SiO_2 (Davisil) (0.90%) despite that it possesses exceedingly high surface silanol.

The fact that the SiO_2 (Davisil) has no the structure confinement, lead to the formation of closely proximity Ga species on the surface, when $Ga(NO_3)_3$ was impregnated. Upon calcination the Ga can be agglomerated to large particle of Ga_2O_3 which provide relatively low activity.

Moreover, the surface silanol and structure confinement affect to the stability of the incorporated Ga as seen by the decrease in the intensity of edge energy upon reduction under H_2+N_2 (1:2) at 900 °C for 3 h (**Figure 4.21**).

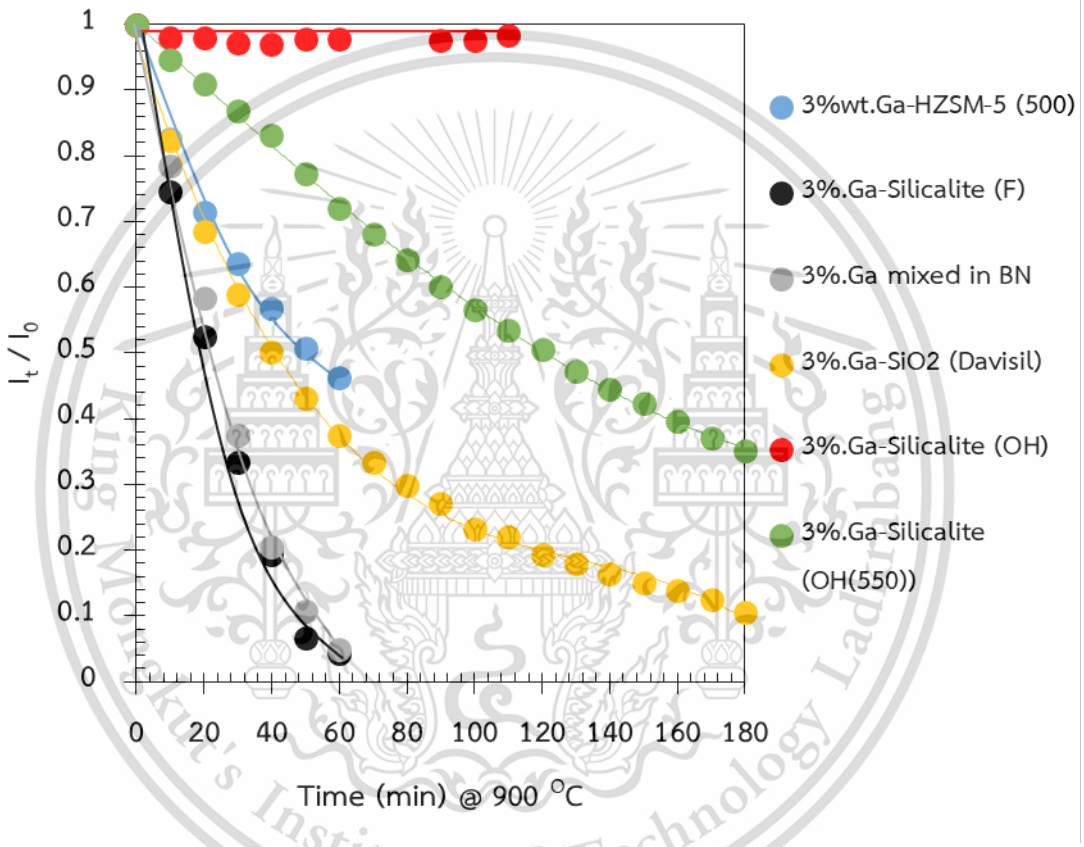

Figure 4.21 I_t / I_0 of the edge energy *vs* Time (min) from In-situ XANES spectra of all catalysts under H_2+N_2 (1:2) at 900 °C for 3 h. (I_t / I_0 of the edge energy is represented to the Ga remaining in the catalysts under reductive gas at 900 °C over time)

When the incorporated Ga is reduced at 900 °C, Ga_2O may well be formed and then sublimated from the catalyst surface [60]. This can be monitored by the change in the relative intensity of the Ga edge energy (I_t/I_0) over time. The observed relative intensity implies the concentration of Ga species remained on the catalyst.

It can be seen that the relative intensity for 3%.Ga-Silicalite (OH), that possesses structure confinement with high concentration of silanol, remains unchanged. When this support was calcined at 550 °C (Silicalite (OH(550)) and also for HZSM-5 (500)), the relatively intensity is decreased over time, as a result of Ga sublimation. This suggested that stability of Ga species in the Silicalite (OH(550)) and HZSM-5 (500) support is low, presumably due to a decrease in silanol groups. With this analogy, the relative intensity for 3%.Ga-Silicalite (F), that possesses negligible amount of silanol numbers, is rapidly decreased with time. In supporting manner, SEM-EDX (**Table 4.6**) shows that the incorporated Ga is remained after reduction of 3%.Ga-HZSM-5 (500) at 900 °C for 60 min, while no Ga was observed in 3%.Ga-Silicalite (F) after reduction in *in situ* XANES.

Table 4.6 The number of Ga loading (%wt.) before and after XANES experimental.

Catalysts	Number of silanol (count)	Ga loading (%wt.) Before XANES experimental	Ga loading (%wt.) After XANES experimental
Ga-HZSM-5 (500)	186.83	3.13%.	1.11%.
Ga-Silicalite (F)	29.57	3.59%.	N/D

In addition to the silanol groups, the structure confinement seem to strongly affect the stability of Ga catalyst. This is seen from the rapid decrease in relative intensity of 3%.Ga-SiO_2 (Davisil), that no structure confinement, as compared with 3%.Ga-Silicalite (OH). This observation are presumably because the structure confinement makes the silanol groups serve as ligand to dimeric Ga oxide providing the reasonable stability as in solid solution.

It can be concluded at this state that the number of silanol and structure confinement are crucial factor for the Ga dispersion and stability.

CHAPTER 5
CONCLUSIONS AND SUGGESTIONS

5.1 Conclusions

In this thesis, the ethane dehydrogenation over gallium loaded supports including HZSM-5 with various Si/Al ratio (28, 40, 250 and 500) and SiO_2 (Devicil, Silicalite (OH), Silicalite (OH(550)), Silicalite (F)) catalysts were investigated. All catalysts are referred to high surface area materials (310-450 m^2/g) with expected metal loading about 2%-4%. as evidenced by ICP-MS and XRF. The acidity is increased by incorporated Ga as Lewis acid. The structure deterioration and phase change of the supports were not found after Ga loaded. Moreover, bulk Ga_2O_3 is not observed in XRD pattern due to the incorporated Ga was possessed in high dispersed gallium oxide. According to H_2-TPR result, the catalyst with surface silanol and structure confinement provide high Ga dispersion. Moreover, the highly Ga dispersed is formed on the extra-framework Ga species.

The high activity was obtained after Ga incorporated with HZSM-5 (28) and HZSM-5 (40) due to the Ga can especially facilitate the dehydrogenation (C-H activation). However, BTX is highly produced and the severe deactivation can be observed, as the high acidity. When acidity is significantly decreased, the high ethylene selectivity and stability is increased. Therefore, the observed high activity and severe deactivation, when acid presence (3%.Ga-HZSM-5 (28) and 3%.Ga-HZSM-5 (40)), is a result of synergistic effect between the exchangeable Ga species and the Brønsted acid site that promoted the side reaction. In contrast, the observed high selectivity (99%) and stability, when acid absence (3%.Ga-HZSM-5 (250) and 3%.Ga-HZSM-5 (500)), is derived from the extra-framework Ga species, as an active species for ethane dehydrogenation. In addition, the conversion is also enhanced with the increase of the extra-framework Ga species. Nevertheless, small amount of BTX and low ethylene selectivity is observed in high Ga loading. It is because the ethylene concentration is increased promoting secondary reactions including, oligomerization and aromatization.

The extra-framework Ga species is highly dispersed in tetrahedral environment with oxidation state of 3+. Together with the observed overlapping feature of Ga-O-Ga in Morlet wavelet transform, it is likely that the dimeric Ga oxide $[Ga_2O_2]^{2+}$ could be the extra-framework Ga species. The dimeric Ga oxide $[Ga_2O_2]^{2+}$ species, that is an active site for ethane dehydrogenation, can be reduced to two hydrido hydroxyl Ga species $[HGaOH]^{+}$ at 900 ^{o}C ,that facilitates for ethane hydrogenolysis. The deviation between $[Ga_2O_2]^{2+}$ and $[HGaOH]^{+}$ species is controlled by H_2 partial pressure. At low H_2 partial pressure, the dimeric Ga oxide species $[Ga_2O_2]^{2+}$ is predominant, while the two hydrido hydroxyl Ga species $[HGaOH]^{+}$ is favorable at high H_2 partial pressure. With different support, the extra-framework Ga oxide shows the different activity. The observed high activity is an effect of the high Ga dispersion which is the consequence of the surface silanol abundance and structure confinement. Moreover, the Ga stability is also improved.

5.2 Suggestions

1. The reduction of dimeric Ga oxide species should be further studied using deuterium labeling method in order to verify the actual mechanism.

2. To improve the thermodynamics of the dehydrogenation reaction, highly selective oxidation of the H_2 produced might be a possible way.

References

[1] F. Cavani, N. Ballarini, and A. Cericola. 2007. **"Oxidative dehydrogenation of ethane and propane: How far from commercial implementation."** *Catalysis Today.,* 127: 113-131**.**

[2] R. S. Vincent, R. P. Lindstedt, N. A. Malik, I. A. B. Reid, and B. E. Messenger. 2008. **"The chemistry of ethane dehydrogenation over a supported platinum catalyst."** *Journal of Catalysis.,* 260: 37-64.

[3] J. J. H. B. Sattler, J. Ruiz-Martinez, E. Santillan-Jimenez, and B. M. Weckhuysen. 2014. **"Catalytic Dehydrogenation of Light Alkanes on Metals and Metal Oxides."** *Chemical reviews.,* 114: 10613–10653.

[4] "https://en.wikipedia.org/wiki/Ethylene," [Online].

[5] "http://www.eia.gov/dnav/pet/hist/LeafHandler.ashx?n=PET&s=METFPUS1&f=A," [Online].

[6] Y. Cheng, H. Gong, C. Miao, W. Hua, Y. Yue, and Z. Gao. 2015. **"Ga_2O_3/HSSZ-13 for dehydrogenation of ethane: Effect of pore geometry of support."** *Catalysis Communications*., 71: 42–45.

[7] Z. Shen, J. Liu, H. Xu, Y. Yue, W. Hua, and W. Shen. 2009. **"Dehydrogen.ation of ethane to ethylene over a highly efficient Ga_2O_3/HZSM-5 catalyst in the presence of CO_2."** *Applied Catalysis A: General.,* 356: 148–153.

[8] Y. Cheng, C.Miao, W. Hua, Yi. Yue, and Z. Gao. 2017. **"Cr/ZSM-5 for ethane dehydrogenation: Enhanced catalytic activity through surface silanol."** *Applied Catalysis A: General*., 532: 111–119.

[9] A. Ausavasukhi and T. Sooknoi. 2014. **"Tunable activity of [Ga]HZSM-5 with H_2 treatment: ethane dehydrogenation."** *Catalysis Communications.,* 45: 63-68.

[10] Z. Wu, Evan C. Wegener, H. Tseng, J. R. Gallagher, J. W. Harris, R. E. Diaz, Y. Ren, F. H. Ribeiroa, and J. T. Miller. 2016. **"Pd–In intermetallic alloy nanoparticles: Highly selective ethane dehydrogenation catalysts."** *Catalysis Science and Technology*., 6: 6965.

[11] E. C. Wegenera , Z. Wua , H. Tsenga , J. R. Gallagherb , Y. Renc , R. E. Diazd , F. H. Ribeiroa , and J. T. Miller. 2018. **"Structure and reactivity of Pt–In intermetallic alloy nanoparticles: Highly selective catalysts for ethane dehydrogenation."** *Catalysis Today.,* 299: 146–153.

[12] K. Nakagawa, M. Okamura, N. Ikenaga, T. Suzuki and T. Kobayashi. 1998. **"Dehydrogenation of ethane over gallium oxide in the presence of carbon dioxide."** *Chemical Communications.,* 1025-1026.

[13] C. Shao, W. Lang, X. Yan and Y. Guo. 2017. **"Catalytic performance of gallium oxide based catalysts for the propane dehydrogenation reaction: Effects of support and loading amount."** *RSC Adv.,* 7: 4710.

[14] "https://en.wikipedia.org/wiki/Ethane," [Online].

[15] "https://www.britannica.com/science/ethane," [Online].

[16] "https://www.icis.com/resources/news/2007/11/05/9075777/ethylene-uses-and-market-data," [Online].

[17] "https://en.wikipedia.org/wiki/Petrochemical," [Online]

[18] "http://cpmaindia.com/ethylene_about.php," [Online].

[19] "https://en.wikipedia.org/wiki/Dehydrogenation," [Online].

[20] B. M. Weckhuysen and R. A. Schoonheydt. 1999. **"Alkane dehydrogenation over supported chromium oxide catalysts."** *Catalysis Today.,* 51: 223-232.

[21] B. Fu, J. Lu, P. C. Stair, G. Xiao, M. C. Kung, and H. H. Kung. 2013. **"Oxidative dehydrogenation of ethane over alumina-supported Pd catalysts. Effect of alumina overlayer."** *Journal of Catalysis.,* 297: 289–295.

[22] "http://www.explainthatstuff.com/zeolites.html," [Online].

[23] P. A. Jacobs, E. M. Flanigen, J. C. Jansen and H. V. Bekkum. 2001. **"Introduction to zeolite science and practice 2nd edition."** The Netherlands: Elsevier : Amsterdam

[24] P. Ploynisa, K. Supanat and S. Settawat. 2014. **"Conversion of ethanol to gasoline over metal transition loaded H-ZSM-5 zeolite catalysts."** Bachelor degree of science, Industrial Chemistry, Faculty of Science, King Mongkut's Institue of Tenchnology Ladkrabang.

[25] L. Sirinuch. 2008. **"Synthesis of zeolite beta as a support of metal supported catalysts for toluene hydrogenation and application of in situ XAS on catalysis characterization."** Nakhonratchasima: Suranaree University of Technology.

[26] P. J. Smeets, J. S. Woertink, B. F. Sels, E. I. Solomon and R. A. Schoonheydt. 2010. **"Transition-metal ions in zeolites: Coordination and activation of oxygen."** *Inorganic Chemistry.,* 49: 3573-3583.

[27] P. J. Grobet, W. J. Mortier, E. F. Vansant and G. Schulz-Ekloff. 1988. **"Innovation in zeolite materials science 1st edition."** The Netherlands: Elsevier : Amsterdam

[28] C. Novara, A. Alfayate, G. Berlier, S. Maurelli and M. Chiesa. 2013. **"The interaction of H_2O_2 with TiAlPO-5 molecular sieves: probing the catalytic potential of framework substituted Ti ions."** *Physical Chemistry Chemical Physics.,* 15: 11099-11105.

[29] J. N. Armor. 1998. **"Metal-exchanged zeolites as catalysts."** *Microporous and Mesoporous Materials.,* 22: 451-456.

[30] Y. Li and J. N. Armor. 1992. **"Catalytic reduction of nitrogen oxides with methane in the presence of excess oxygen."** *Applied Catalysis B: Environmental.,* 1: L31-L40.

[31] Y. Li and J. N. Armor. 1994. **"Catalytic combustion of methane over palladium exchanged zeolites."** *Applied Catalysis B.,* 3: 275-282.

[32] Y. Li and J. N. Armor. 1992. **"Catalytic decomposition of nitrous oxide on metal exchanged zeolites."** *Applied Catalysis B: Environmental.,* 1: L21-L29.

[33] "https://en.wikipedia.org/wiki/Gallium," [Online].

[34] "http://nautilus.fis.uc.pt/st2.5/scenes-e/elem/e03130.html," [Online].

[35] V. R. Choudhary, K. Mantri and C. Sivadinarayana. 2000. **"Influence of zeolite factors affecting zeolitic acidity on the propane aromatization activity and selectivity of Ga/H-ZSM-5."** *Micropourous and Mesoporous Meterials.,* 37: 1-8.

[36] J. H. B. Sattler, Javier Ruiz-Martinez, Eduardo Santillan-Jimenez, and Bert M. Weckhuysen. 2014. **"Catalytic Dehydrogenation of Light Alkanes on Metals and Metal Oxides."** *Chem. Rev.,* 114: 10613−10653.

[37] P. Sabatier. 2004. **"History of Chemistry and Chemical Technology."** *Russian journal of applied Chemistry.,* 77(11): 1909-1912.

[38] H. Dyrbeck., 2007. **"Selective Catalytic Oxidation of Hydrogen and Oxygen-assisted Conversion of Propane."** Norwegain University of Science and Technology. 194.

[39] N. S. Gnep, J. Y. Doyemet, A. M. Seco, F. R. Ribeiro, and M. Guisnet**.** 1988. **"Conversion of light alkanes to aromatic hydrocarbons: II. Role of gallium species in propane transformation on GaZSM5 catalysts."** *Applied Catalysis*., 43: 155-166.

[40] B. Xu, B. Zheng, W. Hua, Y. Yue, and Z. Gao. 2006. **"Support effect in dehydrogenation of propane in the presence of CO_2 over supported gallium oxide catalysts."** *Journal of catalysis.,* 239: 470.

[41] I. Nowak, J. Quartararo, E. G. Derouane, and J. C. Védrinel. 2003. **"Effect of H_2–O_2 pre-treatments on the state of gallium in Ga/H-ZSM-5 propane aromatisation catalysts."** *Applied Catalysis A : General.,* 251: 107–120

[42] J. Wang, F. Zhang, W. Hua, Y. Yue, and Z. Gao. 2012. **"Dehydrogenation of propane over MWW-type zeolites supported gallium oxide."** *Catalysis Communications,* 18: 63-67.

[43] A. L. Petre, A. Auroux, P. Gélin, M. Caldararu, and N. Ilonescu. 2001. **"Acid–base properties of supported gallium oxide catalysts."** *Thermochimica Acta*, 379: 117-185.

[44] X. Zhao, L. Wei, J. Julson, Q. Qiao, A. Dubey, and G. Anderson. 2015. **"Catalytic cracking of non-edible sunflower oil over ZSM-5 for hydrocarbon bio-jet fuel."** *New Biotechnology,* 32(2): 300-312

[45] A. Ausavasukhi, and T. Sooknoi. 2009. **"Additional Brønsted acid sites in [Ga]HZSM-5 formed by the presence of water."** *Applied Catalysis A: General,* 361: 93-98.

[46] N. A. S. Amin, and D. D. Anggoro. 2003. **"Characterization and Activity of Cr, Cu and Ga Modified ZSM-5 for Direct Conversion of Methane to Liquid Hydrocarbons."** *Journal of Natural Gas Chemistry,* 12: 123-134.

[47] K. Trangwachirachai. 2018. **"Dehydrogenation of propane over gallium loaded H-ZSM-5 zeolite catalysts."** Master degree of science, Petrochemical, Faculty of Science, King Mongkut's Institue of Tenchnology Ladkrabang.

[48] C. Shao, W. Lang, X. Yan, and Y. Guo. 2017. **"Catalytic performance of gallium oxide based catalysts for the propane dehydrogenation reaction: effects of support and loading amount."** *Royal Society of Chemistry Advances,* 7: 4710-4723

[49] M. Saito, S. Watanabe, I. Takahara, M. Inaba, and K. Murata. 2003. **"Dehydrogenation of Propane over a Silica-Supported Gallium Oxide Catalyst."** *Catalysis Letters,* 89: 213-217

[50] V. O. Rodrigues, J. Eon, and A. C. Faro Jr. 2010. **"Correlations between Dispersion, Acidity, Reducibility, and Propane Aromatization Activity of Gallium Species Supported on HZSM5 Zeolites."** *Journal of Physical Chemistry C,* 114(10): 4557-4567.

[51] J. Shi, J. Guan, D. Guo, J. Zhang, L.J. France, L. Wang, and X. Li. 2016. **"Nitrogen Chemistry and Coke Transformation of FCC Coked Catalyst during the Regeneration Process."** *Scientific Reports,* 6(1): 27309.

[52] G. S. Pokrovski, J. Schott, J. Hazemann, F. Farges, and O. S. Pokrovsky. 2002. **"An X-Ray Absorption Fine Structure and Nuclear Magnetic Resonance Spectroscopy Study of Gallium–silica Complexes in Aqueous Solution."** *Geochimica et Cosmochimica Acta,* 66: 4203–4222.

[53] M. Ju, X. Wang, W. Liang, Y. Zhao, and C. Li. 2014. **"Tuning the energy band-gap of crystalline gallium oxide to enhance photocatalytic water splitting: mixed-phase junctions."** *Journal of Material Chemistry A,* 2: 17005-17014.

[54] N. M. Phadke, J. Van der Mynsbrugge, E. Mansoor, A. Getsoian, M. Head-Gordon, and A. T. Bell. 2018. **"Characterization of Isolated Ga^{3+} Cations in Ga/H-MFI Prepared by Vapor-Phase Exchange of H-MFI Zeolite with $GaCl_3$."** *ACS Catalysis,* 8: 6106-6126.

[55] P. L. Higby, J. E. Shelby, J. C. Phillips, and A. D. Legrand. 1988. "EXAFS study of alkali gallosilicate glasses." *Journal of Non-Crystalline Solids*, 105: 139–148.

[56] B.K. Teo. 1986. **"Basic Principles and Data Analysis (Inorganic Chemistry Concepts) 9th edition."** Springer: New York.

[57] E. J. M. Hensen, E. A. Pidko, N. Rane, and R. A. Santen. 2007. **"Water-Promoted Hydrocarbon Activation Catalyzed by Binuclear Gallium Sites in ZSM-5 Zeolite."** *Angewandte Chemie,* 46: 7273-7276.

[58] A. B. Getsoian, U. Das, J. Camacho-Bunquin, G. Zhang, J. R. Gallagher, B. Hu, S. Cheah, J. A. Schaidle, D. A. Ruddy, J. E. Hensley, T. R. Krause, L. A. Curtiss, J. T. Miller, and A. S. Hock. 2016. **"Organometallic model complexes elucidate the active gallium species in alkane dehydrogenation catalysts based on ligand effects in Ga K-edge XANES."** *Catalysis Science & Technology,* 6: 6339-6353.

[59] E. A. Pidko, V. B. Kazansky, E. J. M. Hensen and R. A. Santen. 2006. **A comprehensive density functional theory study of ethane dehydrogenation over reduced extra-framework gallium species in ZSM-5 zeolite.** *Journal of Catalysis*, 240: 73-84.

[60] D. P. Butt, Y. Park, and T. N. Taylor. 1999. **"Thermal vaporization and deposition of gallium oxide in hydrogen."** *Journal of Nuclear Materials*, 264: 71-77

APPENDICES

Appendix A

CATALYSTS CHARACTERIZATION

A1: Gas adsorption

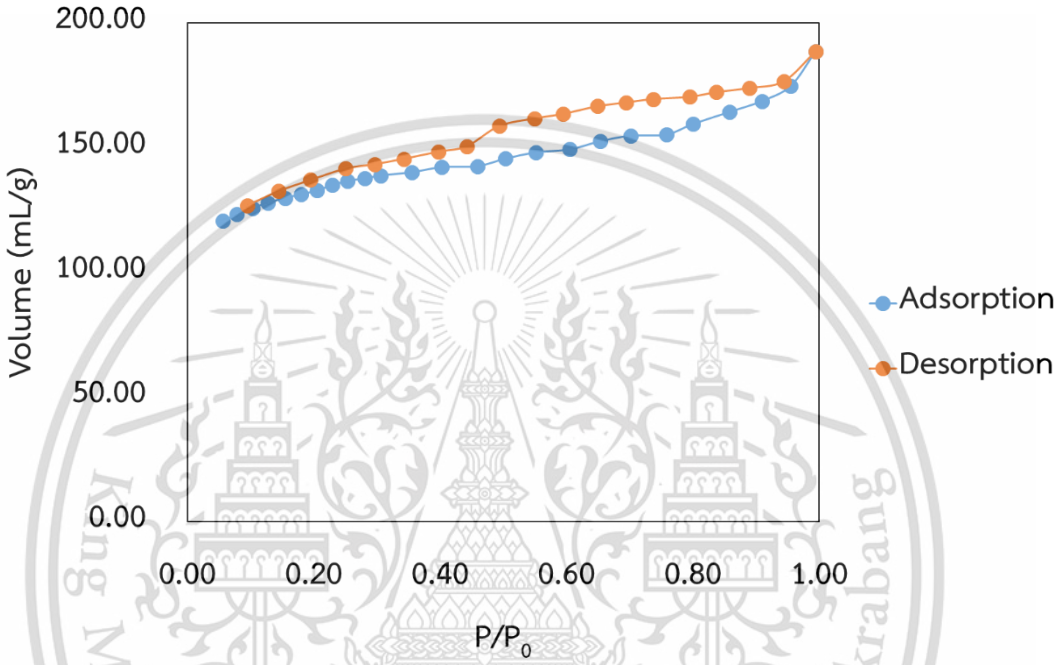

Figure A1 Adsorption isotherm of HZSM-5 (28)

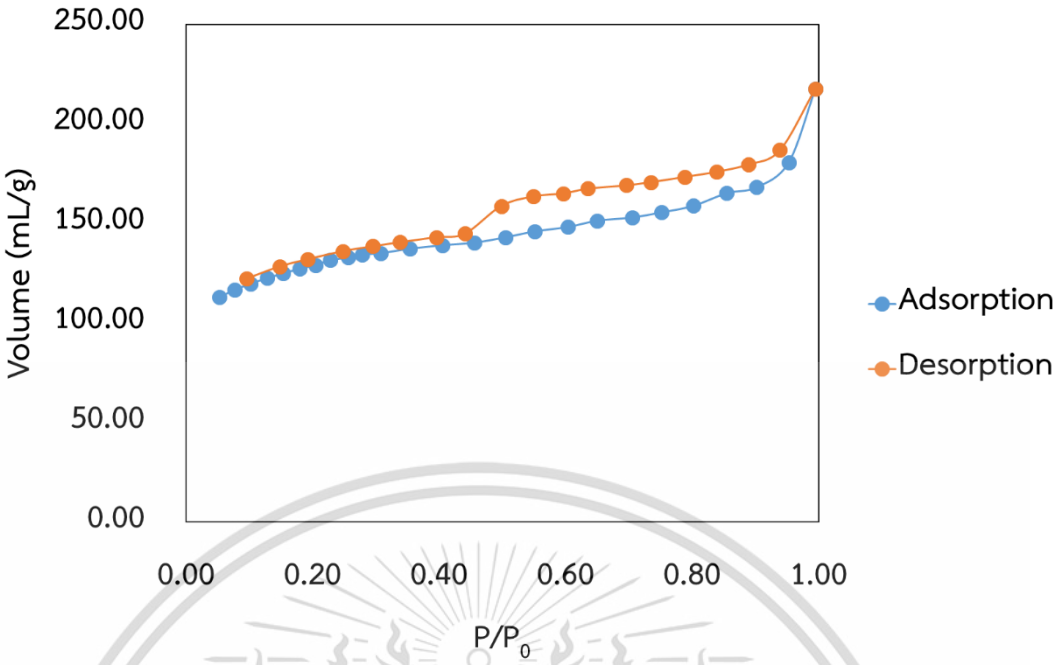

Figure A2 Adsorption isotherm of HZSM-5 (40)

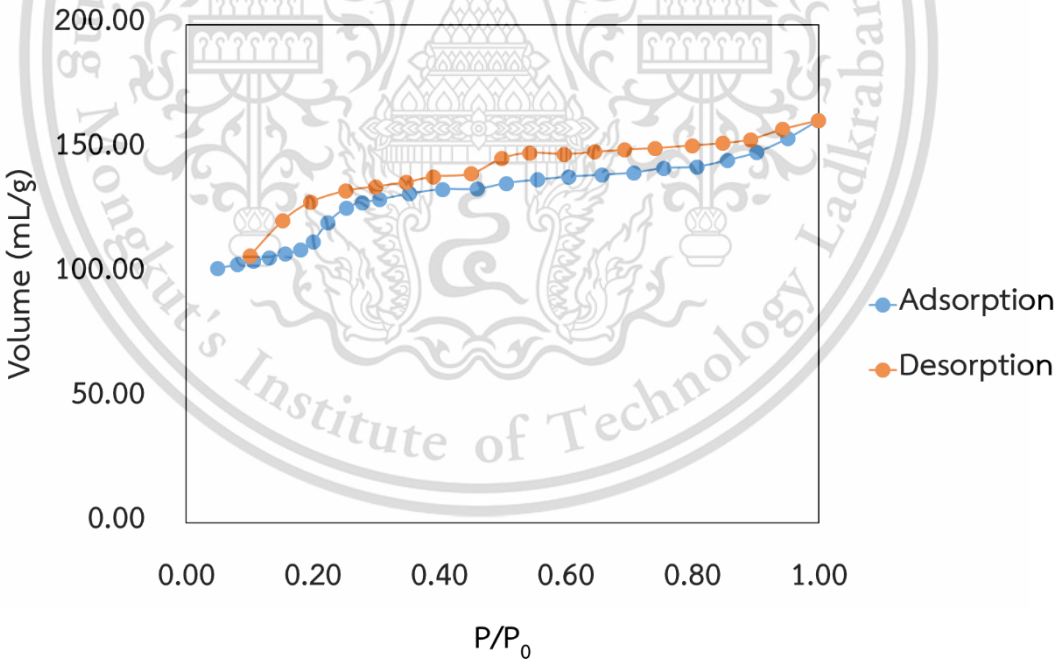

Figure A3 Adsorption isotherm of HZSM-5 (250)

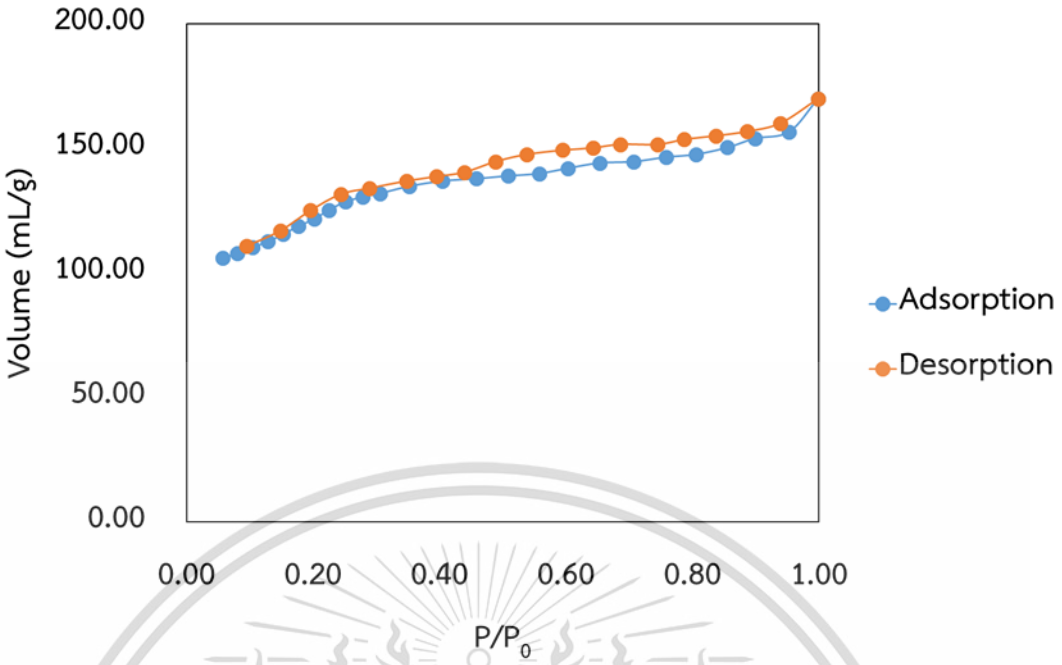

Figure A4 Adsorption isotherm of HZSM-5 (500)

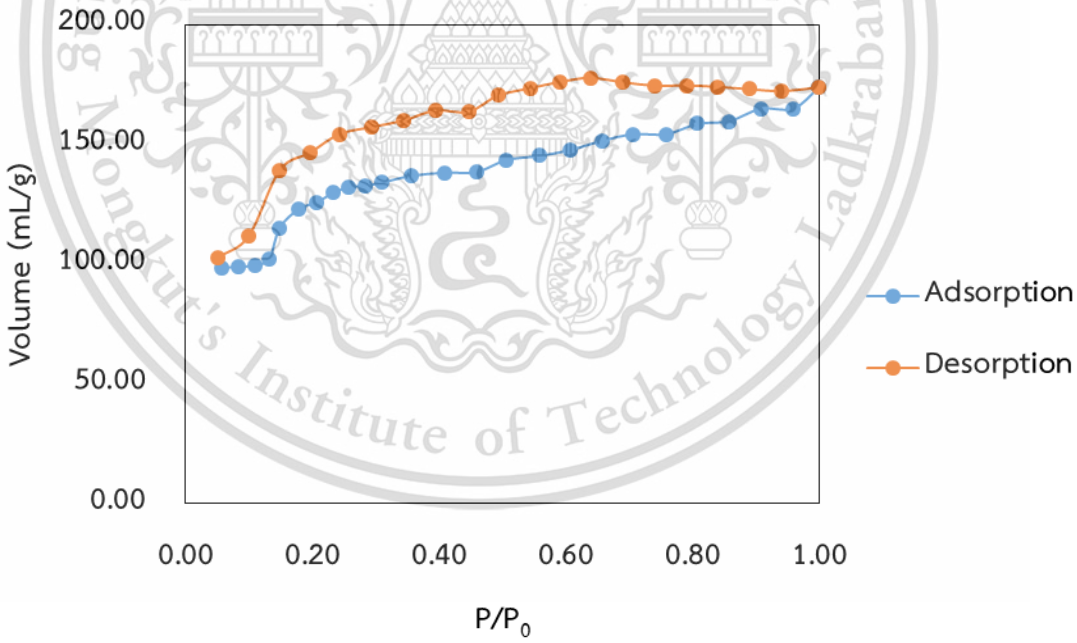

Figure A5 Adsorption isotherm of Silicalite (F)

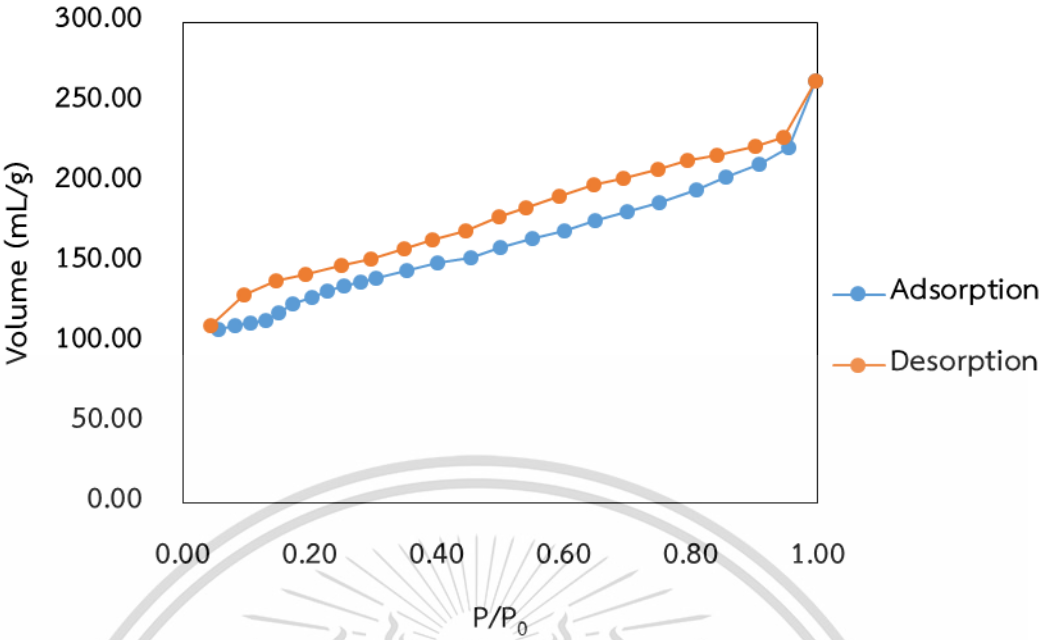

Figure A6 Adsorption isotherm of Silicalite (OH(550))

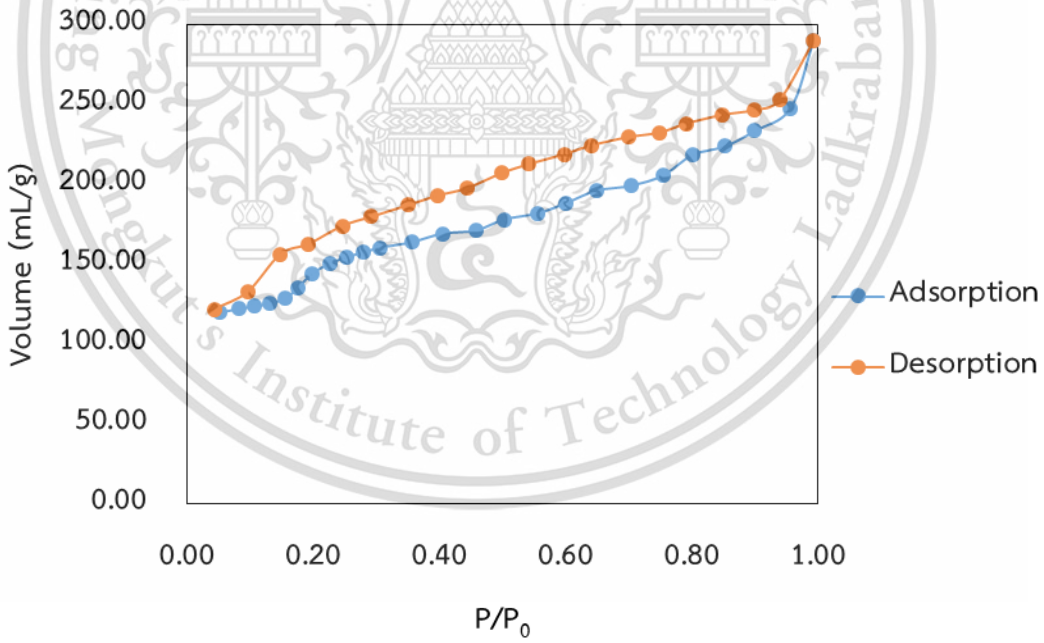

Figure A7 Adsorption isotherm of Silicalite (OH)

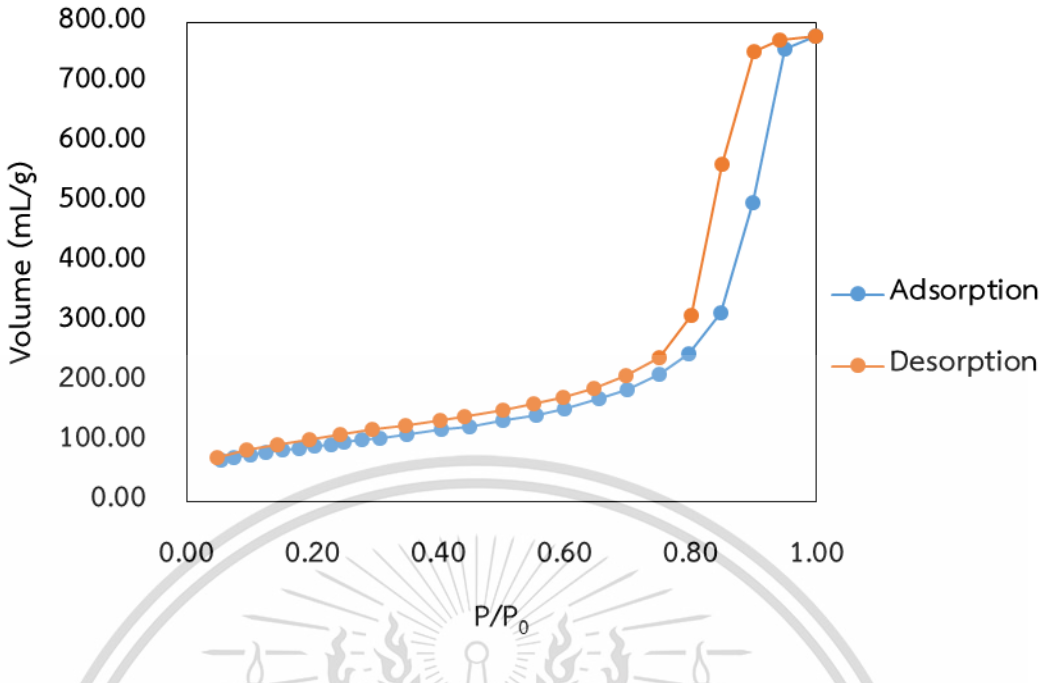

Figure A8 Adsorption isotherm of SiO_2 (Devisil)

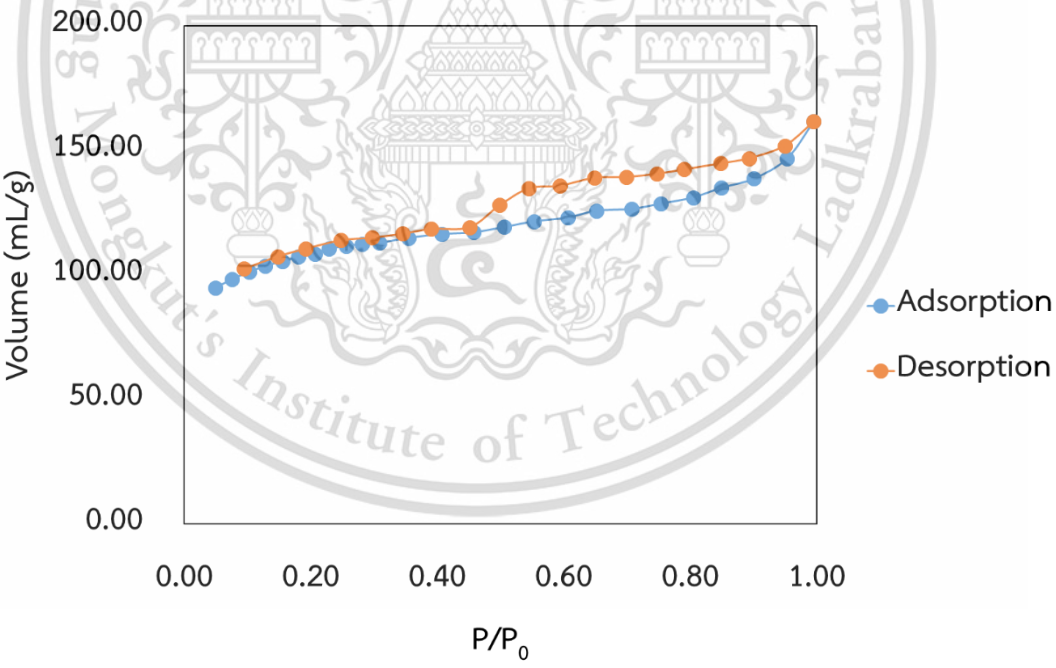

Figure A9 Adsorption isotherm of 2%.Ga-HZSM-5 (28)

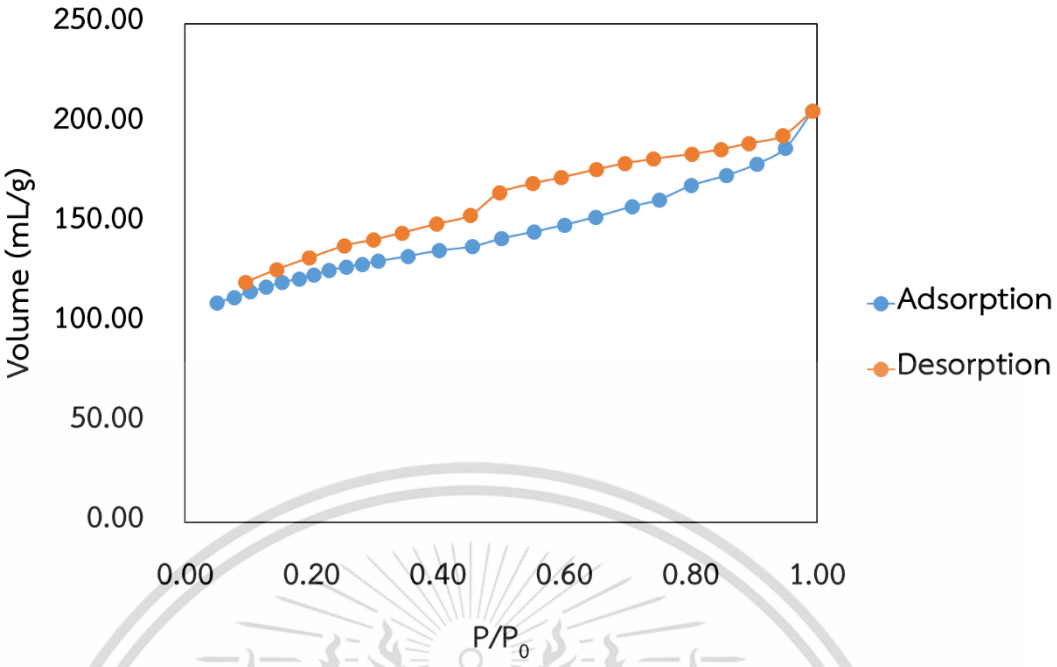

Figure A10 Adsorption isotherm of 2%.Ga-HZSM-5 (40)

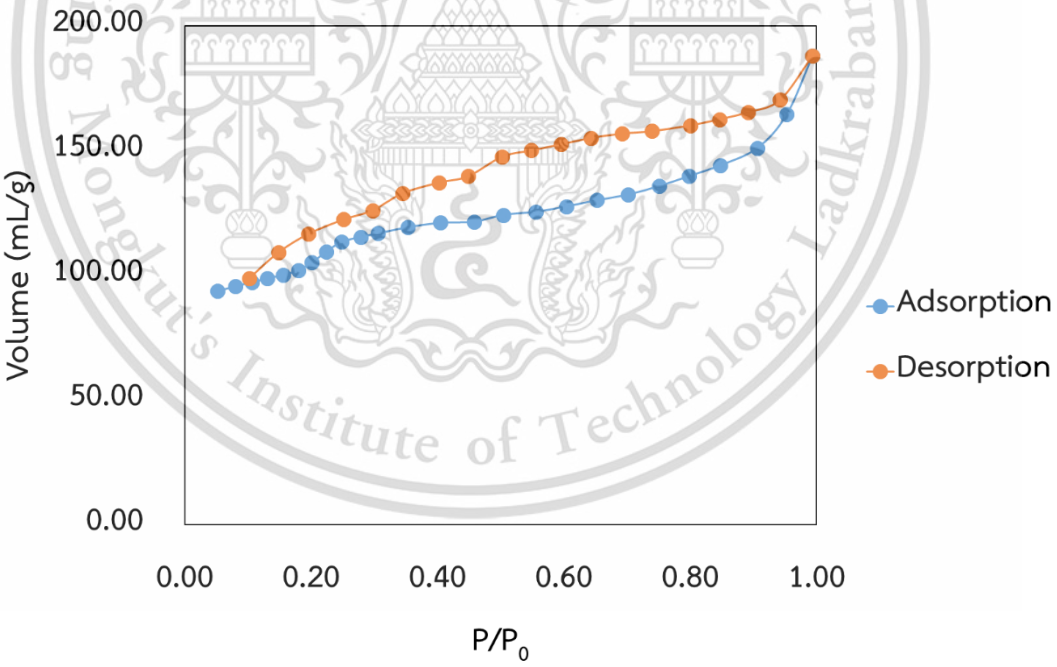

Figure A11 Adsorption isotherm of 2%.Ga-HZSM-5 (250)

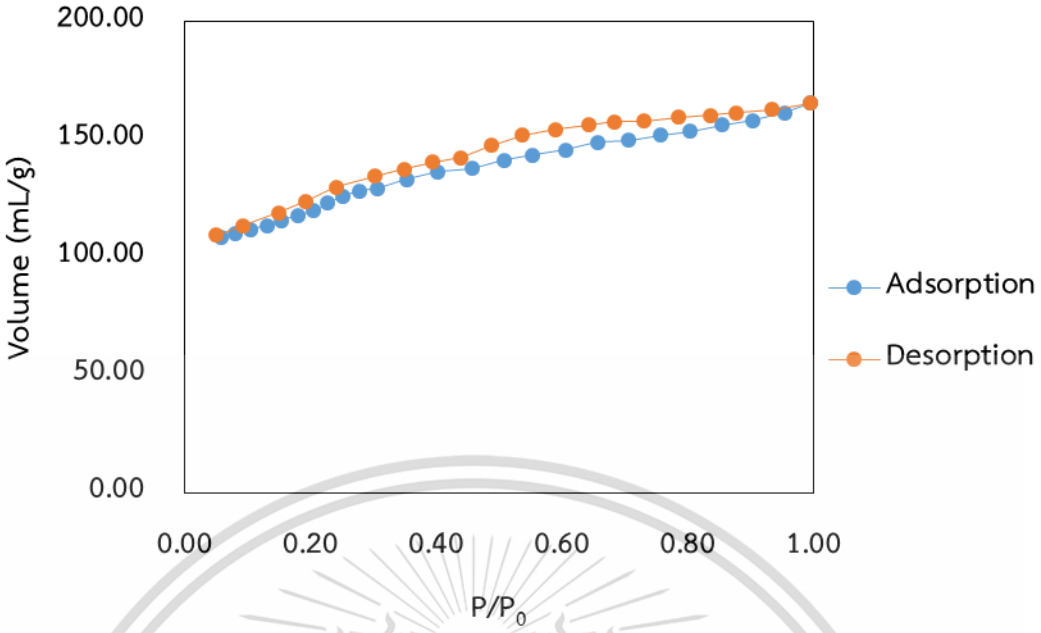

Figure A12 Adsorption isotherm of 2%.Ga-HZSM-5 (500)

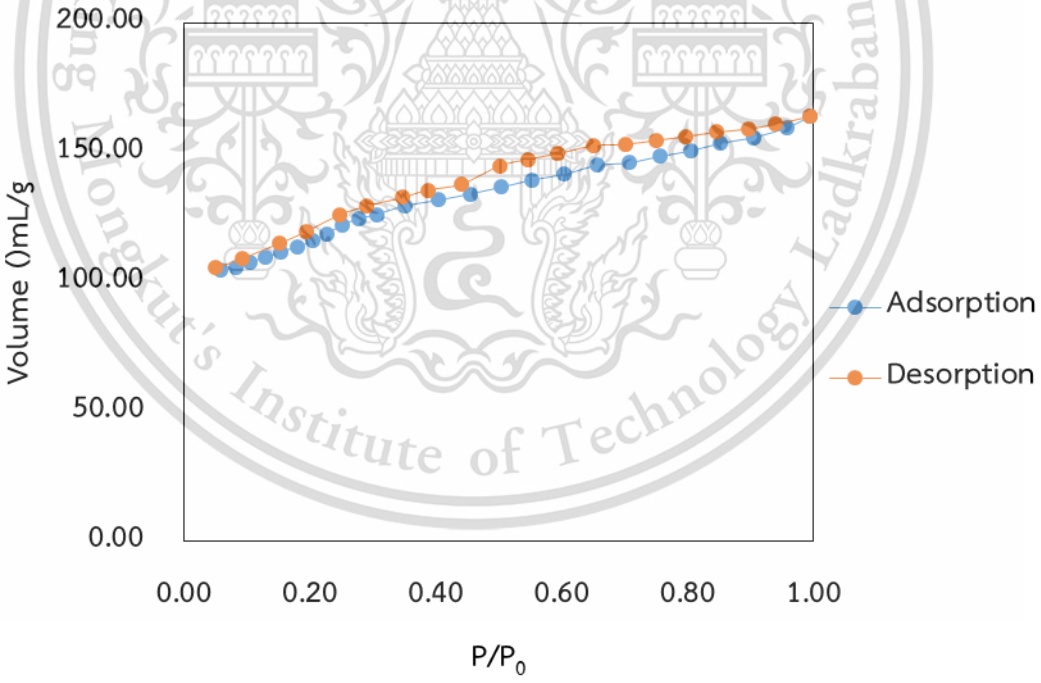

Figure A13 Adsorption isotherm of 3%.Ga-HZSM-5 (500)

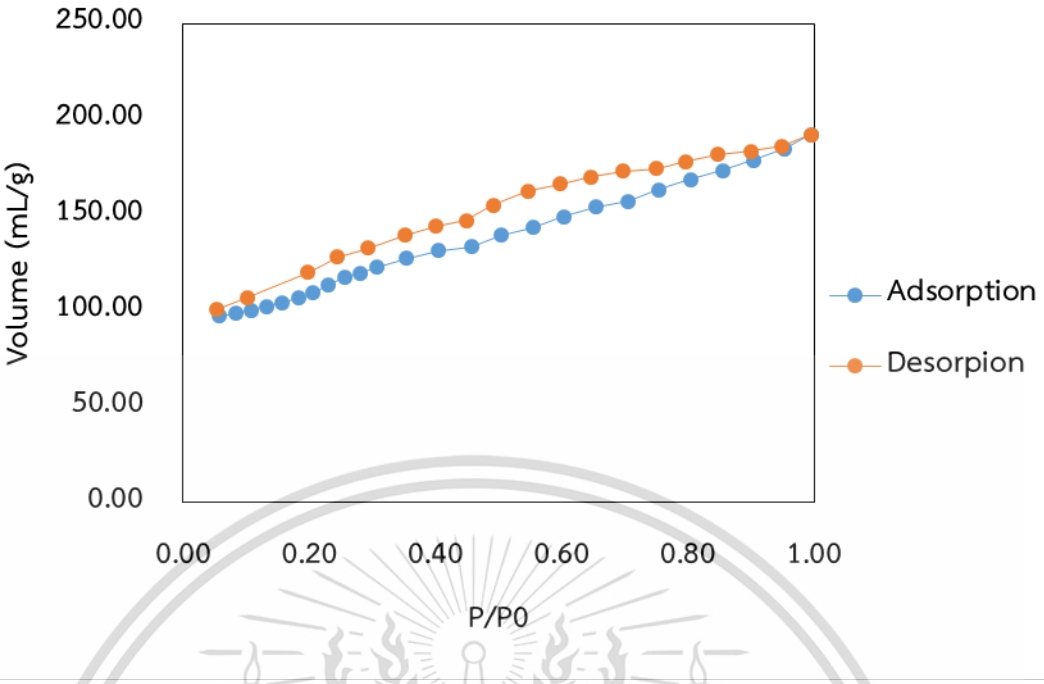

Figure A14 Adsorption isotherm of 4%.Ga-HZSM-5 (500)

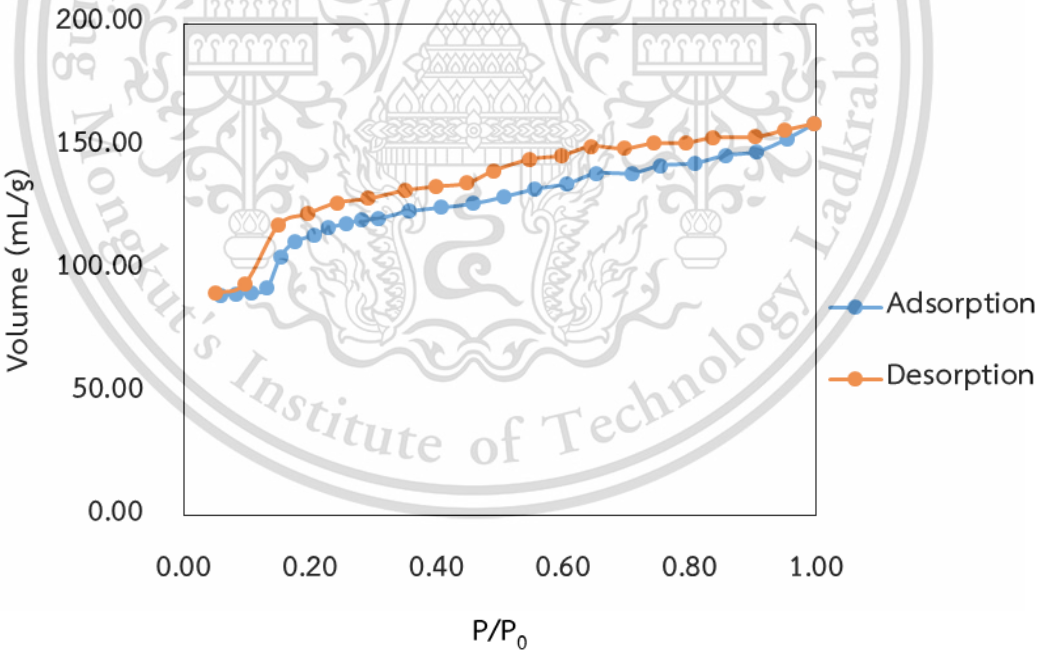

Figure A15 Adsorption isotherm of 3%.Ga-Silicalite (F)

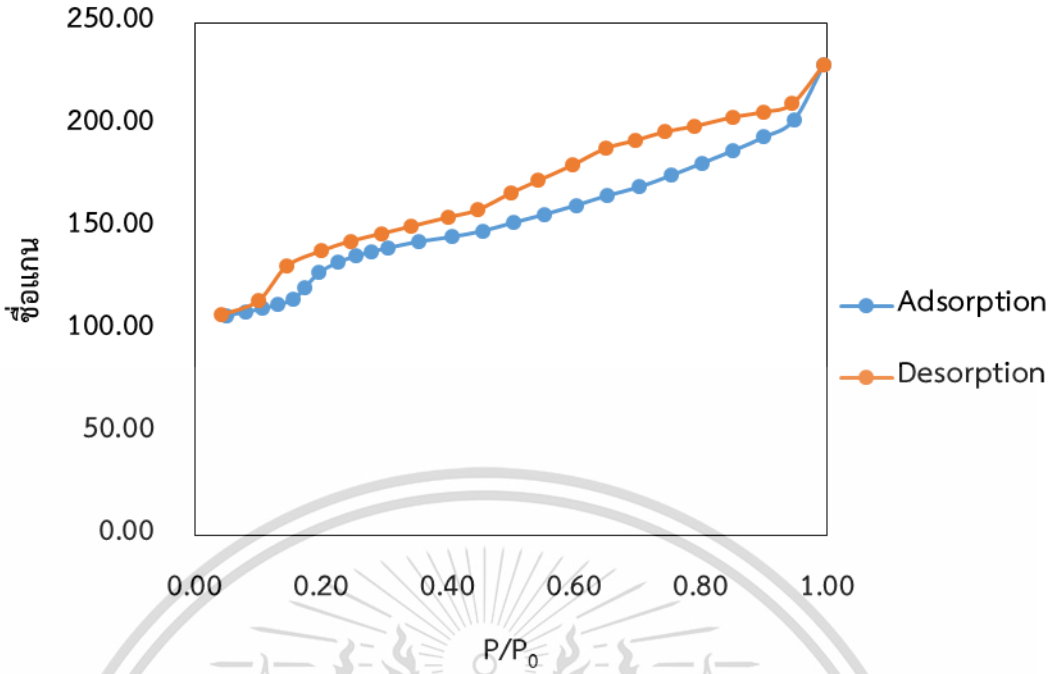

Figure A15 Adsorption isotherm of 3%.Ga-Silicalite (OH(550))

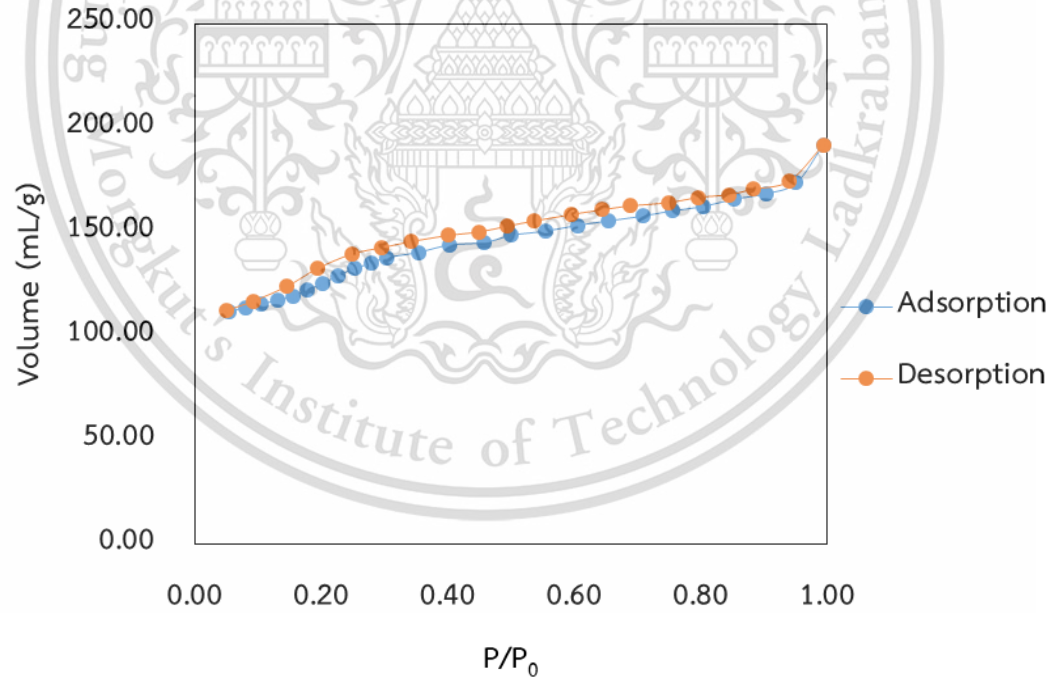

Figure A16 Adsorption isotherm of 3%.Ga-Silicalite (OH)

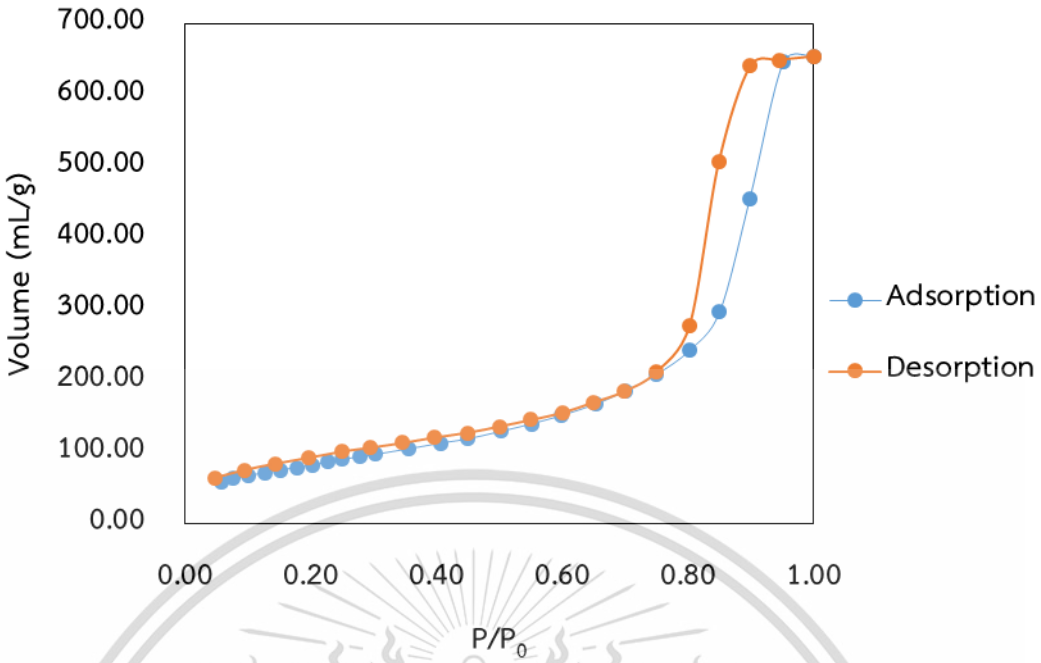

Figure A17 Adsorption isotherm of 3%.Ga-SiO_2 (Devisil)

A2: ICP-MS

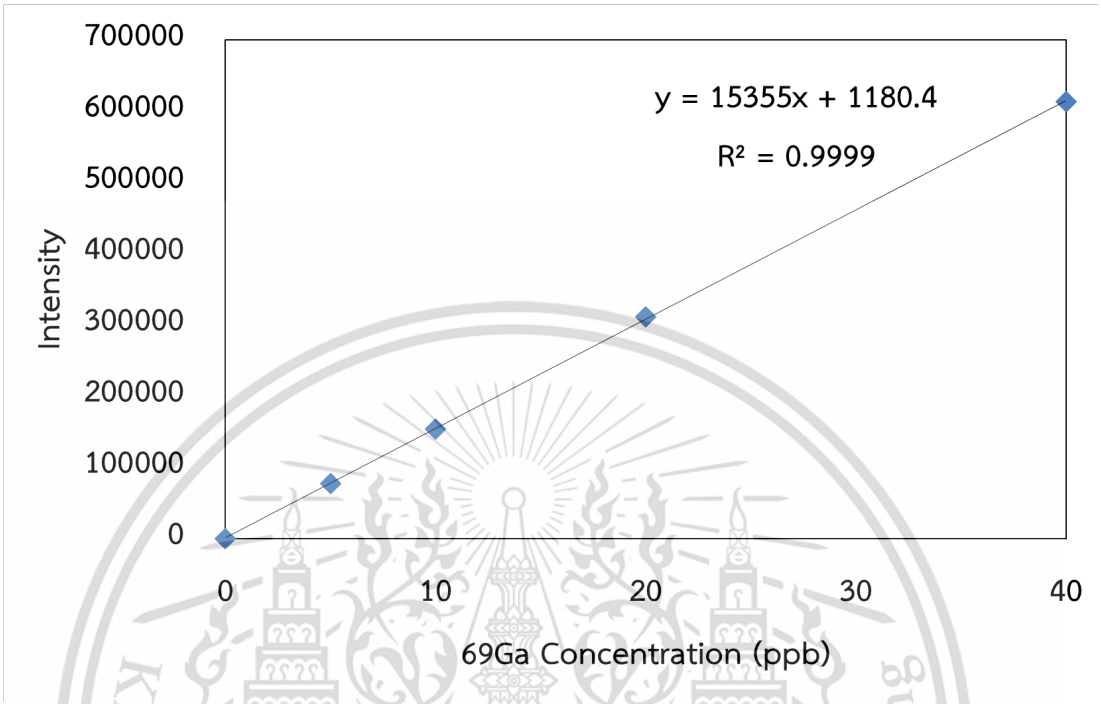

Figure A11 Calibration curve of standard gallium solution

Table A1 Intensity of gallium in catalysts

Catalysts	Intensity	Gallium concentration (ppb)	Gallium loading (wt.%)
3% Ga-HZSM-5 (28)	36496.90	2.30	2.30
3% Ga-HZSM-5 (40)	37150.30	2.34	2.34
3% Ga-HZSM-5 (250)	36971.55	2.33	2.33

Example of gallium loading calculation of 3% Ga-HZSM-5 (28).

Replace the y parameter with 36496.90, then solve for x

$$36496.90 = 15355x + 1180.4$$

$$x = 2.30 \text{ ppb}$$

Dilution factor of catalyst is 1000000, so the concentration = 2300000 ppb = 2300.00 ppm for 0.1 g of catalyst

$$2300 \text{ L}/0.1\ g_{cat} = 2.3\ g/\text{L}/0.1\ g_{cat} = 23\ g/\text{L} = 23\ g/1000\ g = 2.3 \text{ wt.\%}$$

A3: NH_3-TPD

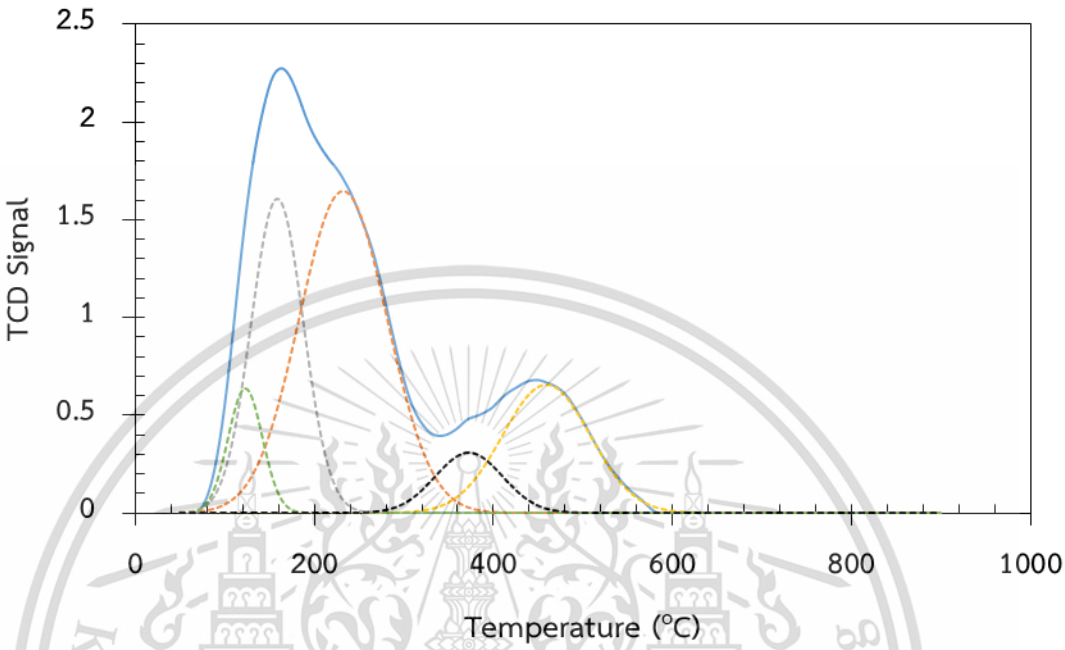

Figure A13 NH_3-TPD of HZSM-5 (28)

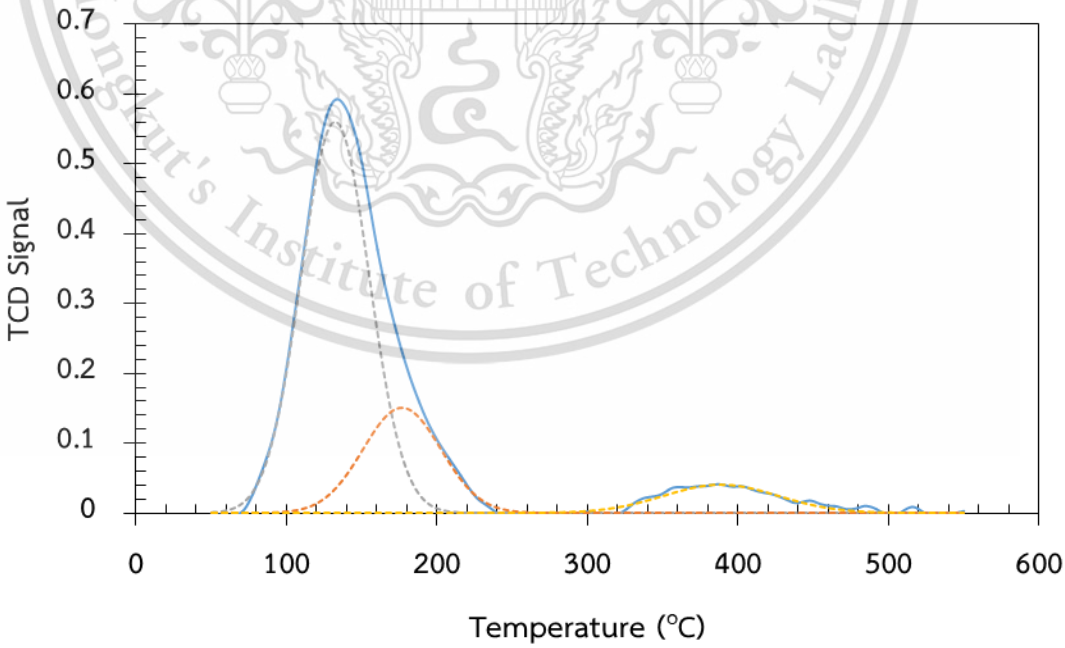

Figure A14 NH_3-TPD of HZSM-5 (500)

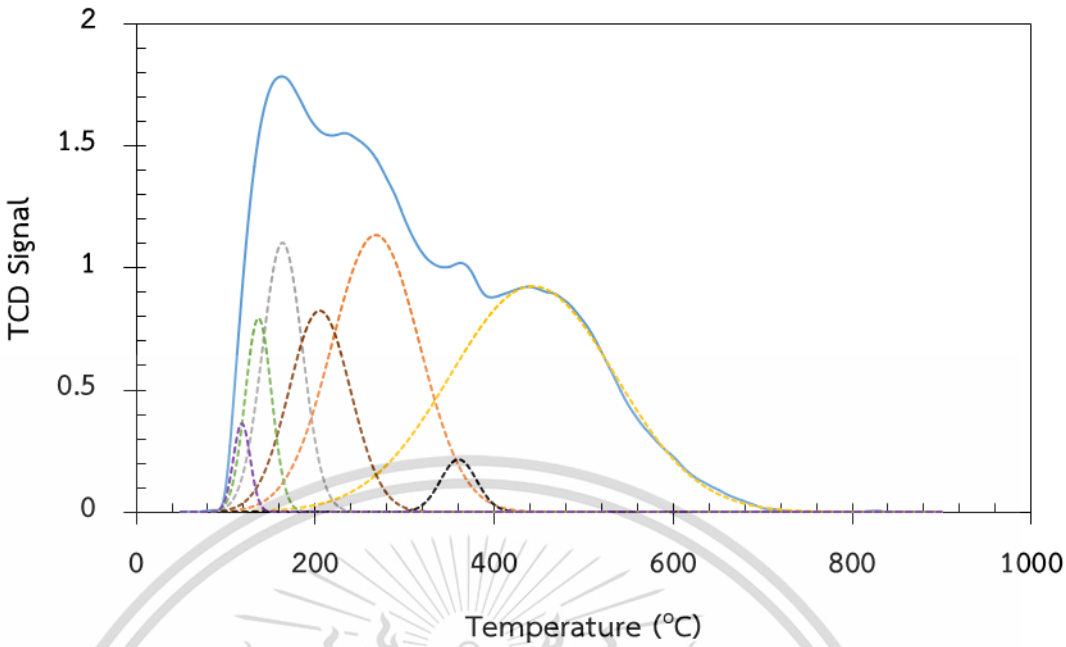

Figure A13 NH_3-TPD of 2%wt.Ga-HZSM-5 (28)

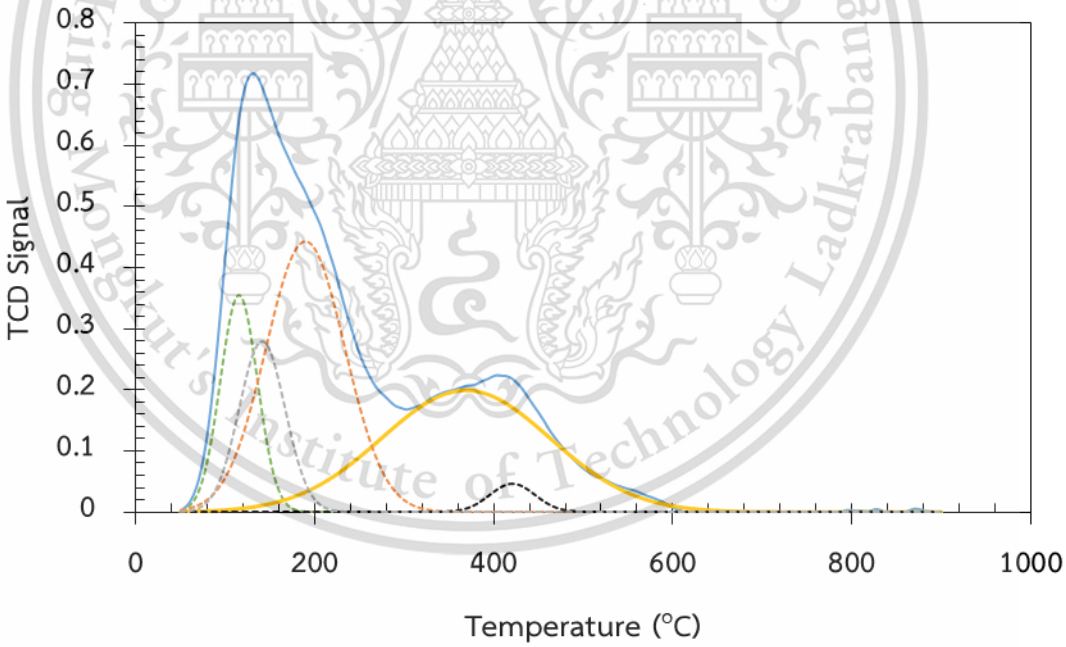

Figure A13 NH_3-TPD of 2%wt.Ga-HZSM-5 (40)

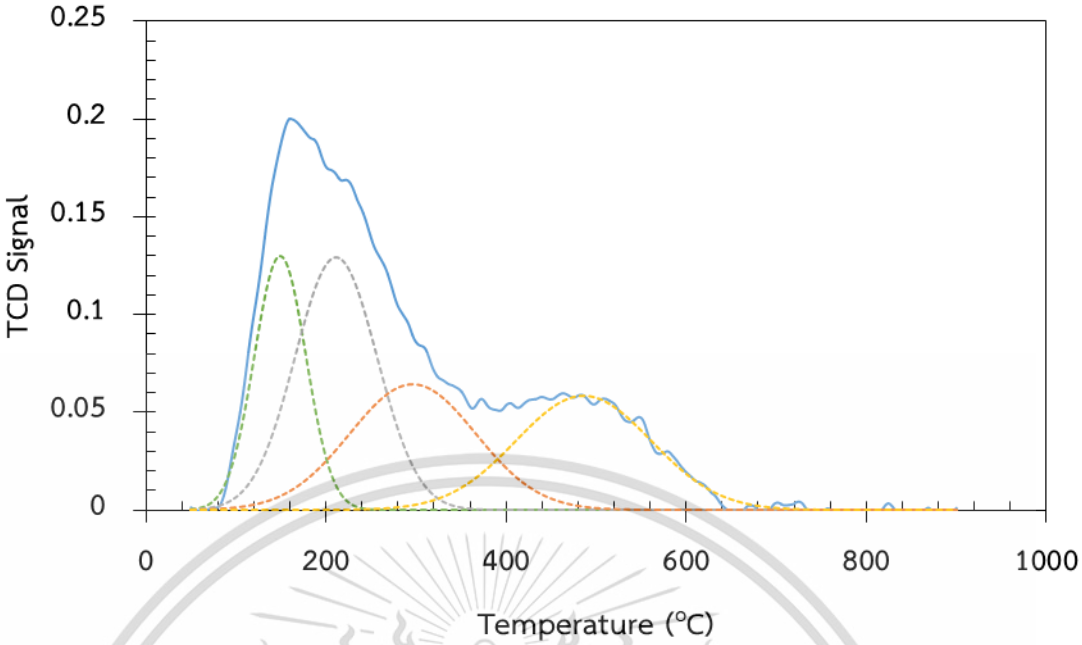

Figure A13 NH_3-TPD of 2%wt.Ga-HZSM-5 (250)

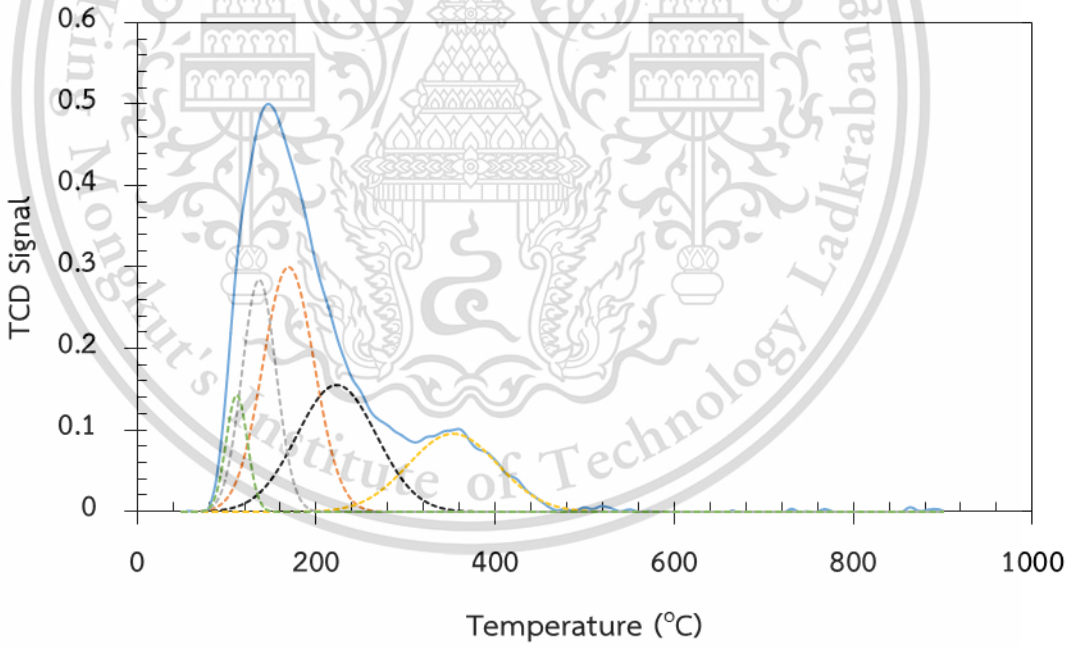

Figure A13 NH_3-TPD of 2%wt.Ga-HZSM-5 (500)

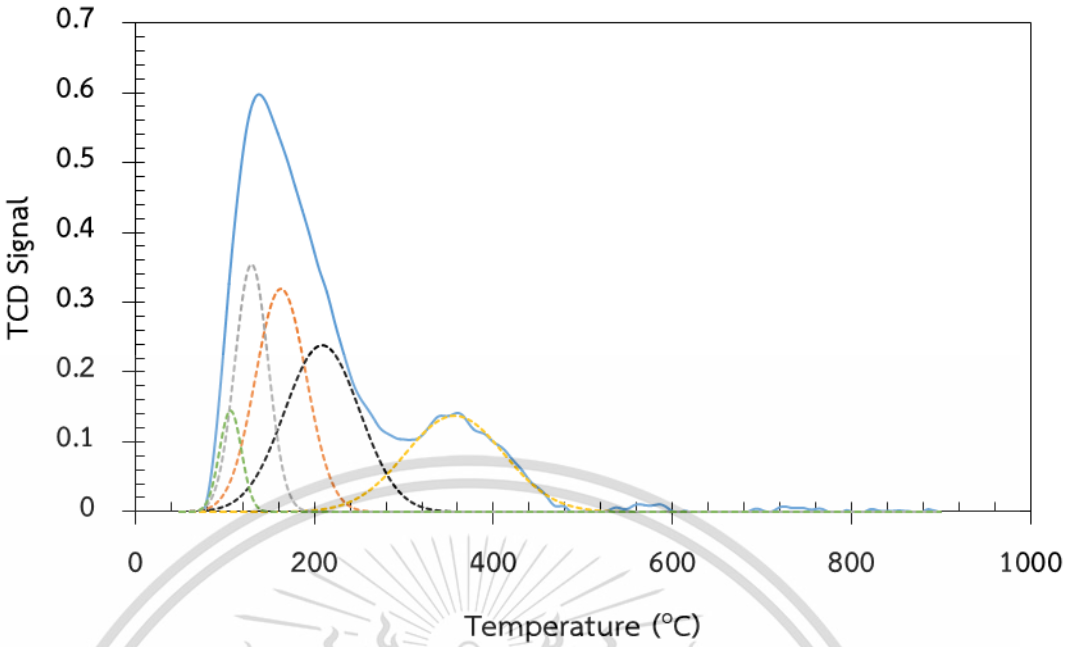

Figure A13 NH_3-TPD of 3%wt.Ga-HZSM-5 (500)

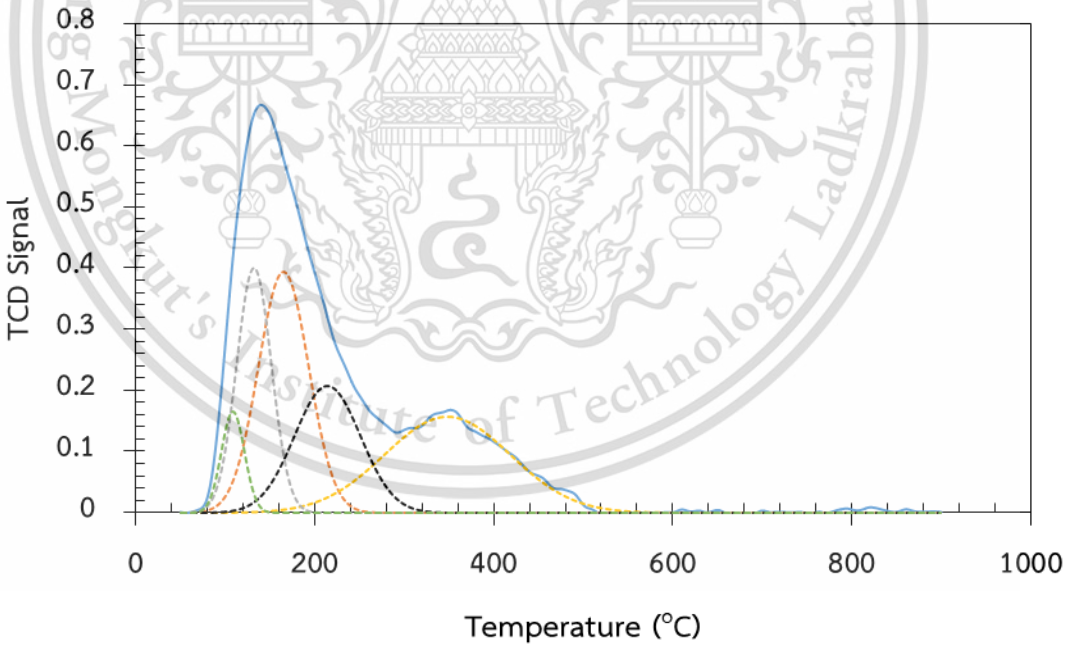

Figure A13 NH_3-TPD of 4%wt.Ga-HZSM-5 (500)

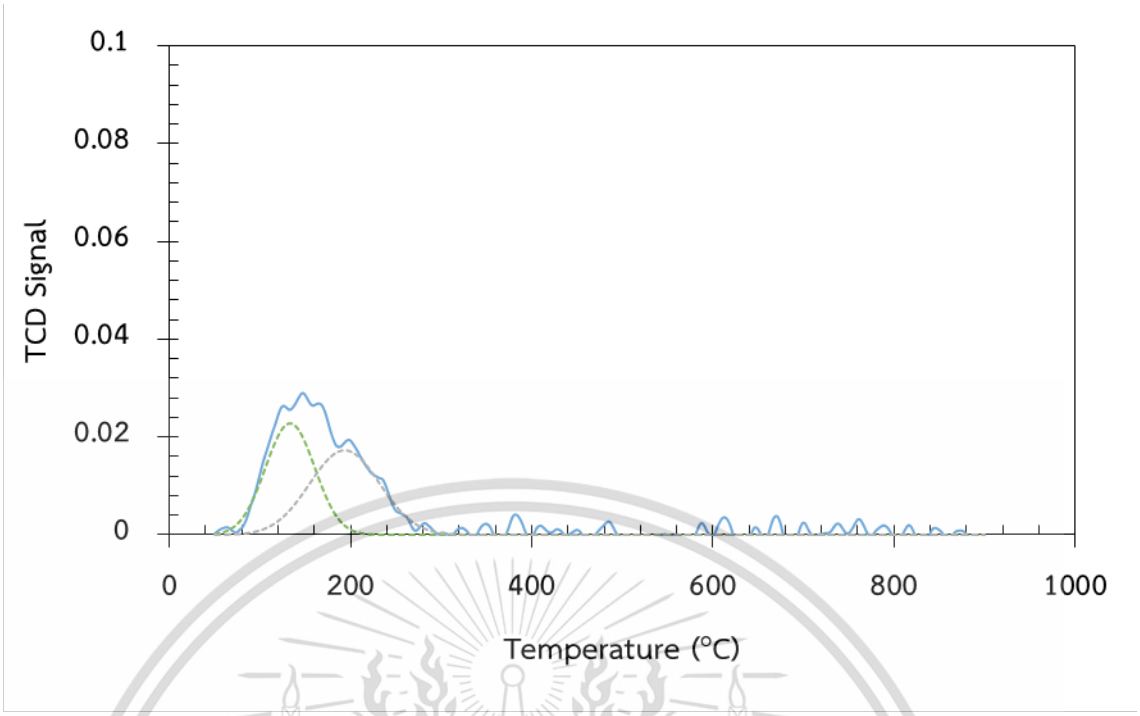

Figure A13 NH_3-TPD of 3%wt.Ga-Silicalite (F)

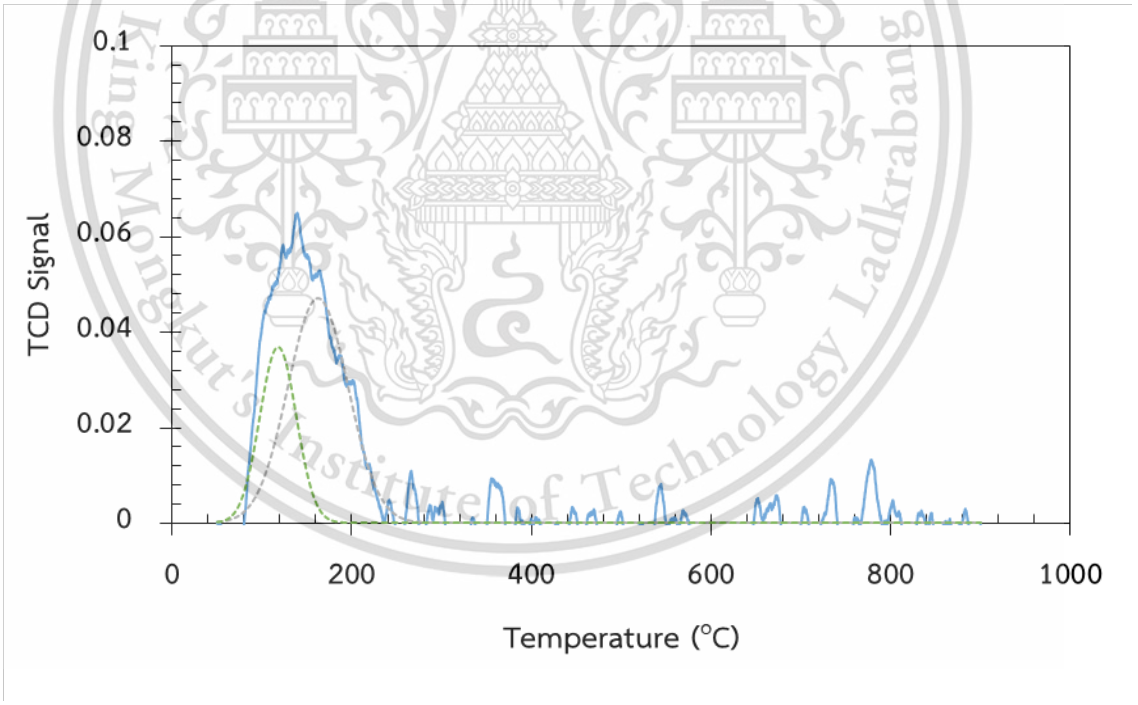

Figure A13 NH_3-TPD of 3%wt.Ga-SiO_2 (Devicil)

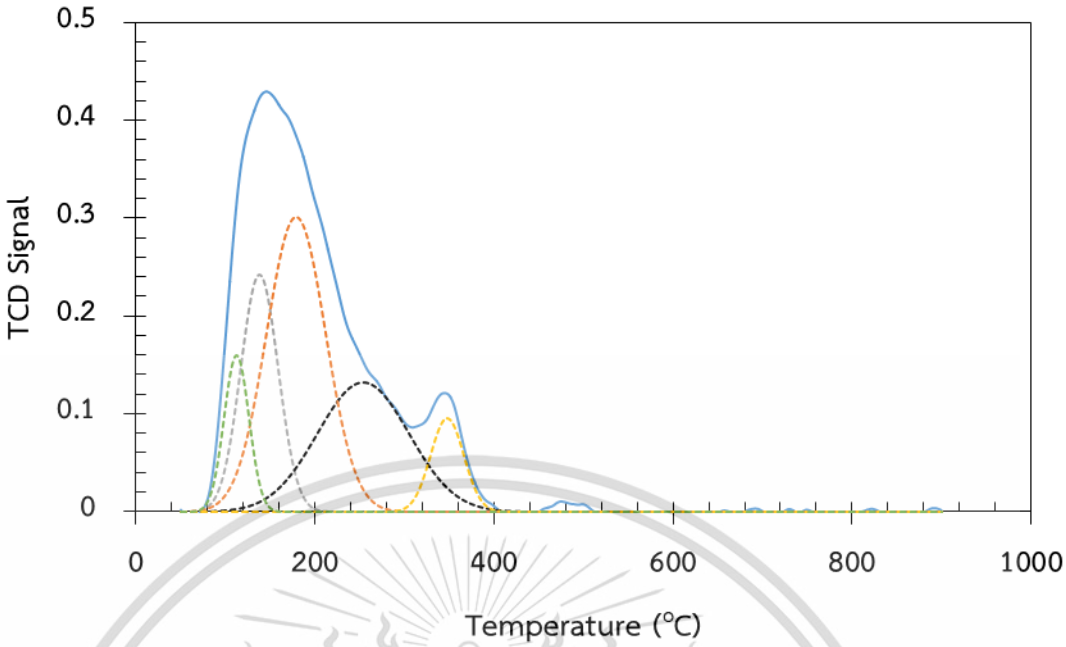

Figure A13 NH_3-TPD of 3%wt.Ga-Silicalite (OH(550))

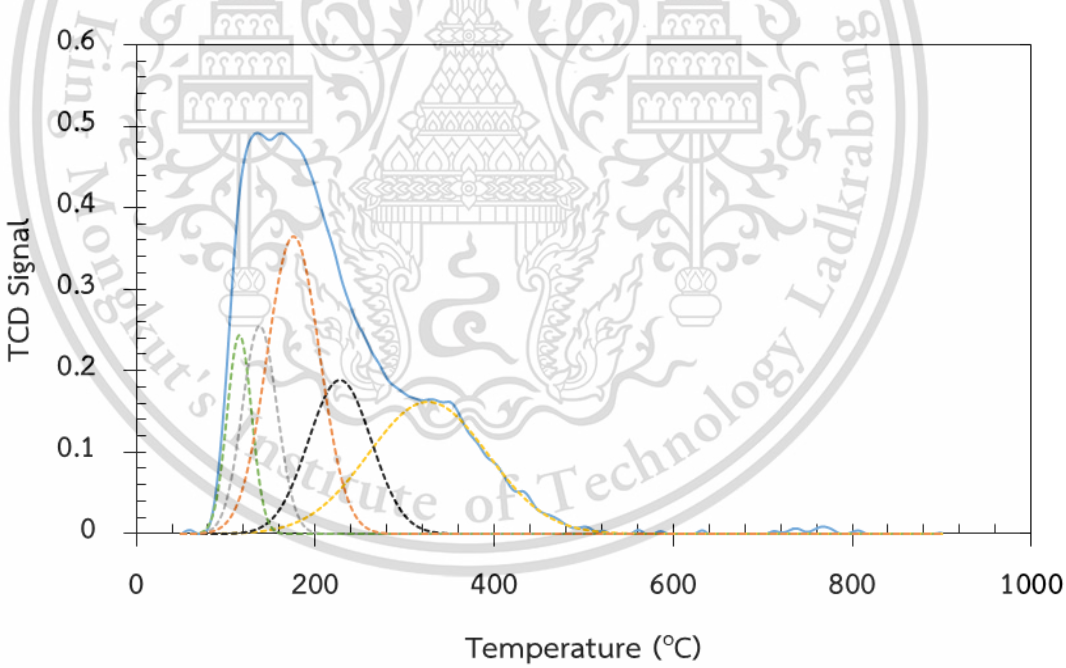

Figure A13 NH_3-TPD of 3%wt.Ga-Silicalite (OH)

Appendix B

GAS CHROMATOGRAM

Analysis gas product from gas chromatography

Prior analysis, GC-MS (gas chromatography with mass spectrometer detector) was used to identify the structure of products in the sample and the GC-FID (gas chromatography with flam ionization detector) was used to determine the quantitative of the product with the condition expressed in **Table B1** and **Table B3**.

Table B1 GC conditions for quantitative analysis for total products

Column	Equity-1, 30 m x 0.53 mmID x 5 μm
Temperature program	35 °C (5 min hold) ramp to 85 °C (2 min hold) at 15 °C/min and ramp to 220 °C (3 min hold) at 10 °C/min
Carrier gas	Nitrogen gas, flow rate 5.2 mL/min
Injector temperature	250 °C
Detector temperature	FID at 280 °C

The products from ethane conversion were identified by comparing the retention time to the standard gas as listed in Table B2.

Table B2 Chromatogram data of feed and products component

Component	Retention time
Light gas	1.62
Cyclopentene	4.40
Benzene	7.90
Toluene	11.00
i-xylene	15.00

Table B3 GC conditions for quantitative analysis for light products

Column	Rt®-Q-BOND, 30 m x 0.53 mmID x 0.2 μm
Temperature program	30 °C (7 min hold) ramp to 85 °C (4 min hold) at 20 °C/min and ramp to 140 °C (3 min hold) at 20 °C/min and ramp to 225 °C (6.83 min hold) at 15 °C/min
Split ratio	100
Carrier gas	Nitrogen gas, flow rate 5.19 mL/min
Injector temperature	250 °C
Detector temperature	FID at 250 °C

The products from ethane conversion were identified by comparing the retention time to the standard gas as listed in Table B4.

Table B4 Chromatogram data of feed and products component

Component	Retention time
Methane	2.48
Ethylene	5.01
Acetylene	5.27
Ethane	6.69
Methyl acetylene	13.56
C_4 - isomers	18.87

Appendix C

CALCULATIONS

C1: Catalytic parameters

Contact time (W/F)

$$\frac{W}{F} = \frac{\text{weight of catalyst (g)}}{\text{feed rate (mol/h)}}$$

Example

In the reaction using 0.0542 mol/h of propane in feed and using 0.2000 grams of catalyst, the W/F is calculated as follow:

$$W/F = (0.2000\ g) / (0.0368\ mol/h)$$

$$W/F = 3.6900\ g.h.mol^{-1}$$

In similar manner; W/F of catalyst with different catalyst weight and different feed rate are calculated.

Calculation of % yield of products from gas chromatography

From the chromatogram, the peaks of each component were identified and summarized using reference standard for comparison. The example of the peak area obtained from chromatogram of a mixture reactor outlet is shown in Table C1.

Table C1 the summation of peak area of all components (information of HZSM-5 (28) at 60 min on stream)

Component	Peak area	Blank
Methane	50.42	29559
Ethylene	161.29	
Ethane	17365.33	
Methyl acetylene	10.74	
Benzene	10.86	
Toluene	8.24	
Total	17609.87	

The %yield of each products was calculated by normalization method as follows:

$$\%yield = \frac{\text{area of product}}{\text{blank area}} \times 100$$

For example

$$\%yield \text{ of ethylene} = \frac{161.29}{29559} \times 100$$

$$= 0.55$$

The yield of each products from this calculation is shown in **Table C2**.

Table C2 %yield of products derived by normalization method

Product	%yield
Methane	0.17
Ethylene	0.55
Methyl acetylene	0.04
Benzene	0.04
Toluene	0.03
Total	0.83

Conversion

%Conversion can be calculated from the following equation:

%conversion = total products yield

For example;

%conversion = 0.17 + 0.55 + 0.04 + 0.04 + 0.03

= 0.83

Selectivity

%Selectivity can be obtained from the following equation:

$$\%selectivity = \frac{\%yield\ of\ product}{\%conversion} \times 100$$

For example;

$$\%selectivity\ of\ ethylene = \frac{0.55}{0.83} \times 100$$

$$= 66.27$$

C2: Equilibrium propane conversion

From

$$\Delta G^0 = \Delta H^0 - T\Delta S^0$$

$\Delta H^0 = \sum h_f^0$ of products - $\sum h_f^0$ of reactants (from Table A-26, Thermodynamics: An engineering approach 8th edition)

$\Delta S^0 = \sum s^0$ of products - $\sum s^0$ of reactants (from Table A-26, Thermodynamics: An engineering approach 8th edition)

ΔH^0 = 136.96 kJ/mol

ΔS^0 = 0.12 kJ/mol/K

So $\Delta G^0 = 136.96 - 0.12T$

At 650 °C (923 K); ΔG^0 = 25.32 kJ/mol

From

$$\Delta G = \Delta G^0 + RT\ln K_{eq}$$

At equilibrium: $\Delta G = 0$

So

$$\Delta G^0 = -RT\ln K_{eq}$$

$$25.32 = -8.3145 \times 10^{-3}\ kJ.mol^{-1}.K^{-1} \times 923\ K \ln K_{eq}$$

$$K_{eq} = 0.0369$$

From equilibrium ethane conversion under an absence of H_2;

$$K_{eq} = X^2 / (1-X)$$

$$0.0369 = X^2 / (1-X)$$

Solve for X; X = 17.46, where X is the equilibrium ethane conversion.

From equilibrium ethane conversion under an excess of H_2;

$$K_{eq} = X / (1-X)$$

$$0.0369 = X / (1-X)$$

Solve for X; X = 3.56, where X is the equilibrium ethane conversion.

The rate equation from these data can be derived as follows;

$$rate = kC / (1 + K_{ad}[H_2])$$

Under an absence of H_2;

$$17.46 = kC / (1 + K_{ad}(0))$$

$$kC = 17.46$$

Under an excess of H_2;

$$rate = kC / (1 + K_{ad}(1))$$

$$3.56 = 17.46 / (1 + K_{ad})$$

$$K_{ad} = 3.91$$

So the rate equation is

$$rate = 17.46 / (1 + 3.91[H_2])$$

The ethane conversion with a presence of H_2 is shown in **Table C3.**

Table C3 equilibrium ethane conversion with a presence of H_2

H_2 (%)	$[H_2]$	X
0	0.0	17.46
10	0.1	12.55
20	0.2	9.80
30	0.3	8.04
40	0.4	6.81
50	0.5	5.91
60	0.6	5.22
70	0.7	4.67
80	0.8	4.23
90	0.9	3.86
100	1.0	3.56

Appendix D

REACTION DATA

D1: The ability of gallium

Table D1 area and product distribution from ethane conversion (contact time 3.69 g.h.mol^{-1})

TOS (h)	Area										Total Area
	Methane	Ethylene	Acetylene	Ethane	Methyl acetylene	C4	Cyclopentene	Benzene	Toluene	Xylene	
1	50.4	161.3	0.0	17368.3	10.7	0.0	0.0	10.9	8.2	0.0	17609.9
2	49.5	157.6	0.0	17190.8	10.4	0.0	0.0	10.0	3.1	0.0	17421.6
3	48.2	154.2	0.0	17249.6	9.3	0.0	0.0	8.2	3.4	0.0	17473.0
4	46.5	150.3	0.0	17068.5	9.5	0.0	0.0	8.4	3.1	0.0	17286.3
5	45.8	149.1	0.0	16988.7	9.2	0.0	0.0	8.8	3.0	0.0	17204.7
6	44.7	147.4	0.0	16800.8	8.9	0.0	0.0	12.0	4.0	0.0	17017.8

TOS (h)	% Yield										
	Conversion	Methane	Ethylene	Acetylene	Methyl acety-lene	C4	Cyclopentene	Benzene	Toluene	Xylene	Blank
1	0.82	0.17	0.55	0.00	0.04	0.00	0.00	0.04	0.03	0.00	29559.00
2	0.78	0.17	0.53	0.00	0.04	0.00	0.00	0.03	0.01	0.00	
3	0.76	0.16	0.52	0.00	0.03	0.00	0.00	0.03	0.01	0.00	
4	0.74	0.16	0.51	0.00	0.03	0.00	0.00	0.03	0.01	0.00	
5	0.73	0.15	0.50	0.00	0.03	0.00	0.00	0.03	0.01	0.00	
6	0.73	0.15	0.50	0.00	0.03	0.00	0.00	0.04	0.01	0.00	

Reaction condition; Catalyst: HZSM-5 (28), Reaction temperature: 650 °C, Reduction temperature: 900 °C, Feed rate: 20 mL/min of ethane, Carrier gas; 55 mL/min of helium, Ambient pressure.

Table D2 area and product distribution from ethane conversion (contact time 3.69 g.h.mol^{-1})

TOS (h)	Area										Total Area
	Methane	Ethylene	Acetylene	Ethane	Methyl acetylene	C4	Cyclopentene	Benzene	Toluene	Xylene	
1	33.5	1916.2	2.2	19722.5	18.2	24.0	2.93	290.3	145.5	34.0	22189.3
2	24.3	1707.6	2.2	19737.5	13.3	19.4	2.23	214.6	94.5	12.7	21828.3
3	19.5	1533.4	1.9	19530.1	10.8	16.6	2.10	166.8	65.4	10.1	21356.6
4	17.2	1440.5	1.8	19456.7	9.6	15.7	2.06	146.3	53.4	7.1	21150.4
5	16.0	1383.5	1.7	19430.3	8.9	15.3	2.05	132.2	47.2	5.2	21042.3
6	14.3	1297.8	1.7	19095.9	7.7	15.2	2.10	114.8	41.6	3.2	20594.1

TOS (h)	% Yield										
	Conversion	Methane	Ethylene	Acetylene	Methyl acetylene	C4	Cyclopentene	Benzene	Toluene	Xylene	Blank
1	8.39	0.11	6.52	0.01	0.06	0.08	0.01	0.99	0.49	0.12	29613.00
2	7.03	0.08	5.81	0.01	0.05	0.07	0.01	0.73	0.32	0.04	
3	6.15	0.07	5.22	0.01	0.04	0.06	0.01	0.57	0.22	0.03	
4	5.70	0.06	4.90	0.01	0.03	0.05	0.01	0.50	0.18	0.02	
5	5.43	0.05	4.71	0.01	0.03	0.05	0.01	0.45	0.16	0.02	
6	5.10	0.05	4.41	0.01	0.03	0.05	0.01	0.39	0.14	0.01	

Reaction condition; Catalyst: 3%wt.Ga-HZSM-5 (28), Reaction temperature: 650 °C, Reduction temperature: 900 °C, Feed rate: 20 mL/min of ethane, Carrier gas; 55 mL/min of helium, Ambient pressure.

D2: Effect of Si/Al ratio

Table D3 area and product distribution from ethane conversion (contact time 3.69 g.h.mol^{-1})

TOS (h)	Area										
	Methane	Ethylene	Acetylene	Ethane	Methyl acetylene	C4	Cyclopentene	Benzene	Toluene	Xylene	Total Area
1	32.4	1883.6	2.1	19266.8	22.0	25.0	5.0	493.9	249.4	60.6	22040.8
2	23.6	1644.6	1.9	18956.0	15.5	21.3	4.0	306.6	138.5	25.8	21137.8
3	19.8	1495.9	1.8	18648.4	12.5	19.6	3.2	231.5	100.2	12.4	20545.4
4	17.7	1399.8	1.8	18321.0	12.3	16.9	3.0	169.5	68.8	6.4	20017.3
5	16.8	1347.5	1.7	18086.9	9.9	13.1	2.6	146.2	64.2	5.8	19694.7
6	15.1	1262.2	1.6	18066.2	9.1	12.5	2.4	127.0	59.6	3.0	19558.6

TOS (h)	% Yield										
	Conversion	Methane	Ethylene	Acetylene	Methyl acety-lene	C4	Cyclopentene	Benzene	Toluene	Xylene	Blank
1	9.43	0.11	6.41	0.01	0.07	0.09	0.02	1.68	0.85	0.21	29413.00
2	7.42	0.08	5.59	0.01	0.05	0.07	0.01	1.04	0.47	0.09	
3	6.45	0.07	5.09	0.01	0.04	0.07	0.01	0.79	0.34	0.04	
4	5.77	0.06	4.76	0.01	0.04	0.06	0.01	0.58	0.23	0.02	
5	5.47	0.06	4.58	0.01	0.03	0.04	0.01	0.50	0.22	0.02	
6	5.08	0.05	4.29	0.01	0.03	0.04	0.01	0.43	0.20	0.01	

Reaction condition; Catalyst: 3%wt.Ga-HZSM-5 (40), Reaction temperature: 650 °C, Reduction temperature: 900 °C, Feed rate: 20 mL/min of ethane, Carrier gas; 55 mL/min of helium, Ambient pressure.

Table D4 area and product distribution from ethane conversion (contact time 3.69 g.h.mol^{-1})

TOS (h)	Area										Total Area
	Methane	Ethylene	Acetylene	Ethane	Methyl acetylene	C4	Cyclopentene	Benzene	Toluene	Xylene	
1	2.0	382.5	0.0	17690.1	1.4	0.0	0.0	0.0	0.0	0.0	18076.0
2	1.9	362.1	0.0	17529.3	1.4	0.0	0.0	0.0	0.0	0.0	17894.6
3	1.8	351.0	0.0	17180.9	1.1	0.0	0.0	0.0	0.0	0.0	17534.7
4	1.8	342.7	0.0	17380.3	1.1	0.0	0.0	0.0	0.0	0.0	17725.9
5	1.8	337.2	0.0	16802.4	1.0	0.0	0.0	0.0	0.0	0.0	17142.3
6	1.7	329.8	0.0	16550.1	0.9	0.0	0.0	0.0	0.0	0.0	16882.5

TOS (h)	% Yield										
	Conversion	Methane	Ethylene	Acetylene	Methyl acety-lene	C4	Cyclopentene	Benzene	Toluene	Xylene	Blank
1	1.31	0.01	1.30	0.00	0.00	0.00	0.00	0.00	0.00	0.00	29403.00
2	1.24	0.01	1.23	0.00	0.00	0.00	0.00	0.00	0.00	0.00	
3	1.20	0.01	1.19	0.00	0.00	0.00	0.00	0.00	0.00	0.00	
4	1.18	0.01	1.17	0.00	0.00	0.00	0.00	0.00	0.00	0.00	
5	1.16	0.01	1.15	0.00	0.00	0.00	0.00	0.00	0.00	0.00	
6	1.13	0.01	1.12	0.00	0.00	0.00	0.00	0.00	0.00	0.00	

Reaction condition; Catalyst: 3%wt.Ga-HZSM-5 (250), Reaction temperature: 650 °C, Reduction temperature: 900 °C, Feed rate: 20 mL/min of ethane, Carrier gas; 55 mL/min of helium, Ambient pressure.

Table D5 area and product distribution from ethane conversion (contact time 3.69 g.h.mol^{-1})

TOS (h)	Area										Total Area
	Methane	Ethylene	Acetylene	Ethane	Methyl acety-lene	C4	Cyclopentene	Benzene	Toluene	Xylene	
1	7.1	900.9	1.9	19894.7	1.4	3.5	0.0	19.3	4.1	0.0	20832.8
2	6.7	787.4	2.1	19503.7	1.1	2.9	0.0	14.5	2.0	0.0	20320.7
3	6.5	736.3	2.1	19456.7	0.0	2.5	0.0	11.6	1.2	0.0	20216.8
4	-	-	-	-	-	-	-	-	-	-	-
5	6.5	673.2	1.9	19380.0	1.0	0.0	0.0	7.3	0.0	0.0	20069.8
6	5.6	632.5	1.9	18877.2	0.0	0.0	0.0	5.7	0.7	0.0	19523.6

TOS (h)	% Yield										
	Conversion	Methane	Ethylene	Acetylene	Methyl acety-lene	C4	Cyclopentene	Benzene	Toluene	Xylene	Blank Me-thane
1	3.50	0.03	3.36	0.01	0.01	0.01	0.00	0.07	0.02	0.00	26815.10
2	3.05	0.02	2.94	0.01	0.00	0.01	0.00	0.05	0.01	0.00	
3	2.83	0.02	2.75	0.01	0.00	0.01	0.00	0.04	0.00	0.00	
4	-	-	-	-	-	-	-	-	-	-	
5	2.57	0.02	2.51	0.01	0.00	0.00	0.00	0.03	0.00	0.00	
6	2.41	0.02	2.36	0.01	0.00	0.00	0.00	0.02	0.00	0.00	

Reaction condition; Catalyst: 3%wt.Ga-HZSM-5 (500), Reaction temperature: 650 °C, Reduction temperature: 900 °C, Feed rate: 20 mL/min of ethane, Carrier gas; 55 mL/min of helium, Ambient pressure.

D3: Effect of Ga loading

Table D6 area and product distribution from ethane conversion (contact time 3.69 g.h.mol^{-1})

TOS (h)	Area										Total Area
	Methane	Ethylene	Acetylene	Ethane	Methyl acetylene	C4	Cyclopentene	Benzene	Toluene	Xylene	
1	8.3	990.7	0.0	20933.2	2.5	2.5	0.0	6.9	0.0	0.0	21944.1
2	6.9	919.7	0.0	20504.7	1.9	2.2	0.0	6.2	0.0	0.0	21441.7
3	6.2	876.8	0.8	20159.7	1.7	2.0	0.0	5.7	0.0	0.0	21053.0
4	5.9	852.7	0.8	19671.6	1.6	2.0	0.0	3.1	0.0	0.0	20537.8
5	5.6	818.2	0.9	19741.8	1.3	2.0	0.0	1.1	0.0	0.0	20570.9
6	5.4	800.3	0.9	19580.7	1.2	2.0	0.0	1.3	0.0	0.0	20391.7

TOS (h)	% Yield										
	Conversion	Methane	Ethylene	Acetylene	Methyl acety-lene	C4	Cyclopentene	Benzene	Toluene	Xylene	Blank
1	3.22	0.03	3.15	0.00	0.01	0.01	0.00	0.02	0.00	0.00	31415.00
2	2.98	0.02	2.93	0.00	0.01	0.01	0.00	0.02	0.00	0.00	
3	2.84	0.02	2.79	0.00	0.01	0.01	0.00	0.02	0.00	0.00	
4	2.76	0.02	2.71	0.00	0.01	0.01	0.00	0.01	0.00	0.00	
5	2.64	0.02	2.60	0.00	0.00	0.01	0.00	0.00	0.00	0.00	
6	2.58	0.02	2.55	0.00	0.00	0.01	0.00	0.00	0.00	0.00	

Reaction condition; Catalyst: 2%wt.Ga-HZSM-5 (500), Reaction temperature: 650 °C, Reduction temperature: 900 °C, Feed rate: 20 mL/min of ethane, Carrier gas; 55 mL/min of helium, Ambient pressure.

Table D7 area and product distribution from ethane conversion (contact time 3.69 g.h.mol^{-1})

TOS (h)	Area										
	Methane	Ethylene	Acetylene	Ethane	Methyl acetylene	C4	Cyclopentene	Benzene	Toluene	Xylene	Total Area
1	13.7	1147.0	0.8	20679.8	4.9	10.8	1.3	83.9	20.2	0.0	21962.3
2	11.2	1057.8	0.9	20584.2	3.7	9.4	0.0	63.9	12.0	0.0	21743.0
3	10.2	1004.5	1.1	20450.9	3.2	7.8	0.0	47.3	8.0	0.0	21532.9
4	9.4	957.1	1.0	20201.0	3.2	7.7	0.0	36.1	6.5	0.0	21221.9
5	9.0	926.5	1.1	20066.1	2.5	7.3	0.0	37.0	4.3	0.0	21053.9
6	8.5	892.5	1.1	19825.5	2.2	7.0	0.0	29.7	4.5	0.0	20771.0

TOS (h)	% Yield										
	Conversion	Methane	Ethylene	Acetylene	Methyl acetylene	C4	Cyclopentene	Benzene	Toluene	Xylene	Blank
1	4.61	0.05	4.12	0.00	0.02	0.04	0.00	0.30	0.07	0.00	27825.00
2	4.16	0.04	3.80	0.00	0.01	0.03	0.00	0.23	0.04	0.00	
3	3.89	0.04	3.61	0.00	0.01	0.03	0.00	0.17	0.03	0.00	
4	3.67	0.03	3.44	0.00	0.01	0.03	0.00	0.13	0.02	0.00	
5	3.55	0.03	3.33	0.00	0.01	0.03	0.00	0.13	0.02	0.00	
6	3.40	0.03	3.21	0.00	0.01	0.02	0.00	0.11	0.02	0.00	

Reaction condition; Catalyst: 4%wt.Ga-HZSM-5 (500), Reaction temperature: 650 °C, Reduction temperature: 900 °C, Feed rate: 20 mL/min of ethane, Carrier gas; 55 mL/min of helium, Ambient pressure.

Table D8 area and product distribution from ethane conversion (contact time 3.69 g.h.mol^{-1})

TOS (h)	Area										Total Area
	Methane	Ethylene	Acetylene	Ethane	Methyl acetylene	C4	Cyclopentene	Benzene	Toluene	Xylene	
1	1.24	96.13	0.00	16073.85	0.00	0.00	0.0	0.00	0.00	0.00	16171.22
2	1.27	97.60	0.00	15997.18	0.00	0.00	0.0	0.00	0.00	0.00	16096.04
3	1.21	92.04	0.00	15727.16	0.00	0.00	0.0	0.00	0.00	0.00	15820.41

TOS (h)	% Yield										
	Conversion	Methane	Ethylene	Acetylene	Methyl acety-lene	C4	Cyclopentene	Benzene	Toluene	Xylene	Blank
1	0.39	0.00	0.38	0.00	0.00	0.00	0.00	0.00	0.00	0.00	
2	0.39	0.01	0.39	0.00	0.00	0.00	0.00	0.00	0.00	0.00	25154.00
3	0.37	0.00	0.37	0.00	0.00	0.00	0.00	0.00	0.00	0.00	

Reaction condition; Catalyst: HZSM-5 (500), Reaction temperature: 650 °C, Reduction temperature: 900 °C, Feed rate: 20 mL/min of ethane, Carrier gas; 55 mL/min of helium, Ambient pressure.

D4: Effect of OH functional surface and Structure confinement

Table D9 area and product distribution from ethane conversion (contact time 3.69 g.h.mol^{-1})

TOS (h)	Area										Total Area
	Methane	Ethylene	Acetylene	Ethane	Methyl acetylene	C4	Cyclopentene	Benzene	Toluene	Xylene	
1	12.4	1383.8	2.9	22995.9	3.8	10.6	0.0	68.5	5.1	0.0	24483.1
2	10.3	1188.5	2.8	22513.3	2.3	7.5	0.0	54.7	6.0	0.0	23785.4
3	9.1	1078.7	2.7	22307.2	2.0	3.8	0.0	33.2	4.4	0.0	23441.1
4	8.5	1011.5	2.7	22481.0	2.0	3.9	0.0	26.2	3.5	0.0	23539.3
5	7.9	948.2	3.0	21704.9	1.5	3.2	0.0	15.5	2.6	0.0	22686.8
6	7.4	902.5	2.3	21514.3	1.3	3.2	0.0	11.6	1.2	0.0	22443.8

TOS (h)	% Yield										
	Conversion	Methane	Ethylene	Acetylene	Methyl acetylene	C4	Cyclopentene	Benzene	Toluene	Xylene	Blank
1	5.23	0.04	4.87	0.01	0.01	0.04	0.00	0.24	0.02	0.00	28415.00
2	4.48	0.04	4.18	0.01	0.01	0.03	0.00	0.19	0.02	0.00	
3	3.99	0.03	3.80	0.01	0.01	0.01	0.00	0.12	0.02	0.00	
4	3.72	0.03	3.56	0.01	0.01	0.01	0.00	0.09	0.01	0.00	
5	3.46	0.03	3.34	0.01	0.01	0.01	0.00	0.05	0.01	0.00	
6	3.27	0.03	3.18	0.01	0.00	0.01	0.00	0.04	0.00	0.00	

Reaction condition; Catalyst: 3%wt.Ga-Silicalite (OH), Reaction temperature: 650 °C, Reduction temperature: 900 °C, Feed rate: 20 mL/min of ethane, Carrier gas; 55 mL/min of helium, Ambient pressure.

Table D10 area and product distribution from ethane conversion (contact time 3.69 g.h.mol^{-1})

TOS (h)	Area										Total Area
	Methane	Ethylene	Acetylene	Ethane	Methyl acetylene	C4	Cyclopentene	Benzene	Toluene	Xylene	
1	8.4	812.6	2.1	18266.9	0.0	3.7	0.0	31.7	5.9	0.0	19131.3
2	6.4	658.4	3.3	18033.9	0.0	2.4	0.0	12.1	1.7	0.0	18718.2
3	5.5	582.1	3.0	17615.4	0.0	0.0	0.0	5.8	0.9	0.0	18212.7
4	5.0	533.1	3.1	18029.5	0.0	0.0	0.0	4.7	0.0	0.0	18575.3
5	4.3	488.8	1.9	17291.7	0.0	0.0	0.0	4.0	0.0	0.0	17790.6
6	4.1	449.1	1.9	16935.5	0.0	0.0	0.0	3.9	0.0	0.0	17394.5

TOS (h)	% Yield										
	Conversion	Methane	Ethylene	Acetylene	Methyl acetylene	C4	Cyclopentene	Benzene	Toluene	Xylene	Blank
1	3.37	0.03	3.16	0.01	0.00	0.01	0.00	0.12	0.02	0.00	25678.53
2	2.66	0.02	2.56	0.01	0.00	0.01	0.00	0.05	0.01	0.00	
3	2.33	0.02	2.27	0.01	0.00	0.00	0.00	0.02	0.00	0.00	
4	2.13	0.02	2.08	0.01	0.00	0.00	0.00	0.02	0.00	0.00	
5	1.94	0.02	1.90	0.01	0.00	0.00	0.00	0.02	0.00	0.00	
6	1.79	0.02	1.75	0.01	0.00	0.00	0.00	0.02	0.00	0.00	

Reaction condition; Catalyst: 3%wt.Ga-Silicalite (OH(550)), Reaction temperature: 650 °C, Reduction temperature: 900 °C, Feed rate: 20 mL/min of ethane, Carrier gas; 55 mL/min of helium, Ambient pressure.

Table D11 area and product distribution from ethane conversion (contact time 3.69 g.h.mol^{-1})

TOS (h)	Area										
	Methane	Ethylene	Acetylene	Ethane	Methyl acetylene	C4	Cyclopentene	Benzene	Toluene	Xylene	Total Area
1	1.2	152.2	0.0	18731.2	0.0	0.0	0.0	0.0	0.0	0.0	18884.6
2	0.9	138.6	0.0	18338.5	0.0	0.0	0.0	0.0	0.0	0.0	18478.0
3	0.8	131.6	0.0	18070.1	0.0	0.0	0.0	0.0	0.0	0.0	18202.5
4	0.9	123.9	0.0	17750.0	0.0	0.0	0.0	0.0	0.0	0.0	17874.8
5	0.9	119.4	0.0	17628.3	0.0	0.0	0.0	0.0	0.0	0.0	17748.6
6	0.8	113.6	0.0	17425.5	0.0	0.0	0.0	0.0	0.0	0.0	17539.9

TOS (h)	% Yield										
	Conversion	Methane	Ethylene	Acetylene	Methyl acetylene	C4	Cyclopentene	Benzene	Toluene	Xylene	Blank
1	0.52	0.00	0.52	0.00	0.00	0.00	0.00	0.00	0.00	0.00	29415.00
2	0.47	0.00	0.47	0.00	0.00	0.00	0.00	0.00	0.00	0.00	
3	0.45	0.00	0.45	0.00	0.00	0.00	0.00	0.00	0.00	0.00	
4	0.42	0.00	0.42	0.00	0.00	0.00	0.00	0.00	0.00	0.00	
5	0.41	0.00	0.41	0.00	0.00	0.00	0.00	0.00	0.00	0.00	
6	0.39	0.00	0.39	0.00	0.00	0.00	0.00	0.00	0.00	0.00	

Reaction condition; Catalyst: 3%wt.Ga-Silicalite (F), Reaction temperature: 650 °C, Reduction temperature: 900 °C, Feed rate: 20 mL/min of ethane, Carrier gas; 55 mL/min of helium, Ambient pressure.

Table D12 area and product distribution from ethane conversion (contact time 3.69 g.h.mol^{-1})

TOS (h)	Area										Total Area
	Methane	Ethylene	Acetylene	Ethane	Methyl acetylene	C4	Cyclopentene	Benzene	Toluene	Xylene	
1	0.9	226.1	0.0	15744.2	0.0	0.0	0.0	0.0	0.0	0.0	15971.24
2	1.1	223.8	0.0	15771.1	0.0	0.0	0.0	0.0	0.0	0.0	15996.07
3	1.0	214.9	0.0	15404.5	0.0	0.0	0.0	0.0	0.0	0.0	15620.45
4	0.9	211.2	0.0	15274.8	0.0	0.0	0.0	0.0	0.0	0.0	15486.87
5	0.9	198.7	0.0	15077.7	0.0	0.0	0.0	0.0	0.0	0.0	15277.37
6	0.9	197.6	0.0	15065.0	0.0	0.0	0.0	0.0	0.0	0.0	15263.53

TOS (h)	% Yield										
	Conversion	Methane	Ethylene	Acetylene	Methyl acetylene	C4	Cyclopentene	Benzene	Toluene	Xylene	Blank
1	0.90	0.00	0.90	0.00	0.00	0.00	0.00	0.00	0.00	0.00	25154.00
2	0.89	0.00	0.89	0.00	0.00	0.00	0.00	0.00	0.00	0.00	
3	0.86	0.00	0.85	0.00	0.00	0.00	0.00	0.00	0.00	0.00	
4	0.84	0.00	0.84	0.00	0.00	0.00	0.00	0.00	0.00	0.00	
5	0.79	0.00	0.79	0.00	0.00	0.00	0.00	0.00	0.00	0.00	
6	0.79	0.00	0.79	0.00	0.00	0.00	0.00	0.00	0.00	0.00	

Reaction condition; Catalyst: 3%wt.Ga-SiO_2 (Devicil), Reaction temperature: 650 °C, Reduction temperature: 900 °C, Feed rate: 20 mL/min of ethane, Carrier gas; 55 mL/min of helium, Ambient pressure.

D5: Effect of contact times

Table D13 area and product distribution from ethane conversion (contact time 7.38 g.h.mol^{-1})

TOS (h)	Area										Total Area
	Methane	Ethylene	Acetylene	Ethane	Methyl acetylene	C4	Cyclopentene	Benzene	Toluene	Xylene	
1	28.6	1164.0	3.2	17758.5	3.7	6.1	0.0	52.5	14.3	0.0	19030.9
2	18.3	1021.8	3.4	17422.0	2.3	4.8	0.0	35.5	5.9	0.0	18513.8
3	14.8	931.9	3.2	17181.9	2.0	3.9	0.0	22.7	4.2	0.0	18164.6
4	12.6	854.9	3.1	16580.3	2.0	3.8	0.0	16.9	3.4	0.0	17476.9
5	11.4	807.7	2.9	16712.6	1.7	3.3	0.0	13.5	2.5	0.0	17555.5
6	9.9	685.7	2.4	14831.6	1.3	3.3	0.0	10.7	1.9	0.0	15546.7

TOS (h)	% Yield										
	Conversion	Methane	Ethylene	Acetylene	Methyl acetylene	C4	Cyclopentene	Benzene	Toluene	Xylene	Blank
1	5.36	0.12	4.90	0.01	0.02	0.03	0.00	0.22	0.06	0.00	23750.27
2	4.60	0.08	4.30	0.01	0.01	0.02	0.00	0.15	0.02	0.00	
3	4.14	0.06	3.92	0.01	0.01	0.02	0.00	0.10	0.02	0.00	
4	3.78	0.05	3.60	0.01	0.01	0.02	0.00	0.07	0.01	0.00	
5	3.55	0.05	3.40	0.01	0.01	0.01	0.00	0.06	0.01	0.00	
6	3.01	0.04	2.89	0.01	0.01	0.01	0.00	0.04	0.01	0.00	

Reaction condition; Catalyst: 3%wt.Ga-HZSM-5 (500), Reaction temperature: 650 °C, Reduction temperature: 900 °C, Feed rate: 20 mL/min of ethane, Carrier gas; 55 mL/min of helium, Ambient pressure.

Table D14 area and product distribution from ethane conversion (contact time 11.07 g.h.mol^{-1})

TOS (h)	Area										Total Area
	Methane	Ethylene	Acetylene	Ethane	Methyl acetylene	C4	Cyclopentene	Benzene	Toluene	Xylene	
1	30.8	2095.5	4.1	22270.4	6.0	10.2	2.3	144.7	32.7	13.7	24610.1
2	24.7	1711.7	3.6	21875.9	4.5	11.2	1.2	79.9	16.9	2.7	23732.2
3	21.7	1559.5	3.4	22098.4	3.7	9.6	1.2	54.3	6.1	0.0	23757.9
4	19.5	1450.7	3.4	21762.9	3.7	9.4	0.0	41.7	2.6	0.0	23293.8
5	17.8	1361.0	3.0	21940.6	3.1	7.2	0.0	32.7	2.7	0.0	23368.0
6	7.4	902.5	2.3	21514.3	1.3	6.8	0.0	11.6	1.2	0.0	22447.4

TOS (h)	% Yield										
	Conversion	Methane	Ethylene	Acetylene	Methyl acetylene	C4	Cyclopentene	Benzene	Toluene	Xylene	Blank
1	8.38	0.11	7.51	0.01	0.02	0.04	0.01	0.52	0.12	0.05	27915.00
2	6.65	0.09	6.13	0.01	0.02	0.04	0.00	0.29	0.06	0.01	
3	5.94	0.08	5.59	0.01	0.01	0.03	0.00	0.19	0.02	0.00	
4	5.48	0.07	5.20	0.01	0.01	0.03	0.00	0.15	0.01	0.00	
5	5.11	0.06	4.88	0.01	0.01	0.03	0.00	0.12	0.01	0.00	
6	3.34	0.03	3.23	0.01	0.00	0.02	0.00	0.04	0.00	0.00	

Reaction condition; Catalyst: 3%wt.Ga-HZSM-5 (500), Reaction temperature: 650 °C, Reduction temperature: 900 °C, Feed rate: 20 mL/min of ethane, Carrier gas; 55 mL/min of helium, Ambient pressure.

Table D15 area and product distribution from ethane conversion (contact time 3.69 g.h.mol^{-1})

TOS (h)	Area										Total Area
	Methane	Ethylene	Acetylene	Ethane	Methyl acetylene	C4	Cyclopentene	Benzene	Toluene	Xylene	
1	82.8	579.0	0.0	25510.4	3.6	0.0	0.0	0.0	0.0	0.0	26175.7
2	78.0	573.6	0.0	25199.9	3.6	0.0	0.0	0.0	0.0	0.0	25855.1
3	73.6	564.1	0.0	24931.2	3.3	0.0	0.0	0.0	0.0	0.0	25572.3
4	73.7	565.4	0.0	24953.8	3.4	0.0	0.0	0.0	0.0	0.0	25596.2
5	-	-	-	-	-	-	-	-	-	-	-
6	52.0	557.4	0.0	24513.4	2.0	0.0	0.0	0.0	0.0	0.0	25124.7

TOS (h)	% Yield										
	Conversion	Methane	Ethylene	Acetylene	Methyl acetylene	C4	Cyclopentene	Benzene	Toluene	Xylene	Blank
1	1.89	0.24	1.65	0.00	0.01	0.00	0.00	0.00	0.00	0.00	35154.00
2	1.86	0.22	1.63	0.00	0.01	0.00	0.00	0.00	0.00	0.00	
3	1.82	0.21	1.60	0.00	0.01	0.00	0.00	0.00	0.00	0.00	
4	1.83	0.21	1.61	0.00	0.01	0.00	0.00	0.00	0.00	0.00	
5	-	-	-	-	-	-	-	-	-	-	
6	1.74	0.15	1.59	0.00	0.01	0.00	0.00	0.00	0.00	0.00	

Reaction condition; Catalyst: 3%wt.Ga-HZSM-5 (500), Reaction temperature: 650 °C, Reduction temperature: 900 °C, Feed rate: 20 mL/min of ethane, Carrier gas; 55 mL/min of hydrogen, Ambient pressure.